

Embedding Space Approach to Lorentzian CFT Amplitudes and Causal Spherical Functions

Pulkit Agarwal^{*}, Richard C. Brower^{**}, Timothy G. Raben⁺, and Chung-I Tan⁺⁺

^{*}National University of Singapore, Singapore

^{**}Boston University, Boston, MA 02215

⁺Michigan State University, East Lansing, MI, 48824

⁺⁺Brown University, Providence, RI 02912

March 20, 2023

Abstract

Conformal Field Theory in a Minkowski setting is discussed in an embedding space approach, paying special attention to causality constraints for four-point amplitudes. The physics of dilatation and Lorentz boost is emphasized in specifying the non-compact Maximal Abelian subgroup (MASG) of $SO(d, 2)$. Reduction of a Conformal Field Theory (CFT) four-point amplitudes as functions of cross ratios is shown to be equivalent to enforcing H bi-invariance, i.e., $F(hgh') = F(g)$, with $g \in SO(d, 2)$ and H an appropriate subgroup. Causality is imposed by introducing appropriate semigroups. Causal zonal spherical functions are constructed, making contact with Minkowski conformal blocks introduced previously.

Contents

1	Introduction	1
2	CFT Amplitudes in Minkowski Limits	7
2.1	Kinematics of Causal Scattering Regions	8
2.2	Group Theoretic Motivated Variables	11
2.3	Wick Rotation and Causal Scattering vs Non-Causal Regions	13
3	Four-point Functions, H-bi-Invariance, and Semigroups	14
3.1	Embedding Space	15
3.2	Embedding Space Realization of Antipodal Frame	18
3.3	H -bi-Invariance	19
3.4	Causal Semigroups	21
4	Principal Series for $SO(d, 2)$	23
4.1	Induced Representation	23
4.2	Multiplier Factor, Roots and Weyl-Vector	25
4.3	Induced Representation for Semigroups and Root Space	27
5	Spherical Functions and Semigroups	29
5.1	A First Look at Group Harmonics	29
5.2	Space of Homogenous Functions for $SO(2, 1)$	30
5.3	Generalized Inductive Character and Doubling Procedure	31
5.4	Minkowski Causal CFT_2	33
5.5	Minkowski CFT_d for $d > 2$	35
6	Discussion	36
A	Summary of Notations	41
B	Kinematics of Minkowski 4-Point CFT Amplitudes	43
C	Some Useful Aspects of $SO(d, 2)$	49
D	Causal Symmetric Spaces	54
E	Spherical Functions for $SO(3)$	58
F	Inductive Characters & Zonal Spherical Functions	60

1 Introduction

Most current CFT studies have been carried out in a Euclidean framework, i.e., working with the group $SO(d+1, 1)$. There has been increasing recent interest in the relation between CFT in an Euclidean setting to its counter part in a Minkowski setting. Most notably is the work of Caron-Huot [1], where a connection was made between OPE expansion coefficients in terms of Euclidean conformal blocks with an integral over matrix elements of double-commutators. Many other interesting recent work have also appeared. In particular, Simmons-Duffin, Stanford and Witten [2] offer a Minkowski spacetime derivation of Caron-Huot’s result and discusses the causal structures involved.

In a Minkowski space, a double-commutator, e.g., $\langle 0 | [\varphi(x_4), \varphi(x_1)] [\varphi(x_2), \varphi(x_3)] | 0 \rangle$, can be identified with the imaginary part of a time-ordered amplitude, $\langle 0 | T(\varphi(x_4)\varphi(x_1)\varphi(x_2)\varphi(x_3)) | 0 \rangle$. Such time-ordered amplitude defines an off-shell Green’s function, and it can be used to study the “s-channel” scattering process ¹,

$$\Phi(1) + \Phi(3) \rightarrow \Phi(2) + \Phi(4). \tag{1.1}$$

Naively, a CFT doesn’t have asymptotically separated states. However, by introducing a confinement scale or considering current flows, “CFT scattering” has been an area of active research [3–21]. Two important related areas are the Out of Time Order Correlators (OTOCs) [22–25] in models like the SYK [26–29], and celestial holography [30–32]. In many of these and related works the issue of CFT Regge behavior has begun to play an increasingly important role. However, in much of the previous CFT scattering work, results are obtained by working in a Euclidean framework and then performing an analytic continuation to Minkowski space at the end. A serious attempt in connecting Euclidean CFTs to their Minkowski counter parts from an axiomatic approach has begun recently by Kravchuk, Qiao and Rychkov [33, 34], (see additional references therein).

In a CFT, correlation functions can be described via a “partial wave analysis” where the dynamics of the process are captured by partial wave amplitudes and the kinematics is encoded in the *conformal blocks* (see [35, 36] for a complete introduction). An initial direct examination of conformal blocks in a Minkowski setting was carried out in [20]. A related work using the analytic continuation approach is found in Kravchuk and Simmons-Duffin [37]. The importance of a direct Minkowski approach was recently emphasized by Mack [38].

The double-commutator is non-vanishing,

$$\langle 0 | [\varphi(x_4), \varphi(x_1)] [\varphi(x_2), \varphi(x_3)] | 0 \rangle \neq 0, \tag{1.2}$$

¹It also describes the reversed process $\bar{2} + \bar{4} \rightarrow \bar{1} + \bar{3}$.

only in certain configurations in Minkowski space: x_{14} and x_{23} time-like separated, while holding all other $x_{ij}^2 > 0$; therefore, the double-commutator is defined as a *distribution*. This configuration of space-time points is the signature of “**causality**”, a concept which is meaningful only in a Minkowski setting. Fig. 1.1 provides a kinematic interpretation in terms of a lightcone diagram, which can also be associated with the notion of what we will refer to as “Minkowski t -channel OPE” limit [3–17, 19–21, 37]. This also ties in with Regge limits for CFT. We shall refer to Eq. (1.2) as the associated causal condition for the “ s -channel” scattering process, $(1 + 3 \rightarrow 2 + 4)$.

The kinematics can also be understood by analogy with that for off-shell Compton scattering, $\gamma^*(1) + \gamma^*(3) \rightarrow \gamma^*(2) + \gamma^*(4)$ (ignoring spin degrees of freedom), i.e., x_{14} and x_{32} time-like, while keeping all other Lorentz invariants space-like, $x_{ij}^2 > 0$ and $x_i^2 > 0$, $i, j = 1, 2, 3, 4$. This corresponds to our causal condition (1.2). With x_i^2 fixed, translational invariance becomes less apparent. It can be restored formally by introducing a fiducial point x_5 so that $x_i^2 \rightarrow x_{i5}^2$. See analogous treatment in Ref. [2].

The corresponding “ u -channel” process, $(1 + 4 \rightarrow 2 + 3$ by $3 \leftrightarrow 4$ crossing) associated with Minkowski t -channel OPE takes place in the region where

$$\langle 0 | [\varphi(x_3), \varphi(x_1)] [\varphi(x_2), \varphi(x_4)] | 0 \rangle \neq 0. \quad (1.3)$$

Note that we have identified scattering channels with partitions: (13)(24) for s -channel, (14)(23) for u -channel and (12)(34) for the t -channel process, $(1 + 2 \rightarrow 3 + 4)$. Our usage here differs from that typically used in an Euclidean OPE/bootstrap treatment. (See Appendix A.1 of Ref. [20], for a more careful discussion.)

The main purpose of this paper is to directly work with CFT in a Minkowski framework using a novel group theoretic approach. The new results here greatly expand on the initial work in [20]. We provide a framework for discussing four-point functions for Lorentzian CFTs by working with the **embedding space**, as done by Dobrev *et al.* for Euclidean CFTs [39]. (That is, we lift the d -dimensional Minkowski space-time to $(d + 2)$ -dimensional and consider functions defined on the null-cone $X^2 = 0$.) Our analysis complements related studies on various mathematical aspects of $SO(d, 2)$ representations carried out in [2, 37, 38, 40]. In particular, we highlight the central role played by **causality**, as specified by (1.2) and (1.3), and how it relates to the notions of *causal symmetric spaces* [41] and *semigroups* [41–47] in an embedding space approach.

For a scattering amplitude defined in terms of a time-ordered Green’s function, its imaginary part in a *causal* domain, e.g., $x_{14}^2 < 0, x_{23}^2 < 0$, can be identified with the double commutator,

$$\text{Im}T(x_i) = \frac{\langle 0 | [\varphi(x_4)\varphi(x_1)] [\varphi(x_2), \varphi(x_3)] | 0 \rangle}{\langle \varphi(x_1)\varphi(x_2) \rangle \langle \varphi(x_3)\varphi(x_4) \rangle}. \quad (1.4)$$

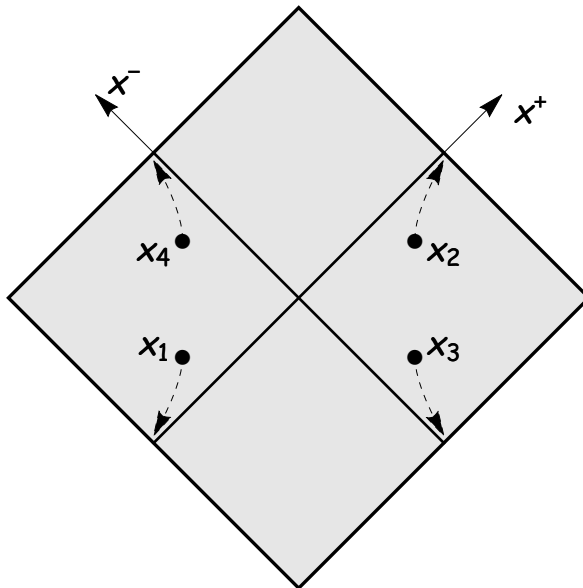


Figure 1.1: The s -channel scattering region. Switching $x_3 \leftrightarrow x_4$ leads to the u -channel scattering. Figure taken from Ref. [15].

where we have normalized the amplitude by $\langle \varphi(x_1)\varphi(x_2) \rangle \langle \varphi(x_3)\varphi(x_4) \rangle$. The amplitude is thus dimensionless. With x_{12} and x_{34} spacelike separated, this choice is appropriate for s - and u -channel scattering as specified by causal conditions (1.2) and (1.3). This choice also maintains s - u symmetry. By focusing on s - and u -channel scatterings², our treatment is not totally s - t - u symmetric. Causal region for t -channel scattering can be treated by permutation.

Lorentzian CFTs are invariant under the symmetry group $SO(d, 2)$, which has a set of mutually commuting generators forming a Cartan subalgebra. In particular, $SO(d, 2)$ contains a rank-2 non-compact Maximal Abelian Sub-Group (**MASG**),

$$A = SO(1, 1) \times SO(1, 1). \quad (1.5)$$

(This is referred to as the split-rank of $SO(d, 2)$ and will be clarified further in Appendix C.) By relating the MASG to the physics of dilatation and Lorentz boosts, it was emphasized in [20] that $\text{Im}T(x_i)$, identified as a discontinuity, can be represented in terms of the **principal series representation** of $SO(d, 2)$ [45–50]

$$\text{Im}T(x_i) = \int_{-i\infty}^{i\infty} \frac{d\tilde{\ell}}{2\pi i} \int_{-i\infty}^{i\infty} \frac{d\tilde{\Delta}}{2\pi i} a^{(\pm)}(\tilde{\ell}, \tilde{\Delta}) \mathcal{G}_{(\tilde{\ell}, \tilde{\Delta}; 0)}(g). \quad (1.6)$$

It should be pointed out that there are other possible choices for the MASG. In this study, we have made a choice appropriate by the physics of Lorentzian CFTs.

²Our treatment is often guided by intuitions gained from studies based on gauge/string duality, e.g., [3]

This is the first of two papers in our current effort on a direct approach to Minkowski CFT ³. We present in this paper a proper derivation for this representation by adopting an embedding space approach, focussing on the scattering region specified by the causal condition, (1.2). We identify the representation functions (or group harmonics) $\mathcal{G}_{\tilde{\Delta}, \tilde{\ell}; 0}(g)$ as “causal” **zonal spherical functions** [41, 45–47, 51] for $SO(d, 2)$, and associate them with Minkowski conformal blocks discussed in [20] ⁴.

This paper consists of two main parts. The key insights can be summarized as follows:

1. Minkowski Fourpoint Functions and Causality:

- *In Sec. 2, we focus on specifying causal scattering regions for (1.2) and (1.3) in terms of cross ratios by introducing a new set of group theoretic motivated variables (w, σ) .*

Kinematic analysis of the 4-point function can be simplified greatly by a new set of variables (w, σ) , Eq. (2.2),

$$w \equiv \frac{1 - \sqrt{v}}{\sqrt{u}}, \quad \sigma \equiv \frac{1 + \sqrt{v}}{\sqrt{u}}.$$

These variables, defined via (\sqrt{u}, \sqrt{v}) , resolve the multi-sheeted structure of the u - v plane by allowing $-\infty < w, \sigma < \infty$ and help to exhibit relevant kinematic singularities for CFT scattering, e.g., at $u = 0$, $v = 0$ or $u = v = \infty$. They delineate clearly transitions from the Euclidean region to Minkowski regions, (see Figs. 2.1, 2.2 and 2.3). They also provide physically intuitive interpretation when adopting a generalized Minkowski antipodal frames. This is also referred to as “double-lightcone” frame in Ref. [20]. It allows a direct connection between variables (w, σ) , (thus (\sqrt{u}, \sqrt{v})), with $SO(d, 2)$ group parameters (y, η) . In particular, it provides a symmetrical identification for the *causal conditions*, (1.2) and (1.3), with causal regions $M_s^{(t)}$ and $M_u^{(t)}$ respectively, (see Fig. 2.3).

- *In Sec. 3, we examine consequences of conformal invariance and causality for Minkowski CFT in an embedding space treatment. This leads to the introduction of H bi-invariance and semigroups. The first accomplishes the reduction to conformal cross ratios and the latter enforces causality. Both of these concepts are needed for introducing causal group harmonics in Sec. 5.*

³A second paper, “Conformal Blocks and Harish Chandra c-Functions”, is being prepared [52]. Some preliminary results were reported in [53].

⁴The term spherical functions is used in several different contexts in literature. For example, bi-invariant functions that are of importance to us are referred to as spherical functions in [51], whereas they are called zonal spherical functions in [45–47]. We adopt the latter definition and reserve the phrase spherical functions for right-invariant functions. This is closer to the familiar physics literature, since $Y_{\ell, m}$ are called spherical harmonics for $SO(3)$ and are associated with right-invariant functions.

Understanding 4-point functions in terms of linear group representations requires first lifting them from functions in the coordinate space to the embedding space. These can then be parametrized as functions over $G = SO(d, 2)$, i.e., functions $F(g)$, with $g \in SO(d, 2)$ acting on the embedding space linearly. A group function of a single-copy of $SO(d, 2)$ in general involves $(d + 2)(d + 1)/2$ variables. It can be reduced to fewer degrees of freedom by acting on the coset G/H , where H is a subgroup characterizing a residual symmetry, e.g., $F(gh) = F(g)$, with $h \in H$. If the symmetry is enhanced when acting on two-sided coset, $F(g) = F(hgh')$, it is “ H bi-invariant”, leading to

$$F(g) = F(hah') = F(a),$$

where $a \in A$, the maximal abelian subgroup, Eq. (3.12)⁵. We demonstrate that reducing to the cross ratio space is equivalent to enforcing H bi-invariance, with H determined by specifying an appropriate basepoint in the embedding space. When causality is imposed, additional structure emerges, e.g., various regions in the w - σ plane are covered via semigroups. This leads to H bi-invariant zonal spherical functions associated with each representation of $SO(d, 2)$. Similar type of analysis has been carried out in early years with emphasis on Lorentz group, e.g., [41–44, 47]. These functions are necessarily constructed piecewise in different regions of the w - σ plane.

2. Representation Theory of Semigroups:

- *In Sec. 4, we discuss induced representations for $SO(d, 2)$ via Iwasawa decomposition and the principal series. We identify the positive root-space structure, dictated by causal consideration.*

The principal series representations for $SO(d, 2)$ can be labelled by the unitary irreducible representation of its MASG via induced representation. This leads to Eq. (1.4), with purely imaginary representation labels $\tilde{\lambda} = (\tilde{\ell}, \tilde{\Delta})$. The induced representation involves introducing a multiplier factor, Eq. (4.5), which can be interpreted as adding real parts to these labels. The Weyl group dictates these real parts be parametrized by a Weyl vector, $\vec{\rho}$, Eq. (4.8) and Table-1. That is, the multipliers are of the form $e^{-\vec{\rho} \cdot \vec{t}}$. Together with the unitary representation of the MASG $e^{\tilde{\lambda} \cdot \vec{t}}$, the representation functions are now labelled by a pair of complex numbers $\vec{\lambda} = -\vec{\rho} + \tilde{\lambda}$, Eq. (4.9). The Weyl vector is in turn fixed by the ordering of positive roots, dictated by the *semigroup* structure. A proper treatment of Weyl vectors leads to a consistent identification with the conventionally defined variables (ℓ, Δ) , [54], done in a

⁵A two-sided coset is often denoted by $H \backslash G / H$ in mathematical literature, with G/H as “left-coset”. We will adopt the alternative notation $G//H$ for two-sided coset.

traditional Euclidean treatment, Eq. (4.12),

$$\ell = -(d-2)/2 + \tilde{\ell}, \quad \Delta = d/2 + \tilde{\Delta}.$$

A comparable analysis has also been carried out in [37]. This in turn leads to the desired boundary condition for Minkowski conformal blocks [20], Eq. (5.21), defined in the causal region $1 < \sigma < w < \infty$,

$$G_{(\Delta, \ell)}^{(M)}(u, v) \sim (\sqrt{u})^{1-\ell} \left(\frac{1-v}{\sqrt{u}} \right)^{1-\Delta},$$

and Euclidean conformal blocks, Eq. (5.22), defined in the region $1 < w < \sigma < \infty$,

$$G_{(\Delta, \ell)}^{(E)}(u, v) \sim (\sqrt{u})^{\Delta} \left(\frac{1-v}{\sqrt{u}} \right)^{\ell}.$$

Note that these are formally related by the (ℓ, Δ) and $(1-\Delta, 1-\ell)$ swap, so necessary in various related treatments, e.g., [1, 2]

- *Finally, in Sec. 5, we construct causal zone spherical functions which serve as group harmonics for the principal series, Eq. (1.6).*

We begin by providing a first look at group harmonics, making use of more familiar examples, e.g., $SO(3)$ and $SO(2, 1)$. The w - σ variables bear a direct connection to the MASG. An explicit construction of causal zonal spherical functions is introduced next for $SO(d, 2)$, leading to the desired group harmonics for CFT as functions of cross ratios. One arrives at an integral representation for these group harmonics, i.e., the resulting causal zonal spherical functions can be expressed as integrals over the subgroup H , Eq. (5.10),

$$\varphi_{\lambda}(a) = \varphi_{\lambda}(h_1 a h_2) = \int_H e^{\vec{\lambda} \cdot \vec{t}(h_1 a)} dh_1,$$

where as before, $\vec{\lambda} = -\vec{\rho} + \tilde{\lambda}$. The integrand is referred to as the inductive character, with $\vec{t}(a) = (y, \eta)$. We present explicit results for $d = 1, 2$. In particular, explicit evaluation of Eq. (5.10) for $d = 2$ leads to Minkowski conformal blocks satisfying boundary condition, Eq. (5.21), in agreement with that derived in [20].

Let us re-state the main goal of this paper: *To clarify the suggestion made in Refs. [20, 37, 38, 40] that Lorentzian CFT 4-point amplitudes can be treated directly in terms of the principal series representation of $SO(d, 2)$, Eq. (1.6), and to construct causal representation functions appropriate for Lorentzian physics directly from an embedding space approach.* Our emphasis in this study is on the discontinuity of connected Minkowski Green's function. It is non-vanishing, due to causality, only within the scattering regions. The full Minkowski amplitude can be

recovered formally via a dispersion relation, after proper consideration is made for analyticity, subtraction, etc. This as well as other pertinent issues will be discussed in Sec. 6.

Some of the materials in this study do not typically appear in standard CFT physics literature. For clarity, our discussions will occasionally appear to be repetitive. Additionally, in the appendices, a deliberate effort is made on being comprehensive rather than brief. Appendix-A summarizes our notational conventions. Appendix-B and Appendix-C contain more traditional background materials. Appendix-B includes clarification on the kinematics of a 4-point amplitude as a function of various equivalent sets of conformal invariant variables. Appendix-C is a brief discussion on the structure of semi-simple Lie groups and, for $SO(d,2)$, the notion of MASG, Eq. (1.5). Other appendices provide supplemental discussions to the text proper. Appendix D summarizes some of the key issues involved in the construction of *causal symmetric spaces* and how lightcone causality is understood using *semigroups*. Appendix E offers a review of zonal spherical functions for the case of $SO(3)$ and Appendix F extends the discussion to non-compact groups.

Note Added: After the completion of this work, we were made aware of the series of papers by Burić, Isachenkov, and Schomerus [55–59]. Some of the key constructions presented here are discussed in their work in the context of Euclidean CFTs. In particular, their K -spherical functions are the Euclidean analogues to our Minkowski H -bi-invariant functions, where their subgroup $K = SO(d) \times SO(1,1)$ is a Wick rotation away from our $H = SO(d-1,1) \times SO(1,1)$. The key distinction is the role played by causality in the determination of H and its association with the embedding space. Further, causality also dictates for us the ordering of roots discussed in [37,57]. The reduction of the Casimir equation to a Calogero-Sutherland Hamiltonian evolution can be understood in terms of our (y, η) variables and was briefly discussed in [53]. Further discussion in related directions is currently being prepared [52]. In this current study, we construct the relevant spherical functions directly in an integral representation.

2 CFT Amplitudes in Minkowski Limits

Minkowski scattering kinematics has often been illustrated schematically by the use of a lightcone diagram, e.g. Fig. 1.1. This necessarily requires adopting a Lorentzian signature. However, this illustration requires specifying a frame and it also lacks precision since the diagram involves *non-causal scattering regions* [2, 4, 12, 15, 20, 37].

The main goal of this section is to introduce a new set of group theoretically motivated conformal invariant variables, (w, σ) . This allows a more precise specification for the *causal scattering* regions for (1.2) and (1.3). This also prepares us for an embedding space treatment in the subsequent sections.

2.1 Kinematics of Causal Scattering Regions

In this subsection, we explain on how causal scattering regions can be reached from the Euclidean region kinematically by extending to regions where $-\infty < \sqrt{u}, \sqrt{v} < \infty$. In particular, reaching causal regions requires crossing certain singular line segments, L_s or L_u .

In a standard Euclidean treatment, after removing a kinematic factor, as done in (1.4), conformal invariance leads to a reduced dimensionless scalar function of two independent cross ratios, $\mathcal{G}(u, v)$, $u = x_{12}^2 x_{34}^2 / x_{13}^2 x_{24}^2$ and $v = x_{23}^2 x_{14}^2 / x_{13}^2 x_{24}^2$, with $u, v > 0$. With x_{ij}^2 defined with Euclidean signature, this scalar function is well-known to be further restricted kinematically, due to Schwarz inequality [54]. The curve bounding this Euclidean region- E , (green shaded region in Fig. 2.1(a)), is quadratic in u and v , and it can be factorized in terms of \sqrt{u} and \sqrt{v} , i.e., $(\sqrt{u} - \sqrt{v} - 1)(\sqrt{u} + \sqrt{v} - 1)(\sqrt{u} - \sqrt{v} + 1)(\sqrt{u} + \sqrt{v} + 1) = 0$. The first quadrant of the u - v plane is now divided into four separate regions, with straight-line segments separating them in the \sqrt{u} - \sqrt{v} plane, Fig. 2.1(b).

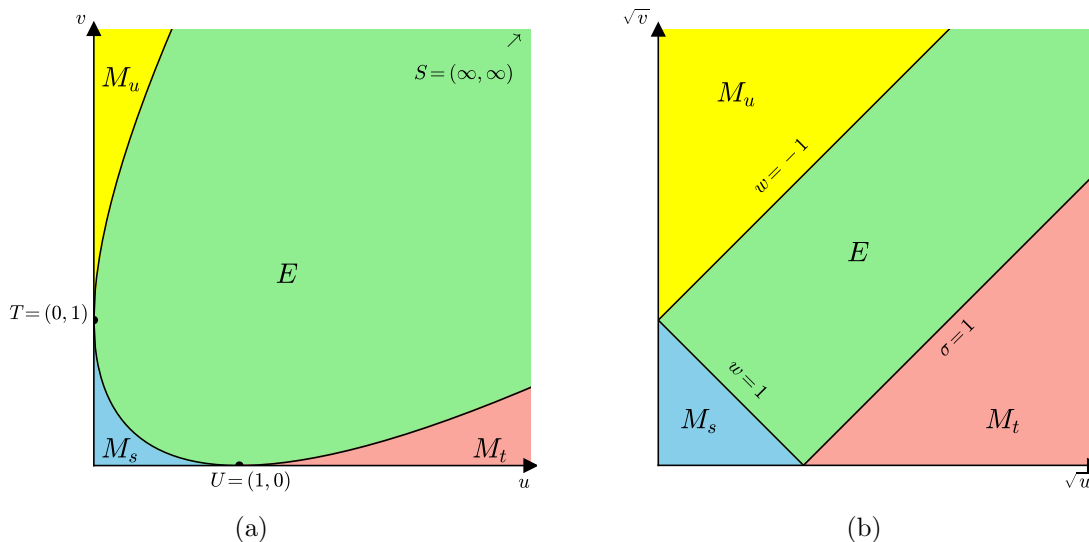


Figure 2.1: Euclidean region E (green) and three Lorentzian extensions, M_s , M_u , M_t , Fig. 2.1(a). S , T and U are three Euclidean OPE points. In Fig. 2.1(b), straight line segments separating these regions, labelled by variables (w, σ) .

It is also important to note that Euclidean CFT scalar amplitudes, e.g., $\mathcal{G}(u, v)$, can be expressed in terms of OPE expansions in region E . There are three options, associated with s -, t - and u -channels, leading to three scalar amplitudes, $\mathcal{G}^{(s)}$, $\mathcal{G}^{(t)}$ and $\mathcal{G}^{(u)}$. They are simply related by kinematic factors, which are singular at $u, v = 0, \infty$. These expansions can be associated with Euclidean OPE points, labelled as S , T and U in Fig. 2.1(a).

Natural Lorentzian Extension of Euclidean CFT: It is natural to first extend a scalar CFT amplitude, e.g., $\mathcal{G}^{(t)}(u, v)$, from region E to cover the whole first quadrant of the \sqrt{u} - \sqrt{v} plane, i.e., extending into regions M_s, M_u, M_t by analytic continuation *without* crossing the expected singularities at $u, v = 0$, (and also at $+\infty$). However, to keep $x_{ij}^2 > 0$, i.e., all points spacelike separated, it necessitates a Wick rotation so that $x^2 = x^\mu x_\mu = \eta^{\mu\nu} x_\mu x_\nu$, defined with *Lorentzian signature*, $\text{dia } \eta = (-, +, \dots, +)$. In this extension, we have

$$\sqrt{u} = \frac{\sqrt{x_{12}^2} \sqrt{x_{34}^2}}{\sqrt{x_{13}^2} \sqrt{x_{24}^2}} \quad \text{and} \quad \sqrt{v} = \frac{\sqrt{x_{23}^2} \sqrt{x_{14}^2}}{\sqrt{x_{13}^2} \sqrt{x_{24}^2}}, \quad (2.1)$$

defined with positive square roots. The first quadrant of u - v plane is in 1-to-1 correspondence with that for the \sqrt{u} - \sqrt{v} plane.

From a group theoretic perspective, moving away from region E corresponds to a shift from $SO(d+1, 1)$ to $SO(d, 2)$. However, regions M_s, M_u, M_t do not correspond to *causal scattering regions* since all points remain space-like separated. We will loosely refer to them as **Minkowski non-causal scattering regions**. In particular, with $0 < \sqrt{u}, \sqrt{v} < \infty$, region M_s is bounded, with $0 < \sqrt{u} + \sqrt{v} < 1$, with M_u and M_t unbounded.

In place of (u, v) , it is often convenient to treat Euclidean four-point functions, e.g., $\mathcal{G}^{(t)}(u, v)$, in terms of other equivalent variables. The most often used is a pair (z, \bar{z}) where $u = z\bar{z}$ and $v = (1-z)(1-\bar{z})$, with $z^* = \bar{z}$ in the Euclidean region E . To continue outside of the Euclidean region, it is necessary to treat z and \bar{z} as independent complex variables, with $\mathcal{G}^{(t)}(u, v)$ having singularities at z or $\bar{z} = 0, 1$. To reach M_s, M_u, M_t , one needs to approach the limit z and \bar{z} on the real axis, $-\infty < z, \bar{z} < \infty$. There are many possible paths, so long as they stay on the “physical sheet” by not crossing the singular lines at $u, v = 0$ or at $+\infty$. (See Appendix B for the notion of “first sheet” or “physical sheet”, and also for the equivalence among various sets of variables, e.g., (\sqrt{u}, \sqrt{v}) , (z, \bar{z}) , $(\rho, \bar{\rho})$ and (q, \bar{q}) .)

In our approach, we will stay on the slice where \sqrt{u} and \sqrt{v} are real. This slice can be described by a set of group theoretic motivated variables, (w, σ) . Transitions from E to regions M_s, M_u, M_t are smooth and can be understood in terms of Wick rotations. This also fixes our convention in specifying our causal regions, (1.2) and (1.3).

Causal Scattering Regions: To reach *causal scattering regions*, it is necessary to cross singularities at $\sqrt{u} = 0$ and/or $\sqrt{v} = 0$, (or at $+\infty$), thus extending from the first quadrant to the whole \sqrt{u} - \sqrt{v} plane, Fig. 2.2. Consider s-channel causal scattering, (1.1), subject to causal constraint (1.2). With both x_{14} and x_{23} timelike, (i.e., both $\sqrt{x_{14}^2}$ and $\sqrt{x_{23}^2}$ purely imaginary with same signs), it leads to $\sqrt{u} > 0$ and $\sqrt{v} < 0$, i.e., the fourth quadrant in the \sqrt{u} - \sqrt{v} plane. Let us focus on the bounded region, $0 < \sqrt{u} + |\sqrt{v}| < 1$ in the fourth quadrant, (shaded blue in Fig. 2.2 and will be designated as $M_s^{(t)}$ in what follows). This region is bounded by three

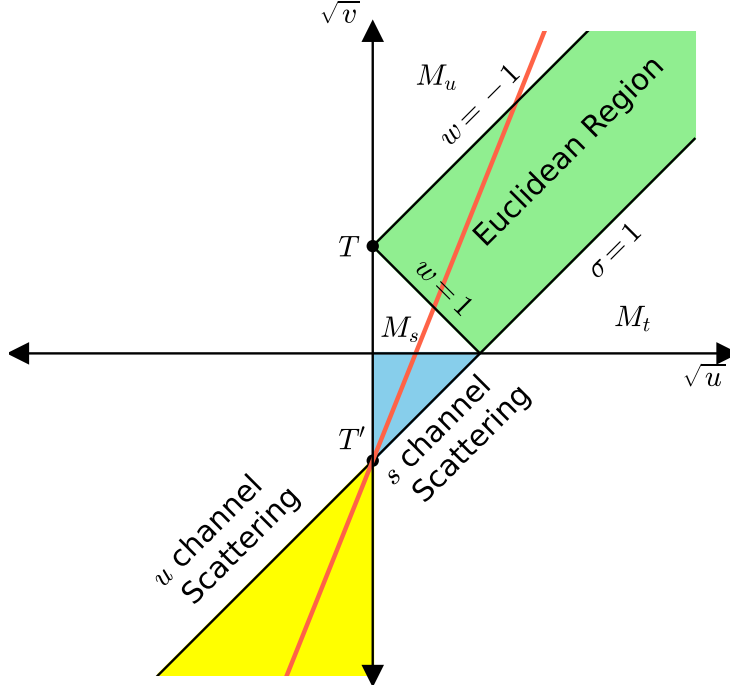


Figure 2.2: Extension into \sqrt{u} - \sqrt{v} plane, with s - and u -channel causal scattering regions shown, shaded blue and yellow respectively.

line segments. Of particular interest is the segment L_s : $0 < \sqrt{u} < 1$, $\sqrt{v} = 0$, which separates it from the non-causal region, M_s .

It can be shown that this region corresponds to where the causal condition (1.2) holds. This can best be carried out in a generalized antipodal frame. (See Secs. 2.2 and 2.3. The superscript for $M_s^{(t)}$ will also be explained shortly.) Region $M_s^{(t)}$ will be referred to as the s -channel causal region, with M_s as the s -channel non-causal region.

Similarly, the u -channel causal region, specified by (1.3), corresponds to having $\sqrt{u} < 0$ and $\sqrt{v} < 0$, i.e., in the third quadrant, with $1 < |\sqrt{v}| - |\sqrt{u}| < \infty$. This region will be designated as $M_u^{(t)}$, (shaded yellow region in Fig. 2.2). The corresponding line segment L_u separating it from non-causal region M_u is less explicit in Fig. 2.2. It corresponds to the limit $\sqrt{u}, \sqrt{v} \rightarrow \pm\infty$, with $\sqrt{v}/\sqrt{u} > 1$. (Line segments L_s and L_u can be better described in terms of group theoretic variables (w, σ) to be introduced below. They are shown symmetrically in Fig. 2.3. In particular, our group theoretic approach maintains s - u symmetry.) The straight-line (colored red) in Fig. 2.2 corresponds to $\sqrt{v} = -1 + \sigma\sqrt{u}$, with a fixed slope, $1 < \sigma < \infty$, (in Fig. 2.3, the corresponding line is identified).

The corresponding region $M_t^{(t)}$ for causal t -channel scattering lies in the second quadrant, (not shown in Fig. 2.2 but can be read off Fig. 6.2 in Sec. 6). It can be better understood

intuitively in a “direct-channel picture”. It can also be treated in terms of group theoretic variables (w, σ) . However, since it does not directly lead to a principal series representation, we will not deal directly with this region in what follows.

Minkowski OPE: In analogy with Euclidean OPE, it is equally meaningful to introduce OPE for Minkowski scattering [3–15, 20]. We will return to this in Sec. 6. Here we simply mention the fact that the antipodal frame adopted here can be associated with Minkowski t -channel OPE [20], thus the superscript for $M_s^{(t)}$, $M_u^{(t)}$ and $M_t^{(t)}$. Regions $M_s^{(t)}$, $M_u^{(t)}$ can also be identified with Minkowski t -channel OPE point, $T' = (0, -1)$, which is conjugate to the Euclidean point $T = (0, 1)$, as indicated in Fig. 2.2. More importantly, for causal scatterings, Minkowski OPE’s can in turn be associated with Regge limits for CFT [3–15, 20].

2.2 Group Theoretic Motivated Variables

In this subsection, we introduce a set of variables, (w, σ) , in terms of which causal regions can be identified more clearly, together with the transition lines L_s and L_u .

Instead of $\sqrt{u}-\sqrt{v}$, let us define a new set of variables

$$w \equiv \frac{1 - \sqrt{v}}{\sqrt{u}}, \quad \sigma \equiv \frac{1 + \sqrt{v}}{\sqrt{u}} \quad \Leftrightarrow \quad \sqrt{u} = \frac{2}{\sigma + w}, \quad \sqrt{v} = \frac{\sigma - w}{\sigma + w}. \quad (2.2)$$

Since (w, σ) is given in terms of (\sqrt{u}, \sqrt{v}) , they provide a natural extension into the whole $\sqrt{u}-\sqrt{v}$ plane. The map is 1-to-1, as can be seen as follows. From $\sqrt{v} = -1 + \sigma\sqrt{u}$, straight lines through T' with slope $-\infty < \sigma < \infty$ cover the entire $\sqrt{u}-\sqrt{v}$ plane. It is also easy to verify that the range for each line covers $-\infty < w < \infty$. In Fig. 2.2, such a line with $1 < \sigma < \infty$ is shown. Correspondingly, this line with $\sigma > 1$ is shown in Fig. 2.3. We emphasize the important fact that s - u crossing, $(u, v) \leftrightarrow (u/v, 1/v)$, corresponds to $(w, \sigma) \leftrightarrow (-w, \sigma)$. (In Ref. [20], this was discussed via another set of variables, $w' = \sqrt{q\bar{q}}$ and $\sigma' = (\sqrt{q/\bar{q}} + \sqrt{\bar{q}/q})$. For practical purpose, $(w', \sigma') \simeq (w, \sigma)$. Of course, manifest crossing symmetry proves useful for discussing dispersion relations and inversion. A related discussion for $d = 1$ is presented in [60].)

These variables can be understood intuitively in a generalized antipodal frame and they help to pave the way for group theoretic analysis in sections to come.

Regions E, M_s, M_u, M_t : These regions now correspond to $E : (-1 < w < 1, 1 < \sigma < \infty)$, $M_s : (1 < w < \infty, 1 < \sigma < w)$, $M_u : (-\infty < w < -1, 1 < \sigma < |w|)$ and $M_t : (-1 < w < 1, 0 < \sigma < |w|)$, shown in Fig. 2.3), with line segments L_s and L_u simply labelled. Note also that, the Euclidean t -channel OPE point, $T = (\sqrt{u}, \sqrt{v}) = (0, 1)$, has moved to $\sigma = +\infty$, with $w/\sigma \rightarrow 0$. It can be reached from regions E , M_s and M_u .

best be interpreted by adopting the **Euclidean Antipodal Frame** where [61,62]

$$-1 \leq w = \cos \theta \leq 1 \quad \text{and} \quad 1 < \sigma = \cosh \tau < \infty. \quad (2.4)$$

(In fact, this is nothing but the equivalent of ‘‘CM frame’’, i.e., $x_1 = -x_2$ and $x_3 = -x_4$.)

For non-causal regions M_s, M_u as well as for causal regions $M_s^{(t)}, M_u^{(t)}$, we adopt **Minkowski Antipodal frame**, (also known as the **double-lightcone** frame in Ref. [20]), where, for the light-cone components, $x_1^\pm = -x_2^\pm$ and $x_3^\pm = -x_4^\pm$, and, for transverse components, $x_{\perp,1} = x_{\perp,2}$ and $x_{\perp,3} = x_{\perp,4}$. It follows that (w, σ) can be parametrized by

$$1 < |w| = \cosh y < \infty \quad \text{and} \quad 1 < \sigma = \cosh \eta < \infty. \quad (2.5)$$

(See Appendix B.2 and Ref. [20].) We shall show in Sec. 3 how to attach group theoretic interpretations for all these regions.

2.3 Wick Rotation and Causal Scattering vs Non-Causal Regions

In this subsection, we provide further clarification on how causal regions can be reached from Euclidean region: first by Wick rotation, continuing from $SO(d+1,1)$ to $SO(d,2)$, and next by crossing singular lines L_s or L_u .

Comparing (2.4) with (2.5), the transition from $|w| < 1$ to $1 < |w|$ can be interpreted as a **Wick rotation**. That is, by substituting $\theta \rightarrow iy$ or $\theta \rightarrow \pi + iy$, one moves from $0 \leq |w| \leq 1$ to $1 < |w|$. Group theoretically, this corresponds to a formal continuation from $SO(d+1,1)$ to $SO(d,2)$. Kinematically, one moves from E to M_s or M_u initially.

However, various Wick rotations take on different interpretations in different frames. Consider first transitions from E to M_s or M_u . Immediately after a Wick rotation, by crossing $|w| = 1$, region E is smoothly connected to the region $1 < |w| < \sigma < \infty$, i.e., non-causal regions M_s and M_u . Next, by subsequently crossing $|w| = \sigma$, it is possible to move to $1 < \sigma < |w| < \infty$, the causal scattering regions $M_s^{(t)}$ and $M_u^{(t)}$, i.e., crossing line segments L_s or L_u . These are singular lines.

Consider $\theta \rightarrow iy$ first. In the Minkowski antipodal frame, a quick check, using Eqs. (B.6) and (B.7), establishes that

$$x_{14}^2 = x_{23}^2 = \sigma - w = \cosh \eta - \cosh y, \quad (2.6)$$

with all other x_{ij}^2 spacelike. The Minkowski non-scattering region M_s corresponds to $x_{14}^2 = x_{23}^2 > 0$, leading to $0 < y < \eta < \infty$, consistent with $0 < \sqrt{u}$, $0 < \sqrt{v}$ and $0 < \sqrt{u} + \sqrt{v} < 1$, i.e., remaining in the 1st quadrant.

Since the line segment L_s corresponds to $w = \sigma$, crossing L_s enters the causal region $M_s^{(t)}$. With $\sigma < w$, i.e., $\cosh \eta < \cosh y$, the causal condition is achieved with $x_{14}^2 = x_{23}^2 < 0$. The **causality constraint** can also be expressed as

$$0 < \eta < y < \infty. \quad (2.7)$$

Consider next $\theta \rightarrow \pi + iy$. A similar analysis also follows for the u-channel causal region, e.g., with $w = \cosh(y - i\pi) = -\cosh y < 0$,

$$x_{13}^2 = x_{24}^2 = \sigma + w = \cosh \eta - \cosh y, \quad (2.8)$$

all other x_{ij}^2 spacelike, and consistent with the u-channel causal constraint when (2.3) is imposed. Moving into u-channel causal region $M_u^{(t)}$ corresponds to crossing the line segment L_u , leading again to causal constraint, (2.3).

The most significant fact here is the presence of two unbounded parameters, y and η as well as the causal restriction, (2.7). As emphasized in [20], variables y and η are nothing but group parameters characterizing boosts and dilations in the context of $SO(d, 2)$. (See Secs. 3 and 4.) We will also show in Sec. 3 that the causal restriction, (2.7), interpreted group theoretically, leads to the structure of a “semi-group”.

Before leaving this section, we point out that transition from region E to M_t can be interpreted via a double Wick rotations, or a “twisted” $SO(d, 2)$, i.e., moving from $0 < |w| < 1$ and $1 < \sigma < \infty$ to $0 < |w| < 1$ and $|w| < \sigma < 1$, with both w and σ “compact”. (This can better understood in an embedding space treatment.) The transition from M_t to $M_t^{(t)}$ can be accomplished by changing the sign of σ . (Equivalently, $\sqrt{u} \rightarrow \sqrt{u'} = -\sqrt{u}/\sqrt{v}$, $\sqrt{v} \rightarrow \sqrt{v'} = -1/\sqrt{v}$.) This can again be carried out via a more involved Wick rotations. We will not follow up on these possibilities here since it does not lead to the principal series representation for $SO(d, 2)$.

We also note that the relation between the invariant Euclidean four-point functions, $\mathcal{G}(u, v)$ and our Minkowski discontinuity functions, $\text{Im } T$, has traditionally been discussed via analytic continuation, e.g., via (z, \bar{z}) . In [1], an important identification between $\text{Im } T$ and a “double discontinuity”, $\text{dDisc}G$, was made. This relation is briefly reviewed in Appendix B.4 in connection with crossing line segments L_s and L_u and illustrated by the Ising and generalized mean-field models. In the following sections, we focus mostly on the causal regions where Minkowski discontinuity functions, $\text{Im } T$, are defined. We will return to this issue in Sec. 6 and also in [52]. In this paper, we will focus mostly on the kinematic aspect of this transition.

3 Four-point Functions, H -bi-Invariance, and Semigroups

In this section, we begin the effort to understand CFT scattering in the context of group functions. In Sec. 2, we, in essence, described the left hand side of Eq. (1.6) as functions over

conformal invariants, e.g., by adopting the antipodal frame, the Minkowski analog to the setup for radial quantization in the Euclidean setting. Describing the right hand side of Eq. (1.6), requires an understanding on the class of group functions that can be associated with causal fourpoint functions. In other words, does understanding the group theory associated with the right hand side of Eq. (1.6) naturally lead to the condition in Eq. (2.7)?

This is answered in several steps. Our key results for this section can be stated as follows:

1. An invariant fourpoint scalar amplitude, after lifting to embedding space, can be treated as a group function, $F(g)$, over $G = SO(d, 2)$. A reduction to cross ratios can be identified group theoretically as “ H -bi-Invariance”, $F(hgh') = F(g)$, with an appropriate subgroup $H \subset SO(d, 2)$. This subgroup can be found as the isometry of certain basepoints in the embedding space. (Not surprisingly, it is directly related to that identified by Mack [40] in his discussion on Minkowski space-time symmetry.) We prove this through a formal reduction using a particular coordinate realization appropriate for Minkowski t -channel OPE, and also just by counting that showcase that the number of degrees of freedom after imposing H -bi-invariance is 2, for general dimensions, $d \geq 2$.
2. Causality in this context can be intuitively understood in terms of lightcones that can group theoretically be identified with “semigroups”, $S \subset SO(d, 2)$, a proper subset. We show that this semigroup admits a Cartan-like decomposition HA_+H , with the restriction to A_+ given precisely by Eq. (2.7). That is, our causal condition can be understood as semigroup restrictions due to causality. Ultimately, in studying Eq. (1.6), we want to construct representation functions over this semigroup.

We begin by a short review of embedding space. The answer to the first part listed above will be dealt with in Secs. 3.2 and 3.3. The second will be discussed in Sec. 3.4.

3.1 Embedding Space

In this subsection, we review an embedding space approach to CFT. This involves a projection via a null-cone and a particular choice of a “parabolic slice” with its associated basepoint, ξ_0 . We also briefly discuss the notion of cosets and group decomposition, e.g., Eq. (3.14).

Following the same procedure as done for $SO(d + 1, 1)$, e.g., Ref. [39], we again introduce $(d + 2)$ -dimensional embedding space, $\xi = (X_{-2}, X_{-1}; X_0, \dots, X_{d-1})$, which provides a linear realization for $SO(d, 2)$. The group leaves quadratic form $B(\xi, \xi) = \xi^T \eta \xi = -X_{-2}^2 + X_{-1}^2 - X_0^2 + X_{d-1}^2 + X_{b_\perp}^2$ invariant, where η is a diagonal metric with two time-like directions, $\text{diag } \eta = (-1, 1; -1, 1, \dots, 1)$. Note that we have adopted a particular partition by separating (X_{-2}, X_{-1}) from (X_0, X_{d-1}) , (that leading to lightcone), and $X_{b_\perp} = (X_1, X_2, \dots, X_{d-2})$, with X_{b_\perp} standing

for the $(d-2)$ -dimensional transverse coordinates.

Null-Cone and Physical Slice: Now we consider a restriction to the conic section of a null sub-manifold,

$$B(\xi, \xi) = 0, \quad (3.1)$$

which allows a projective identification with the Minkowski space, i.e.,

$$x_\mu = \frac{X_\mu}{X_{-2} + X_{-1}}, \quad (3.2)$$

for $\mu = 0, 1, 2, \dots, d-1$. In particular, under a “boost” (dilatation)⁶ where $(X_{-2} + X_{-1})$ changes by a scale, λ^{-1} , while leaving X_μ unchanged, it leads to scaling in physical coordinates, $x_\mu \rightarrow \lambda x_\mu$. This reduces the $(d+2)$ -dimensional embedding manifold down to d -dimensional spacetime. Further, we also have that: $x^2 = (X_{-2} - X_{-1})/(X_{-2} + X_{-1})$. Note also, by scaling all embedding coordinates uniformly by a factor, i.e., $\xi \rightarrow a\xi, \forall a > 0$, it leads to the same point on the physical spacetime manifold. (This is a classic property of projective spaces.) Therefore, we can choose to set $X_{-2} + X_{-1} = 1$ leading to a parametrization of the null cone given by:

$$\xi = \left(\frac{1+x^2}{2}, \frac{1-x^2}{2}; x_\mu \right). \quad (3.3)$$

This can be identified as a parabolic “slice” (section) of the null cone containing the “basepoint” $\xi_0 = (1/2, 1/2; 0, 0, \dots)$ ⁷. In the embedding space, we have that:

$$\xi_a \cdot \xi_b = \left(\frac{1+x_a^2}{2}, \frac{1-x_a^2}{2}; x_{a,\mu} \right) \cdot \left(\frac{1+x_b^2}{2}, \frac{1-x_b^2}{2}; x_{b,\mu} \right) \quad (3.4)$$

$$= -\frac{1}{2}|x_a - x_b|^2. \quad (3.5)$$

The basepoint ξ_0 , up to a scale, corresponds to the coordinate origin in the physical space, $x_\mu = 0$. It can play a special role in providing intuition for introducing *causality*, e.g., via the notion of a forward lightcone. For our purposes, it is also useful to consider different basepoints, e.g., Eq. (3.7), which correspond to adopting different slices in CFT applications. We will return to this in the next section.

Coset Spaces and Group Decompositions: In standard field theory, the identification of the Lorentz invariant spacetime manifold $R^{1,3}$ is done through the Poincaré group via a

⁶We use the term “boost” as a catch all phrase for hyperbolic rotations, and “rotations” will refer to all circular rotations. For example, a boost in (X_{-2}, X_{-1}) direction is physically associated with a dilatation whereas a boost in (X_0, X_3) direction is a Lorentz boost.

⁷This parabola is seen when we go to the “lightcone” in (X_{-2}, X_{-1}) , that is, $(X_{-2} + X_{-1}, X_{-2} - X_{-1}; X_\mu) = (1, x^2; x_\mu)$. This is a *maximal* parabola in the sense that x^2 involves all remaining free parameters.

semidirect product. In the conformal group $SO(d, 2)$, this identification can best be carried out in the so-called Gauss decomposition $G = Q_0^+ H_0 Q_0^-$. That is, a separation into translations, Q_0^+ , Lorentz group plus dilatation, H_0 , and special conformal transformations, Q_0^- . The spacetime manifold is then identified as a coset $G/H_0 Q_0^-$ ⁸.

The subgroup $H_0 Q_0^-$ is the isometry group of a basepoint $\xi_0 = \{1, 1; 0, 0, \dots\}$, which corresponds to $x_\mu = 0$ in physical space-time. Treating H_0 and Q_0^- separately can be cast in the language of symmetric spaces where we divide the algebra into three parts ($\mathcal{Q}_0^+, \mathcal{H}_0, \mathcal{Q}_0^-$) by their spectrum $(+1, 0, -1)$, relative to the generator of dilatations D by commutators. (See Appendix D for details.) For $d = 2$, \mathcal{H}_0 is particularly simple, consisting of a pair of commuting generators, Eq. (D.17). For $d = 4$, \mathcal{H}_0 is given by Eq. (D.18).

In Section 4, we will introduce another decomposition, the Iwasawa decomposition, which is important in defining unitary irreducible representations for semi-simple groups. Here, we will consider instead a generalization of a group decomposition by Euler angles, familiar in the case of compact groups, e.g., $SO(3)$.

In most standard mathematical literature on semi-simple Lie groups [63], one starts with a decomposition for its Lie algebra, $\mathcal{G} = \mathcal{K} \oplus \mathcal{P}$, with \mathcal{K} for the generators of the maximal compact subgroup and \mathcal{P} for the non-compact generators⁹. These follow the commutation relations

$$[\mathcal{K}, \mathcal{K}] \subset \mathcal{K}; \quad [\mathcal{K}, \mathcal{P}] \subset \mathcal{P}; \quad [\mathcal{P}, \mathcal{P}] \subset \mathcal{K}. \quad (3.6)$$

Using these commutators, one can show that all group elements carry the decomposition $G = KAK$, where K is the group associated with \mathcal{K} and A is a maximal abelian subgroup in \mathcal{P} , which is associated with \mathcal{P} . This group decomposition can be considered as a generalization of decomposition by Euler angles for compact groups, and will also be referred to as ‘‘Cartan decomposition’’. The key idea is that all elements of \mathcal{P} can be generated by conjugating elements of A with a rotation. That is, $p = kak^{-1}$.

This can be further generalized for all symmetric spaces. In particular, we can again consider the decomposition $\mathcal{G} = \mathcal{H}_0 \oplus \mathcal{Q}_0$, where $\mathcal{Q}_0 = \mathcal{Q}_0^+ + \mathcal{Q}_0^-$, and follow similar commutation relations as Eq. (3.6), with $\mathcal{K} \rightarrow \mathcal{H}_0$ and $\mathcal{P} \rightarrow \mathcal{Q}_0$. This can be formalized by introducing an involution, (see Appendix D). Under such an involution, all group elements carry a decomposition of the form $G = H_0 A_0 H_0$, i.e., Cartan-like decomposition. These types of generalized decompositions will play an important role in our harmonic analysis leading to zonal spherical functions.

⁸This identification is also emphasized by Mack in [40]. Our $H_0 Q_0^-$ is what he calls H .

⁹See Appendix C. This is also known as Cartan’s Theorem and this decomposition is also referred to as ‘‘Cartan decomposition’’ for the Lie algebra. This is not to be confused with the usage of ‘‘Cartan-like’’ decomposition for the Lie group to be introduced below.

3.2 Embedding Space Realization of Antipodal Frame

After lifting a fourpoint function to a group function, we show in this subsection that it can be reduced to a function of a single group element, $F(g)$, via the antipodal frame. This in turn leads to a function of two variables, which can be identified with cross ratios. To simplify the discussion, we consider the case $d = 2$ first.

We can lift a fourpoint function from coordinate space to the embedding space, $f(x_i) \rightarrow F(\xi_i)$, where it offers a linear realization of the conformal group. Here, the four points are represented by lines on a null cone. In this lifting, the cross ratios are defined via inner products (or angles) between the four lines and are independent of the length scale. It is interesting to note that, from the perspective of group actions, the amplitude becomes a function over 4 copies of $SO(d, 2)$. Traditionally, using conformal symmetry to fix three points, it can be reduced to a function over a single copy of $SO(d, 2)$. We will adopt a slightly different procedure by moving the four points in a *coordinated* manner by going to the *center-of-mass (COM) frame* of the system along double-lightcones. This is the generalized antipodal frame discussed in Sec. 2.

In an embedding space approach, an antipodal frame can be introduced by identifying two special basepoints ξ_a and ξ_b . These basepoints can be reached directly from the standard basepoint ξ_0 mentioned in Sec. 3.1, by conformal transformations. To be precise, the basepoints in Eq. (3.7) can be reached from ξ_0 by rotation of $\pm\pi/2$ in the (X_{-1}, X_{d-1}) plane. (This also turns out to be important for our causal consideration in Sec. 3.4.) We demonstrate below that this leads to the amplitude as a function over a single copy of the *maximal abelian subgroup* (MASG), A , i.e., a function of group parameters y and η . This choice of maximal abelian subgroup generated by Lorentz boost L and dilatation D is a physical choice we shall explain shortly.

To simplify the discussion, we shall stay with $d = 2$. Consider two special basepoints:

$$\xi_a = \{1, 0; 0, 1\}, \quad \text{and} \quad \xi_b = \{1, 0; 0, -1\}. \quad (3.7)$$

In physical coordinates, (t, z) , they correspond to $x_a = (0, 1)$ and $x_b = (0, -1)$ respectively. The action of group elements $a_{\text{left}}, a_{\text{right}} \in A$, generated by the maximal abelian subalgebra identified in Sec. 4, $\mathcal{A} = \{L, D\}$, leads the antipodal configuration where we identify:

$$\xi_1 = a_{\text{left}} \cdot \xi_b; \quad \xi_2 = a_{\text{left}} \cdot \xi_a; \quad \xi_3 = a_{\text{right}} \cdot \xi_a; \quad \xi_4 = a_{\text{right}} \cdot \xi_b. \quad (3.8)$$

To be precise, $a_{\text{left}} = a_L(y_l)a_D(\eta_l)$ consists of a Lorentz boost and a scale transformation, and similarly for $a_{\text{right}}(y_r, \eta_r)$. This parametrization connects directly with that discussed in Sec. 2 and given by Eq. (B.6). Given ξ_a , the second point ξ_b is also fixed by our choice of antipodal frame. In what follows, when speak of ξ_a , the point ξ_b is implied.

The fourpoint function is a scalar physical quantity and is invariant under a global conformal transformation. That is: $F(\xi_1, \xi_2, \xi_3, \xi_4) = F(g \cdot \xi_1, g \cdot \xi_2, g \cdot \xi_3, g \cdot \xi_4)$. If we choose $g = a_{\text{right}}^{-1}$, this function reduces to a function of a single group element such that $= F(a(y, \eta)\xi_a, a(y, \eta)\xi_b, \xi_a, \xi_b)$, where $a(y, \eta) = a_{\text{right}}^{-1} a_{\text{left}} \in A$ with $y = y_l - y_r$ and $\eta = \eta_l - \eta_r$. That is, it is a function over a single copy of A only, $F(\xi_i) \rightarrow F(a(y, \eta))$, and therefore reduces to a function of just 2 variables. An equivalent identification of this reduction to two variables is through cross ratios. By evaluating Eq. (2.1) in embedding space using Eq. (3.4), one arrives at

$$\sqrt{u} = \frac{2}{(\cosh \eta + \cosh y)}; \quad \sqrt{v} = \frac{(\cosh \eta - \cosh y)}{(\cosh \eta + \cosh y)}, \quad (3.9)$$

justifying the earlier claim with (w, σ) , (2.2), as group theoretic motivated variables. In this view, cross ratios are a simple change of variables. This however covers only a small subset of possible fourpoint configurations. The challenge then is to show that any generic configuration can always be reduced to the one discussed here. We showcase how this can be done next.

3.3 H -bi-Invariance

In this subsection, by identifying H as an isometry of basepoints ξ_a and ξ_b , we demonstrate the reduction to two independent cross ratios follows from H bi-invariance. We also demonstrate that this reduction holds for general d .

The analysis of Sec. 3.2 amounts to the demonstration that reducing a fourpoint function to that of conformal cross ratios is equivalent to reducing a group function to that over the MASG, A . More general fourpoint configurations can be considered by extending the lifting process via $a_{\text{left, right}}$ to elements over the full group $g_{\text{left, right}}$. These configurations can be reached by starting with basepoints (3.7), i.e.,

$$\xi_1 = g_{\text{left}} \cdot \xi_b; \quad \xi_2 = g_{\text{left}} \cdot \xi_a; \quad \xi_3 = g_{\text{right}} \cdot \xi_a; \quad \xi_4 = g_{\text{right}} \cdot \xi_b; \quad (3.10)$$

where $g_{\text{left}}, g_{\text{right}}$ can be any element G . This again leads to a reduction of a fourpoint amplitude to a function of a single copy of $SO(d, 2)$, $F(g)$, with $g = g_{\text{right}}^{-1} g_{\text{left}}$. Incidentally, we note that this also removes the restriction for $d = 2$. We shall make further comments on $d > 2$ in Sec. 5.5.

As was discussed in Sec. 3.1, g can always be expanded in a Cartan-like decomposition, $g = hah'$, $h, h' \in H$. By choosing the subgroup H as isometries of the basepoints, we can show that $F(g)$ is invariant when left- and right-conjugated, i.e.,

$$F(hgh') = F(g). \quad (3.11)$$

(See discussion leading to Eq. (D.17) and also the following subsection.) Functions with this property are called H -bi-invariant. It follows, for this class of functions,

$$F(g) = F(hah') = F(a). \quad (3.12)$$

Let us provide an explicit demonstration, we note that we can decompose the group elements as $g_{\text{left}} = h_l a_{\text{left}} h_l'$ and $g_{\text{right}} = h_r a_{\text{right}} h_r'$. It follows from the reduction to $g = g_{\text{right}}^{-1} g_{\text{left}}$ described above that

$$F(g) = F(hah' \cdot \xi_b, hah' \cdot \xi_a, \xi_a, \xi_b) = F(ha \cdot \xi_b, ha \cdot \xi_a, \xi_a, \xi_b) \quad (3.13)$$

where we have used the H -invariance property of $\xi_{a,b}$. That is, under a shift by $h \in H$, the basepoints ξ_a, ξ_b remain fixed upto an overall scaling. However, in the embedding space, since the cross ratios are given by $u = (\xi_1 \cdot \xi_2 \xi_3 \cdot \xi_4) / (\xi_1 \cdot \xi_3 \xi_2 \cdot \xi_4)$ and $v = (\xi_1 \cdot \xi_4 \xi_2 \cdot \xi_3) / (\xi_1 \cdot \xi_3 \xi_2 \cdot \xi_4)$, the scaling drops out, making them invariant under shifts by h . A final global shift by h^{-1} of this function, i.e., $F(g) \rightarrow F(h^{-1}g)$, proves the H -bi-invariance property of the fourpoint function, Eq. (3.12).

Stated differently, a scalar fourpoint amplitude reducing to a function of conformal invariant cross ratios, e.g., (u, v) , can be identified with a function of a single copy of G which is H -bi-invariant, which also reduces to be a function of the MASG, A . The subgroup A is parametrized by 2 variables which are related directly to cross ratios by Eq. (3.9).

One might wonder if the H -bi-invariance discussion makes sense from a purely counting perspective. That is, is requiring H -bi-invariance sufficient to restrict us to a function of two variables for general d ? It is instructive to consider this purely in terms of reduction of variables without requiring additional constraints.

After reducing to a single copy of the group, the fourpoint function, as a group function, is a function of $(d+2)(d+1)/2$ independent variables. The subgroup H has $d(d-1)/2 + 1$ independent generators. Note that H is conjugate to H_0 by a discrete rotation, with H_0 made up of the Lorentz group and dilatations (see App. D). However, there is a $(d-2)(d-3)/2$ dimensional subgroup of rotations $R \in H$ that commutes with our MASG A . Therefore, in the group decomposition

$$G = H_1 A H_2, \quad (3.14)$$

we can commute those rotations through A . Imposing H -bi-invariance therefore has $(d-2)(d-3)/2$ fewer constraints. That is, total number of independent variables after imposing H -bi-invariance is:

$$\frac{(d+2)(d+1)}{2} - \left(\frac{d(d-1)+2}{2} + \frac{d(d-1)+2}{2} - \frac{(d-2)(d-3)}{2} \right) = 2. \quad (3.15)$$

This is the expected reduction of variables to 2 cross ratios. This counting applies to both the Euclidean and Minkowski settings.

Our discussion of H -bi-invariance is in contrast with possible utility of the traditional Cartan decomposition $G = KAK$, that might be more familiar from standard mathematical literatures. With $g = hah' = ka'k'$, one finds

$$f(g) = f(hah') = f(a) = f(ka'k') \neq f(a'). \quad (3.16)$$

This showcases an important feature of our discussion. Although both representations are allowed, i.e., $f(g) = f(ka'k') = f(hah') = f(a)$, only the element $a \in A$ parametrizes the cross ratios. Since $a' \neq a$ in general, the cross ratios are still functions of k, a', k' .

For Euclidean signature $SO(d+1,1)$, K -bi-invariant functions reduce to a function of a single variable. Although four-point functions are not K -bi-invariant in the CFT setting, a class of functions that are K -bi-invariant do feature prominently in AdS/CFT studies under other contexts. An example of particular relevance here is that of Euclidean $\text{AdS}_{d+1}^E = SO(d+1,1)/SO(d+1)$. Geometrically, this is identified with the two sheeted hyperboloid H_{d+1} and can be studied using various familiar models of hyperbolic geometry such as the upper half plane or the Poincaré disk. True AdS, however, still requires a non-compact H by definition.

3.4 Causal Semigroups

In this subsection, we turn to causal constraints, leading to a restricted subset S of G , which forms a semigroup. The semigroup can be characterized by Eq. (3.17) below, which also connects with earlier independent discussion in Sec. 2.3.

As stressed in the Introduction, a key difference between Minkowski and Euclidean CFT involves causal constraints. In Sec. 2, in terms of variables $\{w, \sigma\}$, we have identified kinematically causal scattering regions where Eqs. (1.2) or (1.3) hold, leading to (2.3). From a group theoretic perspective, in an embedding-space treatment, understanding these constraints leads to new elements: *causal symmetric spaces* [41] and *semigroups* [42–44]. A thorough discussion on causal symmetric spaces is beyond the scope of this study. A summary is provided in Appendix D. Instead, we present below various new ideas intuitively, leading to the emergence of a causal semigroup.

Starting with an appropriately chosen basepoint, we have demonstrated that a CFT fourpoint functions can be lifted to be a group function, $F(g)$, with $g \in G = SO(d,2)$. By adopting an antipodal frame, one can move to cover different regions in the cross ratio space, expressed in terms of $\{w, \sigma\}$, as illustrated in Sec. 2. Our choice of basepoints, ξ_a and ξ_b , Eq. (3.7), corresponds to starting from $(0,1)$ and $(0,-1)$ in physical space for (t,z) . A group action can move these points in physical space, for example the moving coordinates in the lightcone diagram, Figs. 1.1 and B.1. We are interested in using the group action to move in different regions in Fig. 2.3, starting with $w = \sigma = 1$. We are interested in finding restriction on group parameters which map within the causal region.

As demonstrated earlier, conformal invariance is now realized as H bi-invariance, i.e., it is a function of a MASG, A . Clearly, a minimal requirement for mapping within the causal region

is the restriction to a subset of MASG, $A^+(y, \eta)$, where

$$y - \eta > 0; \quad y > 0. \quad (3.17)$$

(This restriction can be made more mathematically precise by introducing additional concepts of causal symmetric spaces and semigroups [41–44].)

Given a basepoint, the key step involved for imposing causal constraint is by invoking forward lightcone. Recall that, in an embedding space approach, the spacetime manifold can be identified with the coset space $\mathcal{M} = G/H_0Q_0^-$ defined against the basepoint $\xi_0 = \{1, 1; 0, 0\}$, which corresponds to the space-time origin. Relative to ξ_0 , a *causal* map can be made moving to each point in its future lightcone. Restricting to the forward light cone of ξ_0 requires the constraints $z^2 - t^2 < 0$ for $0 < t$. A parametrization of the group elements that preserves this map is $S_0 = H_0 e^{tT_t}, t > 0$, where H_0 contains the Lorentz group and dilatation, and T_t is the generator of time translations. (This map doesn't carry any information about the trajectory and therefore does not contain the inverse of its elements.) Elements of S_0 that obey this restriction therefore form a *causal semigroup*. The group G carries the decomposition $H_0A_0H_0$ where $A_0 = \{B_{0,-1}, B_{-2,3}\}$ with parameters (y_0, η_0) respectively. Restricting to the forward lightcone leads to $S_0 = H_0A_0^+H_0$ where A_0^+ is a restriction to $y_0 - \eta_0 > 0$ with $y_0 > 0$. (See Appendix D.2 for more details.)

The relevant basepoint ξ_a , for our fourpoint function, can be mapped from ξ_0 by a discrete rotation. A corresponding causal structure about ξ_a can now be constructed by applying this discrete rotation. In particular, this takes A_0 to

$$A = \{L, D\}. \quad (3.18)$$

Furthermore, it maps the subgroup H_0 to H , given by (D.17) for $d = 2$ and (D.18) for $d = 4$. Note that H also serves as a subgroup of the isotropy for our basepoint, as claimed. More explicitly, the resulting semigroup is

$$S = HA^+H. \quad (3.19)$$

Here A^+ is a restriction of MASG by $y - \eta > 0; \quad y > 0$, (3.17). This semigroup preserves the causal ordering of our four points. (See Appendix D.3 for more details.)

A partial wave expansion of the imaginary parts of a four-point function are therefore identified with the H -bi-invariant representation functions with support only over a causal semigroup. This is one of our key insights. This restriction was discussed in Sec. 2 via kinematics. In our current approach, we arrive at the same restriction by working directly with four copies of the group and using global conformal invariance to restrict to a single copy along with the basepoint $\xi_a = \{1, 0; 0, 1\}$. We will return to the case $d = 4$ in Sec. 5.5.

4 Principal Series for $SO(d, 2)$

Having discussed the space of functions relevant for expansion in the causal scattering region, let us turn to the problem of constructing a basis. We begin in this section the task of clarifying the claim [20] that the four-point discontinuity function, $\text{Im } T(X_i)$, can be expressed in terms the principal series of unitary irreducible representation of $SO(d, 2)$, leading to a double-Mellin-like representation, Eq. (1.6). This is done by working in the $(d + 2)$ -dimensional embedding space, thus providing a linear realization for the group $SO(d, 2)$. We will see that causal considerations fix how positive roots are organized. This in turn provides the necessary connection with Minkowski conformal blocks discussed in [20].

4.1 Induced Representation

In this subsection, we provide a short discussion on the standard procedure of constructing unitary irreducible representations for semi-simple groups via an induced representation and Iwasawa decomposition. For $SO(d, 2)$, a semi-simple non-compact group of split-rank 2, this leads to a pair of representation labels, $\{\tilde{\ell}, \tilde{\Delta}\}$, initially defined for its MASG. We also discuss the structure of multipliers, which amounts to appending real parts to these representation labels.

Building group representations for compact groups by starting with a subgroup is known as an *induced representation* [64]. This procedure can also be applied to non-compact Lie group G [49–51, 63]. The starting point is the *Iwasawa decomposition*,

$$G = PK = NAK, \tag{4.1}$$

where a noncompact maximal abelian subgroup (MASG), A , plays a central role (see Appendix C). The subgroup K is the maximal compact subgroup and N is a set of nilpotents characterized by the set of positive roots of the algebra. One begins by constructing an unitary representation $\pi^{(s)}$ for A . An induced representation, $U^{(s)}$, can next be constructed, by introducing “multiplier factors”. The best known example for such approach was first carried out for 3-d Lorentz group, $SO(2, 1)$, by Bargmann [65], with the Lorentz boosts in the z -direction serving as the MASG, i.e., $A = SO(1, 1)$. Here, we generalize to the conformal group.

For $SO(d, 2)$, $A = SO(1, 1) \times SO(1, 1)$, which is of *split-rank* 2. We shall adopt a “gauge choice” by identifying A with a Lorentz boost (with its generator denoted by $L = L_{tz} = \mathcal{L}_{0,d-1}$) and dilatation (with generator denoted $D = \mathcal{L}_{-2,-1}$), which are parameterized by y and ζ respectively. In general, there are many equivalent choices for a MASG, all with different “orderings” of root vectors¹⁰ for the Iwasawa decomposition. This freedom leads in general to a Weyl group and has been discussed in [37]. In Sec. 3, we have seen that both A and its ordering

¹⁰Different ordering of root vectors for the same choice of Cartan subalgebra naturally leads to a different set of nilpotents that appear in Eq. (4.1). This will be a key point in what follows. Also see App. C.

are in fact completely determined by the identification of the spacetime manifold by cosets and by a causal requirement.

Let us focus first on the unitary representation for the MASG. For a function over A only, group actions lead to two independent Fourier integrals, $-\infty < k_y, k_\zeta < \infty$,

$$F(a(y, \zeta)) = \int_{-\infty}^{\infty} \frac{k_y}{2\pi} \int_{-\infty}^{\infty} \frac{dk_\zeta}{2\pi} e^{ik_y y} e^{-ik_\zeta \zeta} \tilde{F}(k_y, k_\zeta) \quad (4.2)$$

where $a(y, \zeta) = e^{yL_{zt}} e^{\zeta D} \in A = SO(1, 1) \times SO(1, 1)$ and $\tilde{F}(k_y, k_\zeta)$ its Fourier transform. It is conventional to express the integrals along the imaginary axes, with 1-d unitary representations: $L_{zt} \rightarrow \tilde{\ell} = ik_y$ and $D \rightarrow -\tilde{\Delta} = -ik_\zeta$, leading to a double mellin-like representation,

$$\int_{-\infty}^{\infty} \frac{k_y}{2\pi} \int_{-\infty}^{\infty} \frac{dk_\zeta}{2\pi} e^{ik_y y} e^{-ik_\zeta \zeta} \rightarrow \int_{-i\infty}^{i\infty} \frac{d\tilde{\ell}}{2\pi i} \int_{-i\infty}^{i\infty} \frac{d\tilde{\Delta}}{2\pi i} e^{\tilde{\ell} y} e^{-\tilde{\Delta} \zeta}. \quad (4.3)$$

The sign convention is adopted for later convenience. Although notationally unfortunate, there is good reason for this. The equation $\Delta = d/2 + \tilde{\Delta}$ lends a natural interpretation to Δ as an analytic continuation of $\tilde{\Delta}$.

In what follows, we shall designate this unitarity representation for A by $\pi^{(\tilde{\ell}, \tilde{\Delta})}(a(y, \zeta)) = e^{\tilde{\ell} y - \tilde{\Delta} \zeta}$, with $\tilde{\ell}$ and $\tilde{\Delta}$ purely imaginary. In contrast, for an Euclidean CFT, i.e., working with $SO(d+2, 1)$ where the MASG A is 1-dim, it leads to a single Mellin-like representation.

An induced representation, $U^{(\tilde{\ell}, \tilde{\Delta})}(g)$, can be constructed next by extending $\pi^{(\tilde{\ell}, \tilde{\Delta})}$ to the whole group via Iwasawa decomposition. A trivial first step is to extend over P with $\pi^{(\tilde{\ell}, \tilde{\Delta})}(n) = 1$, for $n \in N$, leading to $\pi^{(\tilde{\ell}, \tilde{\Delta})}(p) = \pi^{(\tilde{\ell}, \tilde{\Delta})}(a)$. The next step involves defining a functional space, \mathcal{F} , with an inner product, on which G acts. An induced representation, $U^{(\tilde{\ell}, \tilde{\Delta})}(g)$, can next be defined for G by “shift”, i.e., a linear map: $U^{(\tilde{\ell}, \tilde{\Delta})}(g) : F \rightarrow F_g$ where

$$U^{(\tilde{\ell}, \tilde{\Delta})}(g)F(g_0) = F_g(g_0) = F(gg_0). \quad (4.4)$$

To be more precise, the representation given here is defined via a “left-shift”. It is completely equivalent to instead adopt a “right-shift”, with $U^{(\tilde{\ell}, \tilde{\Delta})}(g)F(g_0) = F(g_0g^{-1})$.

Completing the specification of this map and the proof of unitary irreducibility involves certain mathematical gymnastics [49, 50]; we provide only a brief description here. Consider a space \mathcal{F} of complex-valued function over G with the following invariant property

$$\mathcal{F} = \{F : G \rightarrow \mathcal{C} \mid F(gp) = \varphi(\rho(a))\pi^{(\tilde{\ell}, \tilde{\Delta})}(a)F(g), \quad \forall p = na \in P\} \quad (4.5)$$

where $\varphi(\rho(a))\pi^{(\tilde{\ell}, \tilde{\Delta})}(a)$ serves as a multiplier factor, as done by Bargmann in Ref. [65]. Here $\varphi(\rho(a))$ is a scalar function to be specified below and elaborated further in Sec. 4.2 in relation to root-space structure for $SO(d, 2)$.

It can also be verified that the invariance property specified in Eq. (4.5) renders \mathcal{F} functions over the coset, G/P , only, which can be identified with K . It is then meaningful to introduce a norm with Haar measure $d\mu(k)$, over K , $\|F\|^2 = \int_{K=G/P} |F(kp)|^2 d\mu(k)$, thus elevating \mathcal{F} to a Hilbert space. To establish this as a unitarity representation, one demands $\|F_g\| = \|F\|$, i.e.,

$$\int_K |F_g(k)|^2 d\mu(k) = \int_K |F(k)|^2 d\mu(k). \quad (4.6)$$

Since $F_g(k)$ can be re-written in terms of $F(k(g))$ with $k(g)$ shifted from k specified by the Iwasawa decomposition, this variable change introduces a jacobian. The scalar factor $\varphi(\rho(a))$ is introduced precisely to remove this extra contribution. When this is done, it can be shown that this leads to a unitary irreducible representation for $SO(d, 2)$ [49, 50].

Symbolically, we have: $U^{(\tilde{\ell}, \tilde{\Delta})}(nak) \rightarrow \varphi^{(\tilde{\ell}, \tilde{\Delta})}(\rho(a)) \pi^{(\tilde{\ell}, \tilde{\Delta})}(a) F^{(\tilde{\ell}, \tilde{\Delta})}(k)$. Since our group is of split rank 2, there is certain freedom on how the multiplier factor $\varphi^{(\tilde{\ell}, \tilde{\Delta})}(\rho(a))$ is defined with respect to the “ordering” of its root-space. This in turn leads to a particular relation between representation labels $(\tilde{\ell}, \tilde{\Delta})$ to the conventionally defined (ℓ, Δ) in an Euclidean treatment, Eq. (4.12),

$$\ell = -(d-2)/2 + \tilde{\ell}, \quad \Delta = d/2 + \tilde{\Delta}.$$

Before constructing our representation functions of interest, let us clarify how these labels are understood in the context of ordered roots, and their impact on the leading behaviour of conformal blocks.

4.2 Multiplier Factor, Roots and Weyl-Vector

In this subsection, we further discuss the freedom for the real parts of representation labels associated with the Weyl group, and the choice for organizing the root space.

Let us provide a more precise determination for the multiplier $\varphi(\rho(a))$. For $SO(d+1, 1)$, A is 1-dim, generated by D , i.e., $a(\zeta) = e^{-\zeta D}$, and the multiplier $\varphi(\rho(a))$ also serves as the standard scaling factor, $\varphi(\rho(a(\zeta))) = e^{-\rho(a(\zeta))} = e^{-c\zeta/2}$, with c a real constant. When unitarity is enforced, the constant c is fixed by the above mentioned jacobian, with c given by the dimension d , leading to $\varphi(\rho(a(\zeta))) = e^{-\rho(a(\zeta))} = e^{-d\zeta/2} \equiv e^{-(d/2) \log a}$, where we have also adopted another (abused) short-hand notation, $\zeta = \log a$. The factor $d/2$ can be combined with $\tilde{\Delta}$ to form a single complex variable Δ , considered as the analytically continued conformal dimension from Euclidean analysis. To be precise, we identify $\Delta = d/2 \pm \tilde{\Delta}$ where at this point we have allowed the freedom of defining $\tilde{\Delta}$ up to a sign choice ¹¹.

We next generalize the notation of multiplier to higher dimensional MASG that is appropriate

¹¹For $d = 1$, there is an option for A depending on the choice of Minkowski or Euclidean CFT_1 , leading to $\log a = \zeta$ or $\log a = y$, e.g., for SYK-like models, Ref. [20].

Ordering of Roots	c_y	c_ζ	Leading Behaviour	
(L, D)	d	$d - 2$	$\ell - 1$	$1 - \Delta$
$(L, -D)$	d	$d - 2$	$\ell - 1$	$\Delta - d + 1$
$(-L, D)$	d	$d - 2$	$1 - d - \ell$	$1 - \Delta$
$(-L, -D)$	d	$d - 2$	$1 - d - \ell$	$\Delta - d + 1$
(D, L)	$d - 2$	d	$-\Delta$	ℓ
$(D, -L)$	$d - 2$	d	$-\Delta$	$2 - d - \ell$
$(-D, L)$	$d - 2$	d	$\Delta - d$	ℓ
$(-D, -L)$	$d - 2$	d	$\Delta - d$	$2 - d - \ell$

Table 1: Coefficients for the group parameters in Weyl vector $\vec{\rho}$, (4.8), change with a choice of ordering of the root vectors. The highlighted rows correspond to Minkowski scattering and non-scattering settings respectively. Similar structure was also highlighted in [37, 57] Table 1.

for our Minkowski case. For $SO(d, 2)$, in imposing unitarity, a combined treatment of the jacobian associated with the boost, y , and scaling, ζ , is required. Since these two operations commute, one has

$$\varphi(\rho(a)) = e^{-\rho(a(y, \zeta))} = e^{-(c_y y + c_\zeta \zeta)/2} \equiv e^{-\vec{\rho} \cdot \vec{t}(a)} \equiv e^{-\langle \rho, t(a) \rangle} \quad (4.7)$$

where, for later convenience, we have introduced additional short-hand notations, e.g.,

$$\vec{\rho} = (c_y/2, c_\zeta/2), \quad \text{and} \quad \vec{t}(a(y, \zeta)) = (y, \zeta), \quad (4.8)$$

with $\vec{\rho} \cdot \vec{t}(a) \equiv \langle \rho, t(a) \rangle \equiv (c_y y + c_\zeta \zeta)/2$. This ρ -vector, (or **Weyl-vector**), will play an important role in what follows ¹².

Positive Roots: It is important to stress that $\vec{\rho}$ depends on the choice of the MASG. It also depends on how the “positive root vectors” are handled in organizing the group algebra. This option on how to specify positive roots can be understood intuitively from a Gram-Schmidt perspective. Geometrically, this requires specifying the order of leading root vectors. As will be explained in the following sections, when applied to CFT, physics consideration will determine the ordering of positive roots. This in turn will be correlated with the leading asymptotic behaviors of the associated conformal blocks [20]. Depending on the ordering for the leading positive root, the allowed values for $\vec{\rho}$ are given in Table 1.

To be more precise, the representation functions are labelled by two complex numbers that we write in the shorthand notation

$$\vec{\lambda} = \vec{\tilde{\lambda}} - \vec{\rho} \quad (4.9)$$

¹²We mention the notation $\langle \rho, t(a) \rangle$ as a way of clarifying the notation typically used in mathematical literature.

where $\vec{\lambda} = (\tilde{\ell}, -\tilde{\Delta})$. As will be explained in the next section, in the Minkowski scattering setting of interest to us, the roots are ordered (L, D) . The Weyl vector, as is indicated in Tab. 1, is given by $\vec{\rho} = \{d/2, (d-2)/2\}$. Therefore, the representation functions are labelled by

$$\vec{\lambda}^M = \left(\tilde{\ell}; \quad -\tilde{\Delta} \right) - \left(\frac{d}{2}; \quad \frac{d-2}{2} \right) = \left(\tilde{\ell} - \frac{d}{2}; \quad -\tilde{\Delta} - \frac{d-2}{2} \right) \quad (4.10)$$

where the superscript M denotes that these are labels appropriate for the Minkowski causal scattering case. Similarly, for the non-scattering case, the roots are ordered (D, L) and the representation labels are given by:

$$\vec{\lambda}^E = \left(\tilde{\ell}; \quad -\tilde{\Delta} \right) - \left(\frac{d-2}{2}; \quad \frac{d}{2} \right) = \left(\tilde{\ell} - \frac{d-2}{2}; \quad -\tilde{\Delta} - \frac{d}{2} \right). \quad (4.11)$$

The resulting zonal spherical function in this case can be analytically continued to the standard Euclidean conformal blocks where Δ is real and positive, with ℓ non-negative integers. This will be discussed further in [52]. Identification with the traditional representation labels can now be made by recognizing that $\vec{\lambda}^E = (\ell, -\Delta)$ which leads to

$$\ell = -(d-2)/2 + \tilde{\ell}, \quad \Delta = d/2 + \tilde{\Delta}. \quad (4.12)$$

(Note that Eq. (4.12) is defined upto a sign of $(\tilde{\ell}, \tilde{\Delta})$. As already mentioned earlier, here we have implicitly made a choice.) Note also that this is precisely the identification required in matching the quadratic Casimir obtained from an Euclidean analysis

$$C(\ell, \Delta) = -[\Delta(\Delta - d) + \ell(\ell + d - 2)] = -\tilde{\Delta}^2 - \tilde{\ell}^2 + d^2/4 + (d-2)^2/4. \quad (4.13)$$

More interestingly, we can also translate the labels for representation functions in the Minkowski scattering region into these traditional labels to get $\vec{\lambda}^M = (\ell - 1, 1 - \Delta)$, which recovers the expected leading behavior for Minkowski conformal blocks [20] when the contour is closed.

4.3 Induced Representation for Semigroups and Root Space

In this subsection, we indicate how causal consideration and the structure of semigroup dictate on the choice root ordering for Minkowski CFT scattering.

Induced representations, as introduced so far, rely on the identification of Iwasawa decomposition of the group $G = N^+AK$, where we write N^+ to emphasize that these are nilpotents associated with the set of positive roots. For this case, we noted that the identification of N^+ relies on the ordering of root vectors. For finite dimensional Lie algebras such as $SO(d, 2)$, the vectors in this space are discrete objects in the sense that they are finitely numbered. We can therefore divide them into two equal subspaces by identifying a hyperplane perpendicular to some root (See Appendix C and Fig. 4.1). We can call the subspace containing the specified

root to be the positive set, whereas the complement subspace is negative set. The choice of hyperplane can be described by an appropriate Weyl transformation as illustrated in Table 1. Ultimately, the representation functions constructed via the Iwasawa decomposition cover the full group and an equivalence between representations can be established.

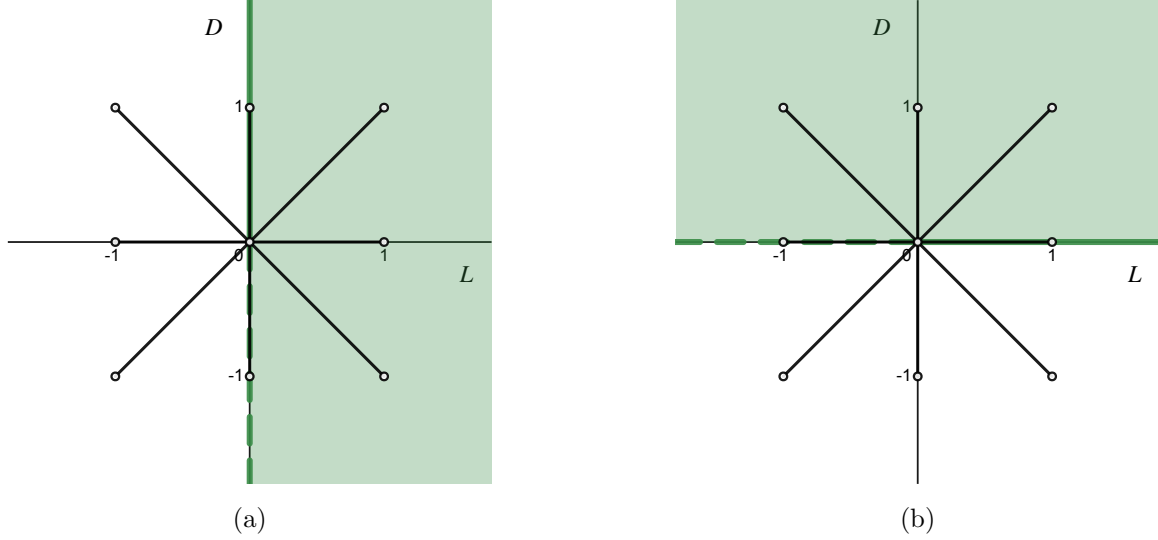


Figure 4.1: The restricted root space diagram for $SO(d, 2)$. The green shaded region contains the set of positive roots. Figure-a corresponds to ordering (L, D) whereas figure-b corresponds to (D, L) . The roots on the solid boundary of this region are included whereas those on the dashed boundary are excluded.

However, the equivalence in representations is not true for representation functions we wish to define over the *semigroup*. This freedom in the choice of positive roots N no longer exists for the semigroup and the ordering of roots is completely determined by S . That is, for $S \subset NAH$ to hold in the scattering region, N is the set of positive roots defined with L as the leading component of root vectors. Intuitively, the idea is that combinations of elements in N can *at most* correspond to null translations on the lightcone to stay within the semigroup (see Table 2 and App. C.2 for an illustration for $d = 2$). The element against which the positive roots are defined is therefore called the cone generating element [41]. (A discussion on this element and how it is completely fixed is presented in App. D.)

Roots	Generators
$(1, -1); (-1, 1)$	$T_t + T_z; C_t + C_z$
$(1, 1); (-1, -1)$	$C_t - C_z; T_t - T_z$

Table 2: Roots for $SO(2, 2)$ ordered as (L, D) . Positive roots that belong in N^+ are therefore $\{T_t + T_z, C_t - C_z\}$.

For our choice of basepoint $\xi_a = \{1, 0; 0, 1\}$ in $d = 2$, the Weyl vector is given by

$$\vec{\rho} = \frac{1}{2} \sum_{\alpha \in \alpha_+} m_\alpha \vec{\alpha} = \frac{1}{2}(2, 0) \quad (4.14)$$

where m_α is called the multiplicity of roots, with the element L dictating that the roots be ordered as (L, D) . The Weyl vector is defined as the half sum of positive roots. As seen in Table 2, for $d = 2$, $m_\alpha = 1$. Therefore, the multiplier in the Minkowski scattering region is $\varphi(\rho(a)) = e^{-y}$. That is, as established in Sec. 2, this applies when $1 < \sigma < w < \infty$.

5 Spherical Functions and Semigroups

The unitary irreducible representation (UIR) also provides the opportunity to represent functions over a group in terms of a set of properly chosen basis functions by specifying $\mathcal{F}(\vec{\ell}, \vec{\Delta})$; this leads to harmonic analysis over the group. The conventional procedure for specifying group harmonics appropriate for fourpoint functions is to consider the second order partial differential equation which follows from the quadratic Casimir operator. Zonal spherical functions can be considered as the solutions to the radial component of Casimir equations. Instead, we show that due to the structure of semi-group and H -bi-invariance, Eq. (3.12), the desired causal zonal spherical functions for $SO(d, 2)$ can be expressed in an integral representation

$$\varphi_\lambda(a) = \varphi_\lambda(h_1 a h_2) = \int_H e^{(-\vec{\rho} + \vec{\lambda}) \cdot \vec{t}(h_1 a)} dh_1, \quad (5.1)$$

with $\vec{\lambda} = (\vec{\ell}, -\vec{\Delta})$. These can be evaluated and identified with Minkowski conformal blocks [20].

5.1 A First Look at Group Harmonics

To introduce zonal spherical functions it is instructive to start with a simple example. We will begin with the group $SO(3)$ and then move on to the noncompact group $SO(2, 1)$ in the next subsection.

UIRs for $SO(3)$ correspond to having the Casimir taking on a value $\lambda = \ell(\ell + 1)$, ℓ a non-negative integer. As reviewed in Appendix E, spherical functions for $SO(3)$ are the standard spherical harmonics, $Y_{\ell, m}(\theta, \varphi) = D_{m0}^\ell(\varphi, \theta, \psi)$, i.e., a restricted subset of Wigner D -functions. They are functions defined over the coset $SO(3)/SO(2)$, thus the absence of dependence on the Euler angle ψ . As group functions, they are right K -invariant, with $K = SO(2)$.

Zonal spherical functions are the Legendre polynomials, $P_\ell(\cos \theta) = D_{00}^\ell(\varphi, \theta, \psi)$. They are functions defined over two-sided cosets, thus independent of both Euler angles φ and ψ . As group functions, they are K -bi-invariant. They are given by matrix elements $\langle \ell, 0 | g(\varphi, \theta, \psi) | \ell, 0 \rangle$ and admit an integral representation, $P_\ell(\cos \theta) = 4\pi \int_0^{2\pi} W(\theta, \varphi; \ell) d\varphi$, where

$$W(\theta, \varphi; \ell) = (\cos \theta + i \sin \theta \cos \varphi)^\ell \equiv e^{i\ell\theta'(\theta, \varphi)}. \quad (5.2)$$

For reason to be explained shortly, it will be referred to as the *inductive character* for $SO(3)$.

5.2 Space of Homogenous Functions for $SO(2, 1)$

Next we construct zonal spherical functions for slightly more complicated examples: first for $SO(2, 1)$ over compact subgroup $K = SO(2)$ and then for non-compact subgroup $H = SO(1, 1)$. Let us begin by providing a geometrically intuitive way of understanding induced representations of groups. Homogeneous functions for $SO(2, 1)$ can be described over a null submanifold in the embedding space since ¹³

$$\xi_1^2 - \xi_2^2 - \xi_3^2 = 0, \quad (5.3)$$

is invariant under simultaneous scaling $\xi_i \rightarrow a \xi_i$. Projective geometry is the natural language of these submanifolds. We start by identifying an appropriate projective plane that “slices” the null cone. A subgroup can be identified that acts transitively on this conic section. Representation functions over this section can be written down and “lifted up” to the full cone by scaling.

Compact Subgroup: For $SO(2, 1)$, we can identify the plane $\Gamma = (1, \xi_2/\xi_1, \xi_3/\xi_1)$ with $\xi_1 > 0$, such that the subgroup $K = SO(2)$ acts transitively on a circle. From Eq. (4.5), unitary representation with $F(k) = e^{im\varphi}$ is lifted up to the complete null cone by the multiplier factor $\pi(na) = \varphi(\rho(a))\pi(a) = e^{(-\rho+\tilde{\lambda})\eta_I}$, where η_I is the boost parameter for a . The representation is labelled by a complex $\lambda = -\rho + \tilde{\lambda} = -1/2 + \tilde{\lambda}$. (The fact that $\rho = 1/2$ will be shown below to be appropriate for $d = 1$. Here λ can be identified with either Δ or ℓ .) Note that we have added a subscript for the boost parameter, η_I , reminding ourselves that this is done through an Iwasawa decomposition. Therefore, the induced representation on the group is

$$\mathcal{F}(g) = e^{(-\rho+\tilde{\lambda})\eta_I} e^{im\theta}. \quad (5.4)$$

Here, we have used the group decomposition $G = NAK$. On the coset space $SO(2, 1)/SO(2)$, we have that $gk = g$. That is, all group elements on the coset are characterized by $g \in NA$. Much in analogy with $SO(3)/SO(2)$, this can be achieved by taking $m = 0$ in Eq. (5.4). This gives the subspace of functions that are right invariant under K .

For the subspace of functions that are K -bi-invariant, the representation functions live on a two sided coset such that $k_1 g k_2 = g$, again in the sense of cosets. It is therefore useful to discuss this space of functions in the Cartan decomposition $G = KAK$, i.e., in terms of an Eulerian-like parametrization for each group element, $g = k_1(\varphi)a(\eta)k_2(\psi)$. Since η_I is independent of ψ due to right K -invariance, the key idea is to write the multiplier $e^{(-\rho+\tilde{\lambda})\eta_I}$ in terms of a function over $k_1(\varphi)a(\eta)$. We can then project out the left invariant function by integrating over k_1 . This is

¹³For this subsection, we shall adopt coordinates ξ_i , $i = 1, 2, 3$, with ξ_1 timelike, for convenience.

carried out in Appendix F.1, leading to, Eq. (F.1),

$$\varphi_\lambda(a) = \varphi_\lambda(k_1 a k_2) = P_\lambda(\cosh \eta) = \int_0^{2\pi} d\varphi (\cosh \eta + \cos \varphi \sinh \eta)^\lambda. \quad (5.5)$$

The integrand is the inductive character for $SO(2, 1)$ over $SO(2)$, (it is also occasionally referred to as the Poisson kernel [44, 46, 47, 51].) Mathematically, the inductive character can be written as

$$W_K(\cosh \eta, \varphi; \lambda) = e^{\lambda \eta_I(k_1 a)} = (\cosh \eta + \cos \varphi \sinh \eta)^\lambda, \quad (5.6)$$

indicating that η_I from the Iwasawa decomposition needs to be evaluated as a function of $k_1(\varphi)$ and $a(\eta)$, from the Cartan decomposition.

Non-Compact Subgroup: We next deal with the more relevant case of non-compact H , which serves a stepping stone for dealing with the case of $SO(d, 2)$. The H bi-invariant functions of interest can be constructed by considering a slice over which the non-compact subgroup $H = SO(1, 1)$ acts transitively. The plane can be chosen as $\Gamma = (\xi_1/\xi_2, 1, \xi_3/\xi_2) = (\cosh s, 1, \sinh s)$, $\xi_2 > 0$, which defines a hyperbolic section of the cone. A basis for the space of functions parametrized by this slice, labelled by $\lambda \in \mathbb{C}$ and $p \in \mathbb{R}$, is given by

$$f_{\lambda,p}(\xi) = (\xi_2)^\lambda \left(\frac{\xi_1 + \xi_3}{\xi_2} \right)^{ip} = (\xi_2)^\lambda e^{ips}. \quad (5.7)$$

In the language of subgroups introduced in Sec. 4, this can be interpreted as the induced representation written as $f(\xi) = \pi(an)F(h)$. On the slice Γ , we have $\pi(an) = 1$ and therefore, $f_{\lambda,p}(\xi) = e^{ips}$. A shift by $a \in A$ takes this to the function $f_{\lambda,p}(\xi') = (\xi'_2)^\lambda \sum_{p'} t(p, p') e^{ip's'}$.

For functions that are H bi-invariant, we need to consider a basis which is independent of s . It follows that we only need the component $t(0, 0)$. This is carried out in Appendix F.2, by projection over H , leading to

$$t(0, 0) = \cosh \eta^\lambda \int_0^\infty ds (1 + \cosh s \tanh \eta)^\lambda. \quad (5.8)$$

This corresponds to an integral representation for the Legendre function of the second kind, $Q_{-\lambda-1}(\cosh \eta)$, Eq. (F.2). From the integrand, one has

$$W_H = (\cosh \eta + \cosh s \sinh \eta)^\lambda, \quad (5.9)$$

as the inductive character for $SO(2, 1)$ over $SO(1, 1)$. The integral is well defined in the region $\eta \geq 0$. This restriction corresponds to that appropriate for a semigroup. This is the unitary ‘‘elementary Spherical functions’’, with $\lambda = -1/2 + \tilde{\lambda}$ and $\tilde{\lambda}$ imaginary.

5.3 Generalized Inductive Character and Doubling Procedure

In this subsection, we motivate the concept of inductive character by Cartan subalgebra and we also introduce a doubling procedure which is useful in dealing for the case of split rank 2.

Generalized Inductive Character: The process of constructing induced unitary representations is essentially building up functions over the group G from known unitary representations of its subgroups. Of particular importance is the Cartan subalgebra which is made up of a direct sum of one dimensional commuting subalgebra such that they can be simultaneously diagonalized. For the principal series of $SO(d, 2)$, this is identified as $SO(1, 1) \times SO(1, 1) \times SO(2) \times \dots \times SO(2)$, for $d > 2$. Each of the compact subgroups has a unitary representation of the form $e^{i\ell\theta}$ with integer ℓ and each noncompact subgroup has a unitary representation of the form $e^{\tilde{\lambda}\eta}$ such that $\tilde{\lambda}$ is imaginary. Under the isomorphism $SO(2) \cong U(1)$, these factors can be identified as the character (trace) associated with the representation. In the context of induced representations, as have already been mentioned above, for definiteness, we shall refer them as generalized inductive characters.

For $SO(d, 2)$, the UIR label can be expressed as a two-vector, $\vec{\lambda} = (\tilde{\ell}, -\tilde{\Delta})$ ¹⁴, for MASG with positive roots ordered as (L, D) . The generalized inductive character can be expressed as $W_{\vec{\lambda}}(a, h_1) = e^{(-\vec{\rho} + \vec{\lambda}) \cdot \vec{t}(h_1 a)}$, with $\vec{\lambda} = -\vec{\rho} + \tilde{\lambda}$. (We have here made use of short-hand introduced earlier, Eq. (4.8).) Once $W_{\vec{\lambda}}(a, h_1)$ is known, zonal spherical function can be calculated as an integral averaging over the non-compact subgroup H , i.e.,

$$\varphi_{\lambda}(a) = \varphi_{\lambda}(h_1 a h_2) = \int_H W_{\vec{\lambda}}(a, h_1) dh_1 = \int_H e^{(-\vec{\rho} + \vec{\lambda}) \cdot \vec{t}(h_1 a)} dh_1. \quad (5.10)$$

Doubling Procedure: For the split-rank 1 case, the inductive character can be derived in several different ways¹⁵, including the explicit demonstration for $SO(2, 1)$ in Appendix F. Here, we present another procedure, which we shall refer to as “doubling”. (See App. F.3 and F.4.) This procedure most easily generalizes to rank 2 case we will be facing.

Let us start in the adjoint representation of the group and consider the space of symmetric matrices by “doubling”, $I(g) \equiv g \cdot g^T$, where g^T stands for the transpose. Of particular importance is the fact that $k^T = k^{-1}$, which means that the subgroup K maps to identity in this space. Consider both Iwasawa and Cartan decompositions, $g = n a_I k$ and $g = k_1 a k_2$, where a_I and a have distinct parametrizations, with η_I and η respectively. Each group element maps to two equivalent product representations

$$I(g) = n (a_I \cdot a_I^T) n^T \quad \text{and} \quad I(g) = k_1 (a \cdot a^T) k_1^{-1}. \quad (5.11)$$

Note that $I(g)$ is independent of k for the first equality and k_2 for the second¹⁶. Therefore, $I(g)$ is associated with group elements explicitly on the coset G/K . Furthermore, since, in a Cayley basis, both a_I and a are diagonal, Eq. (F.13), it follows that one can express η_I in

¹⁴This is the sign choice made in Eq. (4.12).

¹⁵A more conventional derivation can be found in [45–47]. An alternative derivation is to make use of “Radon transform”, or, more explicitly, Abel or Harish transform.

¹⁶The second equality is analogous the standard procedure of SVD for diagonalizable matrices.

terms of η and an angle φ , which specifies k_1 , leading to the same expression obtained earlier, $e^{\eta_I} = \cosh \eta + \cos \varphi \sinh \eta$, Eq. (5.6). (Alternatively, one can express η_I in terms of η and another parameter x specifying n .)

In what follows, we will need to generalize this “doubling procedure” for obtaining the inductive character for the case of split-rank 2. This requires a more refined discussion on the root space structure for $SO(d, 2)$. We will also need to transition to causal symmetric spaces where the subgroup H is non-compact. This requires an understanding of the Iwasawa decomposition NAH as well as Cartan decomposition HAH for semigroups.

5.4 Minkowski Causal CFT_2

We now turn to the main task of this section, treating the case semigroup of split-rank 2. In order to provide an explicit construction, we will deal with the case of $d = 2$ first. Writing down the homogeneous functions similar to Eq. (5.7) on the null cone is more involved when the Cartan subalgebra has dimension greater than 1. We shall adopt a generalized “doubling procedure” similar to the one introduced in the previous section.

Recall from Sec. 3 that the representation functions we are after are the H bi-invariant zonal spherical functions of the semigroup S such that:

$$f(s) = f(ha_+h) = f(a_+) \quad (5.12)$$

where $a_+ \in A = \{L, D\}$ and $y - \eta > 0$. Our choice of basepoint is $\xi_a = \{1, 0; 0, 1\}$ which helps reduce the fourpoint function to a function over the semigroup of a single copy. Since A contains two commuting non-compact generators, the representation functions are labelled by two imaginary continuous parameters $\tilde{\lambda} = (\tilde{\lambda}_1, \tilde{\lambda}_2)$ and the Weyl vector is given by $\vec{\rho} = (1, 0)$, where the roots are ordered as (L, D) since L is the cone generating element.

In this rank-2 case, we have a homogeneity condition involving two parameters

$$f(a_+ \cdot \xi_a) = e^{(\tilde{\lambda}_1 - 1)y_I} e^{\tilde{\lambda}_2 \eta_I} f(\xi_a). \quad (5.13)$$

These homogeneous polynomials define an intertwining representation between a Hilbert space and the manifold. The inductive character W_H is

$$W_H = e^{(\tilde{\lambda}_1 - 1)y_I} e^{\tilde{\lambda}_2 \eta_I}, \quad (5.14)$$

where (y_I, η_I) are functions of the group element $h(\alpha, \beta)a_+(y, \eta)$. That is, the zonal spherical functions can be obtained by integrating the inductive characters W_H over a non-compact subgroup, H .

Consider two alternate expansions for an element of semigroup, Iwasawa and Cartan-like, i.e., $g = na_+(y_I, \eta_I)h$ and $g = h_1 a_+(y, \eta) h_2$. Notice that $g \cdot g^T$ no longer takes us directly to the

coset space G/H since $h^T \neq h^{-1}$. For a coset construction, we therefore introduce a diagonal matrix P that has the property that $h \cdot P \cdot h^T = P$. Since H is the isometry group of our basepoint, we can define P in terms of ξ_a such that $P = \text{diag}\{\xi_{a,-2}^2, \xi_{a,-1}^2, \dots\}$. We now consider the doubling space $I_P(g) = g \cdot P \cdot g^T$ to find that

$$I_P(g) = na_I \cdot P \cdot a_I^T n^T \quad \text{and} \quad I_P(g) = h_1 a \cdot P \cdot a^T h_1^T \quad (5.15)$$

which again maps the coset of interest. Whereas the first representation is independent of h , the second is independent of h_2 . For $d = 2$, subgroup H is of dimension 2 and abelian, making the analysis relatively simple to handle. This analysis applies in general. In particular, our discussion on $SO(2,1)/SO(1,1)$ can be recast in this language to give the same result as presented in the previous subsection. This is discussed in more detail in Appendix F.3.

In the Cayley transformed representation ¹⁷ where A is diagonal and of the form:

$$d = c^{-1}ac = \text{diag}\{e^y, e^\eta, e^{-\eta}, e^{-y}\}, \quad (5.16)$$

we can identify the characters e^{y_I} and e^{η_I} in terms of $h_1 a_+$ by solving for them in Eq. (5.15). Following a procedure analogous to one in [47], since n is nilpotent with 1's on the diagonal, identifying e^{y_I} can be done simply by evaluating the first matrix element of the second representation. Solving for e^{η_I} can be done by considering the 2×2 minor matrix whose determinant is given by $-e^{2y_I} e^{2\eta_I}$ (see App. F.3, F.4 for details). Note that the root-ordering plays an crucial role in arriving at the desired result.

It is interesting to note here the structure of the characters (e^{y_I}, e^{η_I}) . We find

$$e^{y_I} \sim \left(\cosh(y - \eta) \cosh(y + \eta) [1 + \cosh(\alpha - \beta) \tanh(y + \eta)] \right. \\ \left. \times [1 + \cosh(\alpha + \beta) \tanh(y - \eta)] \right)^{1/2}, \quad (5.17)$$

$$e^{\eta_I} \sim \left(\frac{\cosh(y + \eta) [\tanh(y + \eta) \cosh(\alpha - \beta) + 1]}{\cosh(y - \eta) [\tanh(y - \eta) \cosh(\alpha + \beta) + 1]} \right)^{1/2}. \quad (5.18)$$

where α and β are two angles in specifying the abelian h_1 . The character associated with dilatation is a ratio, whereas for the Lorentz boost it is a product. Recall that we are currently working in the causal region, $1 < \sigma < w < \infty$. This is an important observation and will be the key insight when discussing the non-scattering regions, e.g., M_s , where $1 < w < \sigma < \infty$ and continuation into the Euclidean region of $|w| < 1$ in the follow-up paper [52].

Plugging the values of e^{y_I} and e^{η_I} back into the integral form of zonal spherical functions, we get:

$$\varphi_{\vec{\lambda}}(\vec{t}) = Q_{(-\tilde{\lambda}_1 - \tilde{\lambda}_2 - 1)/2}(\cosh(y + \eta)) Q_{(-\tilde{\lambda}_1 + \tilde{\lambda}_2 - 1)/2}(\cosh(y - \eta)) \quad (5.19)$$

¹⁷We use the phrase Cayley transform somewhat loosely in our discussion. It is shorthand for a basis in which the Cartan subalgebra is diagonal. See App. F.3.

upto a normalization. Notice that the integrals are well defined only for $|\eta| < y$, which is our semigroup restriction. These zonal spherical functions therefore have support only in this restricted region. Due to these causal restrictions, covering the full group necessarily requires us to define these functions piecewise for different regions.

Taking into account Eq. (4.12), with $d = 2$, one arrives at

$$\varphi_{\vec{\lambda}}(\vec{t}) = Q_{(-\ell+\Delta)/2-1}(q)Q_{(-\ell-\Delta)/2}(\bar{q}). \quad (5.20)$$

This agrees with the result for Minkowski conformal blocks first presented in Ref. [20], Eq. (III.13), by directly solving the Casimir equation in a symmetric set of variables (q, \bar{q}) , (see Table 3 for their relationship with other variables). Here we have provided an alternative derivation, with $1 < \bar{q} < q < \infty$. They satisfy Minkowski boundary condition,

$$G_{(\Delta, \ell)}^{(M)}(u, v) \sim (\sqrt{u})^{1-\ell} \left(\frac{1-v}{\sqrt{u}} \right)^{1-\Delta} \quad (5.21)$$

We also note that, by evaluating zonal spherical functions defined in the region $1 < w < \sigma < \infty$, one is led to Euclidean conformal blocks,

$$G_{(\Delta, \ell)}^{(E)}(u, v) \sim (\sqrt{u})^{\Delta} \left(\frac{1-v}{\sqrt{u}} \right)^{\ell}. \quad (5.22)$$

Comparing (5.21) and (5.22), observe the (ℓ, Δ) and $(1-\Delta, 1-\ell)$ swap, so necessary in various related treatments, e.g., [1, 2]. It is also interesting to note that (5.22) can be continued into a larger region, $-\sigma < w < \sigma$, (Fig. 2.1). This will be discussed further in [52].

5.5 Minkowski CFT_d for $d > 2$

Harmonics for CFTs in $d > 2$ presents some new challenges. The case for $d = 4$ is particularly interesting for HEP applications. The Cartan subalgebra for this case is 3 dimensional and can be parametrized by $\{L, D, R_{12}\}$. The harmonics are therefore labelled by three indices $(\tilde{\ell}, \tilde{\Delta}, \tilde{m})$: two continuous imaginary numbers and one integer.

The quantum number \tilde{m} allows one in principle to deal with functions with dependence on 2-dim vector \vec{b}_{\perp} . However, by imposing rotational symmetry in the $x-y$ plane, we can restrict ourselves to functions depending on b_{\perp}^2 only. This corresponds to states with $\tilde{m} = 0$, which is reflective of the fact that $R_{12} \in H$. Furthermore, as discussed in Sec. 2, Lorentz invariance allows a further reduction in the dependence on b_{\perp}^2 , leading to

$$\cosh \eta = \cosh \zeta + b_{\perp}^2. \quad (5.23)$$

This can be demonstrated in the embedding space in the following manner.

For the sake of notational brevity, let us consider $d = 3$ where we have a single transverse direction since one can always reduce to this case due to transverse rotational invariance, (that is invariance under R_{xy}). The choice of basepoint analogous to Eq. 3.7 is:

$$\xi_a = \{1, 0; 0, 0, 1\}; \quad \xi_b = \{1, 0; 0, 0, -1\}. \quad (5.24)$$

The fourpoint function is again characterised by Eq. (3.10). For finite impact parameter physics, let us consider the configuration where we have $x_{1\perp} = x_{2\perp} = b_\perp$ and $x_{3\perp} = x_{4\perp} = 0$. Therefore, we are led to consider the group elements $g_{\text{left}} = a_{\text{left}} q^+(b_\perp)$ and $g_{\text{right}} = a_{\text{right}}$, where $q^+(b_\perp)$ generates translation. Notice that this frame is no longer antipodal but can still be characterized as a CM frame. We can therefore choose to parametrize a_{left} by $(y/2, \zeta/2)$ and a_{right} by $(-y/2, -\zeta/2)$, as done previously. Reduction down to a single copy of the group is done by imposing global shift invariance of the fourpoint function under g_{right}^{-1} . Therefore, $g = g_{\text{right}}^{-1} g_{\text{left}} = q^+(b_\perp) a_{\text{left}}^2$. This group element again carries the decomposition $g = hah'$. It is this new group element $a(y, \eta)$ that is related to our (w, σ) variables. It follows that $\cosh \eta = \cosh \zeta + b_\perp^2$, as claimed.

This allows one to restrict to conformal invariant scalar functions with dependence only on 2 variables, (w, σ) , i.e., with scaling parameter ζ and transverse variable \vec{b}_\perp combined into a single variable $\sigma = \cosh \eta$. In the complex w plane, the location of the cut at $w = \sigma$ is therefore dictated by the impact parameter of the collision.

Group theoretically, this corresponds to having partial-wave amplitudes $a(\tilde{\ell}, \tilde{\Delta}, \tilde{m})$ independent of \tilde{m} so that the sum over them can be carried out directly on the conformal harmonics, leading to an “invariant spherical function”, $\mathcal{G}_{(\tilde{\ell}, \tilde{\Delta}, 0)}(w, \sigma)$, as appeared in Eq. (1.6), i.e., with a reduction of variable dependence from $(w, \cosh \zeta, \vec{b}_\perp)$ to (w, σ) .

In our procedure for constructing harmonics, we expect the Weyl vector to be given by $\vec{\rho} = \{2, 1\}$ and the representation labels

$$\vec{\lambda} = \vec{\tilde{\lambda}} - \vec{\rho} = (\tilde{\ell} - 2, -\tilde{\Delta} - 1) \quad (5.25)$$

for the Minkowski case. Calculating the harmonics for $d > 2$ via an integral representation gets tedious, even if it is largely procedural. The structure of semigroups, ordering of roots and the Weyl transformations can also be viewed in the standard procedure of constructing conformal blocks using the Casimir equation. We shall explore this discussion elsewhere [52].

6 Discussion

The goal of this study is to clarify the suggestion made in Refs. [20, 37, 38, 40] that Minkowski CFT 4-point amplitudes can be treated directly in terms of the principal series representation, Eq. (1.6), and to amplify the work of Ref. [20] on Minkowski conformal blocks. We have tried

to limit the scope of this study with emphasis on adopting a direct embedding space approach to $SO(d, 2)$ for 4-point Minkowski CFT amplitudes. In this final section, we highlight some of the key issues and their interplay with the results presented here.

The single most important issue for this study involves causality constraints associated with Minkowski space-time. We introduce a set of variables, (w, σ) in Sec. 2, directly related to cross ratios (\sqrt{u}, \sqrt{v}) . By extending to the whole \sqrt{u} - \sqrt{v} plane, from Minkowski perspective, the w - σ plane is most useful in specifying the causal scattering regions. By associating these variables with Minkowski antipodal frames, they can be identified with Minkowski t -channel OPE, which in turn allows a connection to Regge limit for CFT.

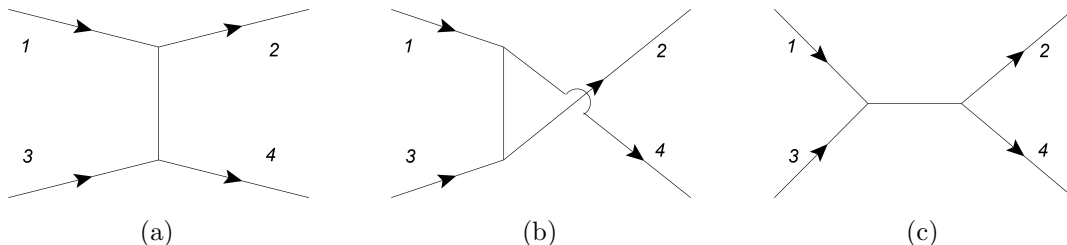


Figure 6.1: Three alternative descriptions for Minkowski s -channel scattering, via OPE connections. (Figure taken from [20].) They can be associated with three distinct regions, $M_s^{(t)}$, $M_s^{(u)}$ and $M_s^{(s)}$, in the extended \sqrt{u} - \sqrt{v} plane, Fig. 6.2(a), and also in Fig. 6.2(b).

Let us next turn to the question of alternative procedure in specifying causal scattering regions. Let us focus on s -channel scattering, (1.1). As pointed earlier, to reach *causal scattering regions*, it is necessary to cross singularities at $\sqrt{u} = 0$ and/or $\sqrt{v} = 0$, (or at $+\infty$). There can be three equivalent modes of descriptions, associated with three possible Minkowski OPE limits [20]. This is schematically illustrated by Fig. 6.1. (This corresponds to three equivalent expansions for Minkowski amplitude, $T(x_i)$.) In terms of the \sqrt{u} - \sqrt{v} plane, they correspond to three distinct regions, $M_s^{(t)}$, $M_s^{(u)}$ and $M_s^{(s)}$, with superscripts associated with the corresponding Minkowski t -channel, u -channel and s -channel OPE's respectively. (See Fig. 6.2(a).) As stress in Sec. 2.2, our choice of antipodal frame singles out the Minkowski t -channel description and it leads to our working with the region $M_s^{(t)}$, i.e., that associated with the t -channel OPE. This in turn leads to (1.2) as our causality condition.

The alternative and equivalent description would be to work with the region $M_s^{(u)}$, in the second quadrant in Fig. 6.2(a), corresponding changing (1.2) to

$$\langle 0 | [\varphi(x_2), \varphi(x_1)] [\varphi(x_4), \varphi(x_3)] | 0 \rangle \neq 0, \quad (6.1)$$

i.e., having x_{12} and x_{34} timelike. Operationally, this is simply $2 \leftrightarrow 4$ exchanging, Fig 6.1(b). Both can be associated with a CFT Regge limit [3–9, 12–15, 20], e.g., with Minkowski t -channel and u -channel OPE points $T' = (0, -1)$ and $U' = (-1, 0)$ labelled in Fig. 6.2(a). Both choices

allow a group theoretic interpretation. The third option leads to $M_s^{(s)}$, which can best be understood in a direct-channel picture. Group theoretically, with w and σ bounded in the range $[-1, 1]$, it suggests that, in place of the principal series, the discrete series for $SO(d, 2)$ is at play. This is a tantalizing possibility worth pursuing further.

The consideration above can equally apply to the t - and u -channel scatterings, e.g., leading to regions $M_t^{(s)}$, $M_t^{(u)}$, etc. This is consistent with the map from the first quadrant of the \sqrt{u} - \sqrt{v} into the whole plane¹⁸, resulting in 16 distinct regions, labelled appropriately in Fig. 6.2. We emphasize that we have adopted (1.2) and (1.3) in this paper as the causality conditions, associated with Minkowski t -channel OPE, by working with regions $M_s^{(t)}$ and $M_u^{(t)}$. We postpone to [52] a more detailed discussion on the connection to CFT Regge limits, together with their group theoretic interpretations.

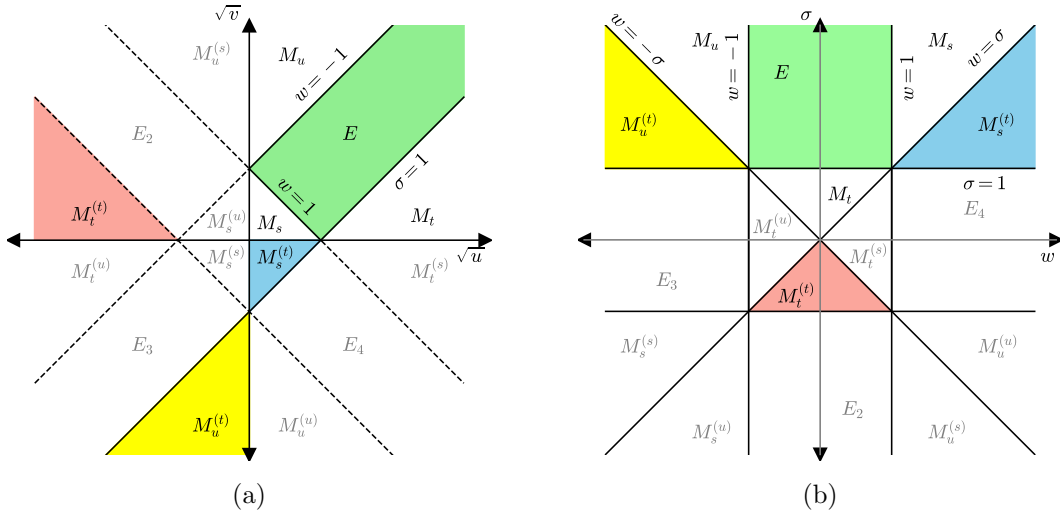


Figure 6.2: By extending to the whole \sqrt{u} - \sqrt{v} plane, it leads to 16 distinct regions in Fig. 2.2(a). In terms of new variables (w, σ) , the corresponding 16 regions are shown in Fig. 2.2(b). Special causal regions $M_s^{(t)}$, $M_u^{(t)}$, $M_t^{(t)}$ are shaded.

For the principal series representation, Eq. (1.6), we have focussed primarily on the s -channel discontinuity, $\text{Im } T_s$, now with an added subscript. Because of $w \leftrightarrow -w$ symmetry, it is simple to combine s -channel and u -channel discontinuities by forming signated discontinuities $\text{Im } T^{(\pm)}(w, \sigma) = \text{Im } T_s(w, \sigma) \pm \text{Im } T_u(-w, \sigma)$. This corresponds to the introduction of signated amplitudes $T^{(\pm)}(w, \sigma)$, as done in classical Regge theory, which, at fixed σ , can be represented by a one-side dispersion relation, (with branch cut along $\sigma < w < \infty$). (This approach allows one to deal with more general CFT applications with mixed s - u symmetry, e.g., see [15, 68].) Some of these issues relating to Minkowski scattering were already emphasized in Ref. [20], where the double sheeted structure of the u - v plane was resolved by taking square roots.

¹⁸For related discussions from a different perspective, see [66, 67].

There is another important issue relating to Eq. (1.6). Strictly speaking, to apply the principal series, functions over the group has to be square-integrable, with a resulting partial-wave amplitude $A(\tilde{\ell}, \tilde{\Delta})$ analytic when $0 < \text{Re } \tilde{\ell}$ ¹⁹. This condition is generically not met for CFTs ²⁰. This can be handled by a subtraction. An alternative approach is to allow $A(\tilde{\ell}, \tilde{\Delta})$ having isolated singularities in the right-half $\tilde{\ell}$ -plane, while distorting the contour for the $\tilde{\ell}$ integral in the principle series representation, Eq. (1.6), by staying to the right of these singularities, as discussed in Ref. [20]. (A subtraction can be interpreted as a contour distortion, e.g., accounting for the leading Regge poles.) As an explicit illustration, considered the case of Minkowski CFT_1 , i.e., $d = 1$, with zonal spherical function given by $Q_{-\ell}(w)$, (identifying $w = \cosh \eta$, $\sigma = 1$ and $\lambda = -1/2 + \tilde{\ell} = \ell - 1$). The partial-wave amplitude, upto a normalization factor, is given by

$$A(\ell) = \int_1^\infty dw \text{Im } T(w) Q_{\ell-1}(w). \quad (6.2)$$

This can be defined initially by keeping $\text{Re } \ell > \ell_0$ and then analytically continued so that $A(\ell)$ is analytic to the right of the line $\text{Re } \ell = \ell_0 = 2$.

It should also be stressed that the principal series representation is kinematic; dynamics for CFT is encoded in the analytic structure of the partial-wave amplitude. It is generally accepted that, for CFT, given (4.12), partial-wave amplitudes, for fixed ℓ is meromorphic in Δ , with pole positions fixed by OPE. Conversely, at fixed Δ , it is also reasonable to assume meromorphy in ℓ , as expected in Regge theories. It has been hypothesized in [3], at least for large-N based theories, these singularities can be simultaneously described by a family of spectral curves, $\tilde{\Delta}_\alpha(\ell)$, i.e., one has a generalized OPE expansion where partial-wave amplitude formally admits an expansion

$$A(\tilde{\ell}, \tilde{\Delta}) = \sum_\alpha \frac{r_\alpha(\ell)}{\tilde{\Delta}^2 - \tilde{\Delta}_\alpha(\ell)^2} = \sum_\alpha \frac{r_\alpha(\ell)}{2\tilde{\Delta}} \left(\frac{1}{\tilde{\Delta} - \tilde{\Delta}_\alpha(\ell)} + \frac{1}{\tilde{\Delta} + \tilde{\Delta}_\alpha(\ell)} \right) \quad (6.3)$$

This becomes immediately apparent in various examples where the spectral curves $\Delta(\ell)$ are symmetric about $\Delta = d/2$. See [3, 4, 6, 7, 9, 12–14, 20, 75–78] for further discussion.

We also see some of the discussion in Ref. [20] in new light, e.g., inversion for the principal series. In particular, the Bethe-Salpeter type equation for SYK-like models can be interpreted in the language of semigroups. Early works, motivated by works of Toller *et al.* on Regge physics [42] via 3 dimensional Lorentz group such as [43, 44, 48, 79, 80], are particularly interesting

¹⁹The subject of square integrability is dealt with appropriate generalizations of the Plancherel theorem. A discussion for Riemannian spaces can be found in [51, 69].

²⁰Discussions for the issue of asymptotic bounds for CFT amplitudes can be found in [3, 70, 71] (see also additional references therein). From a Regge perspective, this is due to the intercept of the so-called ‘‘Pomeron’’ being greater than 1 but bounded by 2 [3, 72]. For a historical perspective on the Pomeron and Bootstrap, see [73] and other contributions in [74].

from current perspective. The integral kernel is of Volterra type and preserves the causality constraints of the scattering region. For $d = 1$, it was shown in Ref. [20] that the partial wave amplitude, (6.2), is given by $A(\ell) = A_1(\ell)/(1 - k(\ell))$, with $k(\ell)$ given by a causal kernel, leading to $A(\ell)$ free of singularity to the right of ℓ_0 . In general, this diagonalization corresponds to a Laplace transform. Conversely, given the partial wave amplitude, the equivalent discontinuity can be reconstructed explicitly via an inverse Laplace transform. This requires invoking the relationship between Legendre functions of first and second kind,

$$P_{\tilde{\lambda}(z)-1/2}(q) = \frac{\cot \tilde{\lambda}\pi}{\pi} \left(Q_{\tilde{\lambda}-1/2}(q) - Q_{-\tilde{\lambda}-1/2}(q) \right). \quad (6.4)$$

(See [38] as well as Appendix E of Ref. [20].) This inversion procedure can be generalized for $d > 1$, framed in the language of spherical Laplace and Abel transforms [41]. This is an interesting application of the semigroup structure developed here. A related issue is the relation of the so-called Froissart-Gribov partial-wave to that obtained directly via $SO(2, 1)$ group theoretically, the so-called Toller analysis [48, 80]. This as well as the question of inversion for our causal harmonics will be explored further in [52].

Our results in this study develop a framework for discussing CFTs by putting the embedding space and the structure of causal symmetric spaces at its core. Our procedure of coset construction restricts us to a single Poincaré patch, avoiding the issues of infinite time windings on the AdS cylinder. Restricting ourselves to representations that trivially depend on the compact part of the Cartan subalgebra (i.e. $\tilde{m} = 0$) made the reduction of variable $(\zeta, \vec{b}_\perp) \rightarrow \eta$ possible. For applications to DIS or near forward scattering, an explicit dependence on \vec{b}_\perp is warranted²¹. Furthermore, studying the geometry of AdS in this perspective can also be very fruitful, e.g., the relationship between Legendre functions of first and second kind, (6.4), can be understood by relating the geometry of $H_2 = SO(2, 1)/SO(2)$ to the geometry of $\text{AdS}_2 = SO(2, 1)/SO(1, 1)$, (Appendix F).

Lastly, let us next turn to some issues on how to relate our work to that where one starts from Euclidean CFT. We have in mind that of [1, 21, 66, 88] and other related works, e.g., [75]. These are beyond the scope here, but nevertheless worth noting. First, it should be pointed out that what we considered as “discontinuity”, (1.4), in a direct Minkowski treatment, has been identified as a “double-discontinuity” in [1]. (See Appendix B.4.) Therefore, starting from a Minkowski treatment, one cannot obtain the Euclidean fourpoint function directly by a one-dimensional dispersion relation, e.g., by that in complex w -plane with $1 < \sigma$ fixed. That is, in

²¹In the short distance limit, it has long been known that BFKL physics [81, 82] involves aspects of Euclidean CFT_2 . For a comprehensive review, see [83]. This has also been done in various related studies such as [3–6, 8, 9, 12, 13, 25, 84–87] among others. Transverse dependence in $d = 4$ comes in via representation functions on $H_3 = SO(3, 1)/SO(3)$. From an AdS_5 perspective, the coordinates on H_3 are (\vec{b}_\perp, β) , where β is the bulk direction and $\vec{b}_\perp = (x, y)$.

terms of Figure 2.3, a dispersion integral at fixed σ , over $1 < \sigma < |w| < \infty$, does not directly leads to Euclidean CFT amplitude in region E , nor its natural continuation into regions M_s and M_u . It at best can be related to appropriate continuation and/or discontinuity of the Euclidean fourpoint function. Indeed, in Refs. [21], an interesting and a relatively involved analysis was carried out in relating the causal discontinuity, (1.4), to Euclidean fourpoint function in the region E , where $|w| < 1 < \sigma < \infty$. It would be interesting if the procedure of [21] can be adopted by making use of simultaneous analyticity in (w, σ) . Equally interesting is the group theoretic interpretation of the work of [75] where one arrives at a Minkowski inversion formula, equivalent to ours. Closer examination on the relation between these different approaches can be fruitful and some will be addressed further elsewhere.

Acknowledgements

The work of RCB is supported by the U.S. Department of Energy (DOE) under Award No. DE-SC0015845. PA is supported by the NUS Research Scholarship. We would like to thank S. Caron-Huot for correspondence and for commenting on a preliminary draft of this paper. We would also like to thank S. Rychkov, I. Burić, M. Isachenkov, and V. Schomerus for their comments. RCB and CIT would also like acknowledge earlier collaboration with J. Polchinski and M. Strassler which paved the way for the current CFT investigations.

A Summary of Notations

In this appendix, we highlight our notational usage, e.g., clarifying the notion of functions over $SO(d, 2)$, $F(g)$, to that over the physical space-time, $f(x_\mu)$ and/or the embedding space, $F(X_\alpha)$.

- Physical spacetime: x_μ : $\mu = 0, 1, \dots, d-1$. Lorentzian metric with signature: $(-, +, +, \dots)$. Occasional alternative notations: $x_\mu = (x_t, x_\perp, x_z)$, and lightcone coordinates: $x_\mu = (x^+, x^-, x_\perp)$ with $x^\pm = x_t \pm x_z$.
- Embedding space: X_α : $\alpha = -2, -1, 0, \dots, d-1$. Lorentzian metric with signature: $(-, +; -, +, +, \dots)$. The standard practice is to define the physical spacetime coordinates, x_μ , as an appropriate projection (a “slice”) of the null-cone, where $X^2 = 0$, thus reducing from $(d+2)$ to d degrees of freedom.
- Function over the physical space-time: $f(x)$, generically using lower letters.
- Function over the embedding space: $F(X)$, generically using capital letters, with X on the null-cone.

- Lifting from physical spacetime to embedding space: A function over the Minkowski spacetime, $f(x)$, can often be “lifted” as a function over the embedding space, $F(X)$, with X on the null-cone. When the context is clear, we often will use $F(X)$ and $f(x)$ interchangeably, e.g., the left-hand side of (1.6).
- Functions over $G = SO(d, 2)$: For each function over the null-cone, $F(X)$, we can introduce a function over G as follows. Let $X = g\hat{\xi}_0$, with $\hat{\xi}_0$ a fixed *base-point* on the null-cone. Since G acts transitively, $F(g\hat{\xi}_0)$ can be treated as a function over G . We will often adopt the same notation $F(g)$ as the group function, with $\hat{\xi}_0$ implicit.
- Functions of several variables: The above constructions generalize to the case of functions of several variables, i.e., $F(X_1, X_2, \dots) \rightarrow F(g_1, g_2, \dots)$. In order to avoid confusion with components X_α for individual embedding coordinate, we will often change notation for embedding variables from X_i to ξ_i , $i = 1, 2, \dots$. We also allow the option of having a different base-point for each g_i , as done in Sec. 3.
- Lie Groups and Associated Algebra: Will generically adopt capital letters, e.g., G, K, Q^\pm, \dots for groups, subgroups, etc.. Their corresponding algebra by capital script letters, $\mathcal{G}, \mathcal{K}, \mathcal{Q}^\pm, \dots$, e.g., generators for $G = SO(d, 2)$ are $\mathcal{L}_{A,B}$, $A, B = -2, -1, 0, \dots, d-1$. This is not followed religiously for various reasons: special considerations, historical, etc., (see below.)
- Basics for $SO(d, 2)$: There are $(d+2)(d+1)/2$ independent generators for $SO(d, 2)$, the same as for $SO(d+1, 1)$, with $\mathcal{L}_{AB} = -\mathcal{L}_{BA}$. Commutation relations for these generators are standard, which can be expressed compactly as,

$$[L_{AB}, L_{CD}] = \eta_{AC}L_{BD} + \eta_{BD}L_{AC} - \eta_{AD}L_{BC} - \eta_{BC}L_{AD}, \quad (\text{A.1})$$

with signature η . Considered as a diagonal matrix, we have $\text{diag } \eta = (-, +; -, +, +, +, \dots)$. We follow the convention where the subgroup generated by \mathcal{L}_{AB} is expressed as $g(\xi) = e^{\xi\mathcal{L}_{AB}}$, with ξ real, i.e., the convention typically adopted in mathematical texts. These commutation relations follow from the fact that $SO(d, 2)$ leaves the quadratic form, $X^2 = X^T\eta X = -X_{-2}^2 + X_{-1}^2 - X_0^2 + X_1^2 + X_2^2 + \dots + X_{d-1}^2$ invariant. In adjoint representation, matrix elements for each generator are real, $\mathcal{L}_{AB} = -\mathcal{L}_{BA}$, with

$$(\mathcal{L}_{AB})_{CD} = \eta_{AD}\delta_{CB} - \eta_{BD}\delta_{CA}. \quad (\text{A.2})$$

- Compact and Non-Compact Subgroups: Generators in adjoint representation, (A.2), are real. The group contains compact subgroups, with generators as *anti-symmetric* matrices, $(\mathcal{L}_{AB})_{CD} = -(\mathcal{L}_{AB})_{DC}$. For non-compact generators, their matrix elements are real and *symmetric*, i.e., $(\mathcal{L}_{AB})_{CD} = (\mathcal{L}_{AB})_{DC}$.

- Rotations and Boosts: In the usual physics usage, compact generators can be characterized as “rotations” and non-compact generators as “boosts”. We will often adopt the convention where compact generators (rotations) are indicated by $\mathcal{K} = (\mathcal{R}_{\alpha,\beta})$, and non-compact generators (boosts) are indicated by $\mathcal{P} = (\mathcal{B}_{\alpha,\beta})$. Although for the most part we will not need these explicit forms, it is nevertheless important to discuss some structural aspects. Illustrative examples for $d = 1, 2$, etc. will be provided below in Appendix C.
- Special Designations for $SO(d, 2)$: The generator for dilatation, $\mathcal{L}_{-1,-2} = -\mathcal{L}_{-2,-1}$ and the generator for Lorentz boost along the “longitudinal” direction, $\mathcal{L}_{d-1,0} = -\mathcal{L}_{0,d-1}$, are designated as D and L respectively. Some other special designations are also provided in Appendix C.2.

B Kinematics of Minkowski 4-Point CFT Amplitudes

This appendix serves several purposes. In B.1, we summarize relations among various sets of conventional variables, with emphasis on continuation beyond the Euclidean region, E . (Table-3(a).) In B.2, we discuss the relation between our group theoretic motivated variables, (w, σ) – expressed in terms of group parameters (y, η) – with the standard sets of variables. (Table-3(b).) In B.3, we provide a more qualitative description for the separation of scattering vs non-scattering regions in a Minkowski light-cone diagram. In B.4, a brief description of the “double discontinuity”, $\text{dDisc}G(\rho, \bar{\rho})$, of Ref. [1] and how it relates to $\text{Im}T(w, \sigma)$ adopted in this work is provided.

B.1 Cross Ratios (u, v) and Alternative Representations

In place of (u, v) , or, equivalently, the pair (\sqrt{u}, \sqrt{v}) , several equivalent sets of independent variables can be introduced, e.g., (z, \bar{z}) , $(\rho, \bar{\rho})$ and (q, \bar{q}) . In terms of the pair (z, \bar{z}) , their relationships are summarized in Table-3a.

Euclidean Region E and OPE Limits: By expressing (z, \bar{z}) in terms of (u, v) while staying within the Euclidean region E , one finds that $\bar{z} = z^*$ and $0 < |z| < \infty$. It also follows that $\bar{\rho} = \rho^*$ and $\bar{q} = q^*$. In particular, in the Euclidean region, one finds

$$\rho = \bar{\rho}^* = r e^{i\theta}, \quad 0 < r < 1, \quad -\pi < \theta < \pi. \quad (\text{B.1})$$

The t-channel OPE limit, associated with the partition $(1, 2)(3, 4)$, corresponds to $x_{12}^2, x_{34}^2 \rightarrow 0$, leading to $u \rightarrow 0, v \rightarrow 1$, or equivalently, the limit $(z, \bar{z}) \rightarrow (0, 0)$. For the Euclidean s-channel OPE, i.e., partition $(1, 3)(2, 4)$, one has $x_{13}^2, x_{24}^2 \rightarrow 0$, corresponding to $u \rightarrow +\infty, v \rightarrow +\infty$, or $(z, \bar{z}) \rightarrow (\infty, \infty)$, and for Euclidean u-channel OPE, partition $(1, 4)(2, 3)$, with $x_{14}^2, x_{23}^2 \rightarrow 0$, $u \rightarrow 1, v \rightarrow 0$, or $(z, \bar{z}) \rightarrow (1, 1)$.

(f_1, f_2)	$f_1(z, \bar{z})$	$f_2(z, \bar{z})$	(g_1, g_2)	$g_1(y, \eta)$	$g_2(y, \eta)$
(u, v)	$z \bar{z}$	$(1-z)(1-\bar{z})$	$(\sqrt{\rho}, \sqrt{\bar{\rho}})$	$e^{-(\eta \pm y)/2}$	$e^{-(\eta \mp y)/2}$
(\sqrt{u}, \sqrt{v})	$\sqrt{z} \sqrt{\bar{z}}$	$\sqrt{(1-z)} \sqrt{(1-\bar{z})}$	(\sqrt{u}, \sqrt{v})	$\frac{2}{(\cosh \eta + \cosh y)}$	$\frac{(\cosh \eta - \cosh y)}{(\cosh \eta + \cosh y)}$
$(\rho, \bar{\rho})$	$\frac{z}{(1+\sqrt{1-z})^2}$	$\frac{\bar{z}}{(1+\sqrt{1-\bar{z}})^2}$	$(\sqrt{\rho\bar{\rho}}, \sqrt{\rho/\bar{\rho}})$	$e^{-\eta}$	e^{-y}
$(\sqrt{\rho}, \sqrt{\bar{\rho}})$	$\frac{\sqrt{z}}{(1+\sqrt{1-z})}$	$\frac{\sqrt{\bar{z}}}{(1+\sqrt{1-\bar{z}})}$	(q, \bar{q})	$\cosh(\eta \pm y)$	$\cosh(\eta \mp y)$
(q, \bar{q})	$\frac{2-z}{z}$	$\frac{2-\bar{z}}{\bar{z}}$	(z, \bar{z})	$\text{sech}^2((\eta \pm y)/2)$	$\text{sech}^2((\eta \mp y)/2)$

(a)
(b)

Table 3: Relationship among variables commonly used in CFT studies. Option for signs in (b) are fixed by convention. With $\rho < \bar{\rho}$, we adopt the upper sign, e.g., (B.8).

The relations between (z, \bar{z}) and $(\rho, \bar{\rho})$ can also be expressed as

$$\rho = \frac{1 - \sqrt{1-z}}{1 + \sqrt{1-z}}, \quad \text{and} \quad \bar{\rho} = \frac{1 - \sqrt{1-\bar{z}}}{1 + \sqrt{1-\bar{z}}} \quad (\text{B.2})$$

One can avoid singularities at $z = 0$ and $z = 1$ by drawing branch cuts along $(-\infty, 0)$ and $(1, \infty)$. The “first-sheet” for the complex z -plane corresponds to the unit disk in ρ , Eq. (B.1).

Lorentzian Extension and Beyond: In moving outside of the region E , e.g., into regions M_s , M_u and M_t , variables (z, \bar{z}) are to be treated as independent variables. Access beyond the first quadrant in the \sqrt{u} - \sqrt{v} plane requires crossing $\sqrt{u} = 0$ and/or $\sqrt{v} = 0$. This is also equivalent to encircling singular points in (z, \bar{z}) at $(0, 0)$ and/or $(1, 1)$ appropriately. That is, with (u, v) as functions of (z, \bar{z}) , it leads to a multiple-sheeted structure. (See Refs. [4, 9, 12–14, 66, 67]).

This structure can be resolved by considering $\sqrt{\rho}$ and $\sqrt{\bar{\rho}}$. By inversion, one finds $z(\rho) = z(\rho^{-1})$ and $\bar{z}(\bar{\rho}) = \bar{z}(\bar{\rho}^{-1})$. The mapping is 1-to-2, dividing the ρ -plane into two regions, $|\rho| < 1$ and $|\rho| > 1$, reflecting again a two-sheeted structure. As functions of $\sqrt{\rho}$ and $\sqrt{\bar{\rho}}$, we have

$$\begin{aligned} \sqrt{z} &= 2(\sqrt{\rho^{-1}} + \sqrt{\rho})^{-1}, & \text{and} & & \sqrt{\bar{z}} &= 2(\sqrt{\bar{\rho}^{-1}} + \sqrt{\bar{\rho}})^{-1}, \\ \frac{1 - \sqrt{v}}{\sqrt{u}} &= \frac{1}{2} \left(\sqrt{\frac{\rho}{\bar{\rho}}} + \sqrt{\frac{\bar{\rho}}{\rho}} \right), & \text{and} & & \frac{1 + \sqrt{v}}{\sqrt{u}} &= \frac{1}{2} \left(\sqrt{\rho\bar{\rho}} + \frac{1}{\sqrt{\rho\bar{\rho}}} \right). \end{aligned} \quad (\text{B.3})$$

This also allows an extension, though less obvious, into the whole \sqrt{u} - \sqrt{v} plane.

The pair of variables q and \bar{q} also leads to kinematic simplification (Ref. [20]). Here we list just one useful relations $q = (\rho + \rho^{-1})/2 = (\sqrt{\rho} + \sqrt{\rho^{-1}})^2/2 - 1$ and $\bar{q} = (\bar{\rho} + \bar{\rho}^{-1})/2 = (\sqrt{\bar{\rho}} + \sqrt{\bar{\rho}^{-1}})^2/2 - 1$.

B.2 Group Theoretic Motivated Variables and Antipodal Frames

We next turn to a discussion of **antipodal frames**, thus providing a more intuitive understanding for invariants (w, σ) , Eq. (2.2),

$$\sqrt{u} = \frac{2}{\sigma + w}, \quad \sqrt{v} = \frac{\sigma - w}{\sigma + w} \quad \Leftrightarrow \quad w \equiv \frac{1 - \sqrt{v}}{\sqrt{u}}, \quad \sigma \equiv \frac{1 + \sqrt{v}}{\sqrt{u}}, \quad (\text{B.4})$$

equivalently, in terms of $(\rho, \bar{\rho})$,

$$w \equiv \cosh y = \frac{1}{2} \left(\sqrt{\frac{\rho}{\bar{\rho}}} + \sqrt{\frac{\bar{\rho}}{\rho}} \right), \quad \text{and} \quad \sigma \equiv \cosh \eta = \frac{1}{2} \left(\sqrt{\rho \bar{\rho}} + \frac{1}{\sqrt{\rho \bar{\rho}}} \right). \quad (\text{B.5})$$

Euclidean Antipodal Frame: For the Euclidean region E , the symmetry group is $SO(d+1, 1)$. Consider the frame where $x_1 = -x_2$ and $x_4 = -x_3$. Each pair corresponds to a diameter within a d -sphere, S^d , with varying radius. Let the relative angle between these two diameters be θ , e.g., $\cos \theta = \hat{x}_1 \cdot \hat{x}_4$. One can also treat the radius for each sphere as a new variable, and denote their ratio by e^τ . These configurations can be visualized as a **cylinder** of length τ , with two unit spheres as ends. This will be referred to as the **Euclidean antipodal frame** [61]. Group theoretically, τ can be identified with a non-compact boost in $SO(d+1, 1)$, leading to **radial-quantization**, and θ with a compact rotation angle. (Eq. (B.1) provides an alternative definition.) In this frame, $\sqrt{u} = 2/(\cosh \tau + \cos \theta)$ and $\sqrt{v} = (\cosh \tau - \cos \theta)/(\cosh \tau + \cos \theta)$, i.e., $\sigma = \cosh \tau$ and $w = \cos \theta = \hat{x}_1 \cdot \hat{x}_4$ (defined shortly via a Wick rotation), as done in [62]. Thus, in region E , $-1 \leq w \leq 1$ and $1 < \sigma < \infty$, Eq. (2.4).

Minkowski Antipodal Frame: For the kinematics of scattering in the Minkowski limit, (1.1), we can again adopt a special frame where the time-components of x_i are ordered oppositely, $-x_1^{(t)} = x_2^{(t)} > 0$ and $-x_3^{(t)} = x_4^{(t)} > 0$. To specify their spatial components, we identify a longitudinal direction, e.g., z -axis, and denote perpendicular components by $x_{\perp, i}$. This naturally lends to a **lightcone** description. (See Fig. 1.1, for a schematic representation.)

To be definite, we parametrize the time and longitudinal coordinates explicitly, with $x_1 = -x_2$ and $x_3 = -x_4$, leading to light-cone coordinates, $x^\pm = x_t \pm x_z$,

$$x_1^\pm = -x_2^\pm = \mp r_1 e^{\pm y/2} \quad \text{and} \quad x_3^\pm = -x_4^\pm = \pm r_3 e^{\mp y/2}, \quad (\text{B.6})$$

or, $(x_1^{(t)}, x_1^{(z)}) = -(x_2^{(t)}, x_2^{(z)}) = (-r_1 \sinh y/2, -r_1 \cosh y/2)$, and $(x_3^{(t)}, x_3^{(z)}) = -(x_4^{(t)}, x_4^{(z)}) = (-r_3 \sinh y/2, r_3 \cosh y/2)$. For transverse components, we choose, for simplicity,

$$x_{\perp, 1} = x_{\perp, 2} = b_\perp, \quad \text{and} \quad x_{\perp, 1} = x_{\perp, 2} = 0. \quad (\text{B.7})$$

We shall refer to this as **Minkowski Antipodal Frame**. (In [20], this is also referred to as the **double-lightcone** frame.) In this frame, evaluating u, v using (B.6) and (B.7), cross ratios can

again be expressed as in Eq. (2.2) and Eq. (2.5), i.e.,

$$1 < w \equiv \cosh y < \infty, \quad \text{and} \quad 1 < \sigma \equiv \cosh \eta = \cosh \zeta + b_{\perp}^2 < \infty.$$

Here, y parametrizes a Lorentz boost, ζ parametrizes a scale transformation, $\cosh \zeta = (r_1/r_3 + r_3/r_1)/2$, and b_{\perp} is the transverse separation between (12) and (34). (We have normalized $2r_1r_3 = 1$ with b_{\perp} dimensionless. See Ref. [20] for more details.) A similar analysis for the u-channel configurations, with $w \rightarrow -w$.

Relationship between Standard CFT Variables and Group Variables (w, σ) : With $w = \cosh y$ and $\sigma = \cosh \eta$, we can express other invariants commonly used in CFT studies as functions of group parameters (y, η) . This is summarized in Table-3b.

As a consistency check, as stated above, by starting with Minkowski antipodal frame, one can directly verify that $w = \cosh y = (1 - \sqrt{v})/\sqrt{u}$ and $\sigma = \cosh \eta = (1 + \sqrt{v})/\sqrt{u}$ i.e., Eq. (2.2), with $\cosh \eta = \cosh \zeta + b_{\perp}^2$. Note that this corresponds to a reduction to two invariants, i.e., either (w, σ) or one of the set from (\sqrt{u}, \sqrt{v}) , (z, \bar{z}) , $(\rho, \bar{\rho})$ or (q, \bar{q}) . For $d = 2, 4$, the choice $(\rho, \bar{\rho})$ or (q, \bar{q}) can also be understood group theoretically, in terms of the concept of Weyl chambers.

Wick Rotation: Consider transition between regions E and M_s . Starting in M_s , we adopt the convention, for group parameters y and η , $\rho = e^{-(\eta+y)}$ and $\bar{\rho} = e^{-(\eta-y)}$, with $0 < y < \eta$. (This also fixes the \pm sign convention in Table-3b.) For later convenience, let

$$t = \sqrt{\rho}/\sqrt{\bar{\rho}} = e^{-y}, \quad r = \sqrt{\rho}\sqrt{\bar{\rho}} = e^{-\eta}. \quad (\text{B.8})$$

Performing next a Wick rotation where $y \rightarrow i\theta$ and also re-express $\eta \rightarrow \tau$, one is led back to region E , with $\rho = \bar{\rho}^* = e^{-\tau + i\theta}$, (B.1), $\sqrt{u} = 2/(\sigma + w) = 2/(\cosh \tau + \cos \theta)$ and $\sqrt{v} = (\sigma - w)/(\sigma + w) = (\cosh \tau - \cos \theta)/(\cosh \tau + \cos \theta)$, as expected.

B.3 Minkowski CFT and Light-cone Diagram

The Minkowski kinematics have often been represented schematically by the use of **light-cone diagrams** [2–4, 6, 7, 9, 12–15, 20, 37]. Relative to any coordinate origin, the limit indicated in Fig. 1.1 covers the s-channel near-forward scattering, with x_{14} and x_{23} timelike. However, it can be shown that the diagram also involves *non-causal (Minkowski) scattering regions*, i.e., x_{14} and x_{23} spacelike. (That is, region M_s in Fig. 2.1. See also Fig. 3 in Ref. [2].)

A precise identification of these regions can be made either through the \sqrt{u} - \sqrt{v} plane or through our new set of variables, (w, σ) , Eq. (2.2). In an antipodal frame, Eq. (B.6), one easily verifies the causal condition, $x_{14}^2 = x_{23}^2 = (\sigma - w)$ and $0 < \eta < y < \infty$, Eqs. (2.6) and (2.7). Here, we provide a qualitative evidence for this fact.

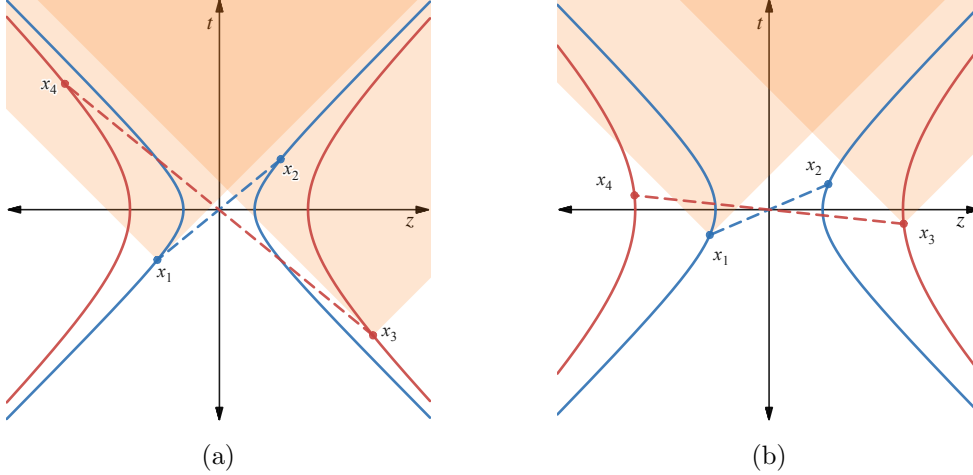


Figure B.1: Antipodal frame in the Minkowski causal-scattering and non-scattering settings respectively.

Fig. B.1a-b showcase a scattering and non-scattering setting respectively for $d = 2$. In Fig. B.1b, lightcones at x_1 and x_3 are shaded in orange to demonstrate that in the non-scattering case, all points are spacelike separated, with x_2 and x_4 outside of the respective lightcone. For the scattering case, Fig. B.1a, (x_1, x_4) and (x_3, x_2) are timelike separated.

It is possible to include transverse components schematically by treating the case of $d = 3$, e.g., Fig. 4 of Ref. [2], with Fig. B.1 as the 2-dim projection onto the t - z plane. Going from a scattering configuration to non-scattering requires increasing σ or lowering w thus broadens the difference in curvature of the two hyperbolae or brings the points in closer respectively. One moves from one region to the other by crossing the line $w = \sigma$. For u-channel, one interchanges x_3 and x_4 .

B.4 Double Discontinuity, $d\text{Disc } G(\rho, \bar{\rho})$, and $\text{Im } T(w, \sigma)$

In Ref. [1], Minkowski discontinuity, $\text{Im } T$, Eq. (1.6), has been related to analytically continued Euclidean fourpoint function G on the “second sheet” through the notion of “double-discontinuity”, denoted by $d\text{Disc } G$. Although we work exclusion with Minkowski CFTs in this study, it is nevertheless useful to spell out this connection thus allowing to clarify further our group theoretically motivated variables (w, σ) in this context. It is convenient to first make use of $(\rho, \bar{\rho})$ before turning to (w, σ) through the use (y, η) .

Given $G(\rho, \bar{\rho})$ in the Euclidean region, $\bar{\rho} = \rho^*$, we first extend into Region M_s where we adopt the convention $\rho = e^{-(\eta+y)}$ and $\bar{\rho} = e^{-(\eta-y)}$, with $0 < y < \eta < \infty$, i.e., $0 < \rho < \bar{\rho} < 1$. Continuation into s-channel scattering region corresponds to switching to $0 < \eta < y < \infty$, leading to $0 < \rho < 1 < \bar{\rho} < \infty$. This corresponds to crossing the line segment L_s , i.e.,

$1 < \sigma = w$. Whereas G is real in the region M_s , it turns complex into the scattering region, one must distinguish values below or above the cut starting at $\bar{\rho} = 1$.

Let's try to be more precise. Let $G(\rho, \bar{\rho}, \pm i\varepsilon)$ be two alternative continuations, from $0 < \bar{\rho} < 1$ to $1 < \bar{\rho} < \infty$, with $0 < \rho < 1$. In analogy with usual S-matrix, $S(\pm i\varepsilon) = \mathbf{I} \pm iT(\pm i\varepsilon)$, one defines Minkowski scattering amplitude $T(\pm i\varepsilon)$ through

$$G(\rho, \bar{\rho}, \pm i\varepsilon) = G_E \pm iT(\rho, \bar{\rho}, \pm i\varepsilon) \quad (\text{B.9})$$

The first factor G_E is evaluated at $(\rho, 1/\bar{\rho})$ where it is real. $T(\rho, \bar{\rho}, \pm i\varepsilon)$ over the cut can be expressed in terms of its real and imaginary parts,

$$T(\rho, \bar{\rho}, \pm i\varepsilon) = \mathcal{R} \pm i\mathcal{I}. \quad (\text{B.10})$$

It follows that

$$\mathcal{I} = G_E - \frac{1}{2}[G(\rho, \bar{\rho}, +i\varepsilon) + G(\rho, \bar{\rho}, -i\varepsilon)] \quad (\text{B.11})$$

and

$$\mathcal{R} = \frac{1}{2i}[G(\rho, \bar{\rho}, +i\varepsilon) - G(\rho, \bar{\rho}, -i\varepsilon)] \quad (\text{B.12})$$

In [1], $\mathcal{I}(\rho, \bar{\rho})$ is referred to as a double discontinuity, designated as $\text{dDisc } G$. (In [1], one makes one additional notational change by replacing $\bar{\rho}$ by $\bar{\rho}^{-1}$ for $G(\rho, \bar{\rho}, \pm i\varepsilon)$. We prefer not to do so to emphasize that causal discontinuity is evaluated in the region $0 < \rho < 1 < \bar{\rho} < \infty$.) One can next express $(\rho, \bar{\rho})$ in terms of (w, σ) , through (y, η) , e.g., (B.5) and (B.8). When $\text{dDisc } G(\rho, \bar{\rho})$ is expressed in terms of (w, σ) , it leads to $\text{Im } T(w, \sigma)$ in this study.

B.5 Illustrations for dDisc from a Spacetime Perspective

Ising Model in 1 + 1 dimensions: Consider the fourpoint correlator $\langle \sigma\sigma\sigma\sigma \rangle$. This is given upto a normalization by:

$$\mathcal{G}_E = \left| \frac{1}{(1-\rho^2)^{1/4}} \right|^2 + \left| \frac{\sqrt{\bar{\rho}}}{(1-\rho^2)^{1/4}} \right|^2 = \left(\frac{1 + \sqrt{u} + \sqrt{v}}{2(\sqrt{v})^{1/2}} \right)^{1/2} \quad (\text{B.13})$$

for Euclidean CFTs where $\bar{\rho} = \rho^*$. In going to the Minkowski space, we make $\rho, \bar{\rho}$ real and independent such that both are bounded at 1. In taking the double discontinuity in the s -channel scattering region step by step, the (u, v) variables prove to be more useful.

Consider first the points where x_{14} become timelike separated. This takes $v \rightarrow -v$ and we get:

$$\mathcal{G} = \left(\frac{1 + \sqrt{u} \pm i|\sqrt{v}|}{2(\pm i|\sqrt{v}|)^{1/2}} \right)^{1/2}, \quad (\text{B.14})$$

where $|\sqrt{v}|$ is positive in the region where a single commutator is non-vanishing. Therefore,

$$\begin{aligned} i \text{Disc}_{14}\mathcal{G} &\equiv \mathcal{G}(+i|\sqrt{v}|) - \mathcal{G}(-i|\sqrt{v}|) \\ &= \left(\frac{1 + \sqrt{u} + i|\sqrt{v}|}{2(|\sqrt{v}|)^{1/2}} \right)^{1/2} e^{-i\pi/8} - \left(\frac{1 + \sqrt{u} - i|\sqrt{v}|}{2(|\sqrt{v}|)^{1/2}} \right)^{1/2} e^{i\pi/8}. \end{aligned} \quad (\text{B.15})$$

For the double discontinuity, we take x_{23} timelike as well which takes us from $-v \rightarrow v$. This leads to another cut in the analytic continuation of $\text{Disc}_{14}\mathcal{G}$ such that $\pm i|\sqrt{v}| \rightarrow \pm|\sqrt{v}| \Rightarrow \pm|\sqrt{v}| \rightarrow \mp i|\sqrt{v}|$. Notice the sign change to \mp is indicative of being in the scattering region. Therefore,

$$\begin{aligned} 2i \text{dDisc}\mathcal{G} &\equiv \text{Disc}_{14}\mathcal{G}(+\sqrt{v}) - \text{Disc}_{14}\mathcal{G}(-\sqrt{v}) \\ &= 2i \left(\frac{1 + \sqrt{u} + |\sqrt{v}|}{2(|\sqrt{v}|)^{1/2}} \right)^{1/2} - 2i \cos(\pi/4) \left(\frac{1 + \sqrt{u} - |\sqrt{v}|}{2(|\sqrt{v}|)^{1/2}} \right)^{1/2} \end{aligned} \quad (\text{B.16})$$

Here, $|\sqrt{v}|$ is in the scattering region. Notice that the first term is visually similar to \mathcal{G}_E , but is evaluated with $|\sqrt{v}| = (\cosh y - \cosh \eta)/(\cosh y + \cosh \eta)$. That is, it is evaluated under a “swap” given by $(w, \sigma) \rightarrow (\sigma, w)$, which is analogous to the map $\bar{\rho} \rightarrow 1/\bar{\rho}$.

Therefore,

$$\begin{aligned} \text{dDisc}\mathcal{G} &= \frac{1}{\sqrt{2}} \left(\frac{1 + \sqrt{u} + |\sqrt{v}|}{(|\sqrt{v}|)^{1/2}} \right)^{1/2} - \frac{1}{2} \left(\frac{1 + \sqrt{u} - |\sqrt{v}|}{(|\sqrt{v}|)^{1/2}} \right)^{1/2} \\ &= \frac{\sqrt{2} \cosh y/2 - \cosh \eta/2}{(\cosh^2 y - \cosh^2 \eta)^{1/4}} = \frac{\sqrt{2}(1+w)^{1/2} - (1+\sigma)^{1/2}}{(4w^2 - 4\sigma^2)^{1/4}} \end{aligned} \quad (\text{B.17})$$

which is in agreement with [1].

Generalized Mean Field Theory: We can perform a similar analysis for the generalized Mean Field Theory where the fourpoint function in the Euclidean setting is given by:

$$\mathcal{G}_E = 1 + (u)^\Delta + \left(\frac{u}{v} \right)^\Delta. \quad (\text{B.18})$$

The double discontinuity is given by:

$$\text{dDisc}\mathcal{G} = \frac{2^{1+2\Delta} \sin^2(\Delta\pi)}{(w - \sigma)^{2\Delta}}. \quad (\text{B.19})$$

C Some Useful Aspects of $SO(d, 2)$

We quickly introduce special features for $SO(d, 2)$ in C.1, leading to Iwasawa decomposition. In C.2, we illustrate several important properties and, in particular, we discuss its root structure. In C.3, we discuss various useful group decompositions, e.g., generalized Cartan-type, $G = HAH$. This is done by making use of the more familiar example of $SL(2, R)$.

C.1 Iwasawa Decomposition for $SO(d, 2)$

The group $SO(d, 2)$ contains a maximal compact subgroup (MCSG), $K = SO(d) \times SO(2)$, with compact generators, \mathcal{K} . It also contains a rank-2 non-compact Maximal Abelian Subgroup (MASG), A , with generators \mathcal{A} , i.e., $\dim(\mathcal{A}) = 2$. It is useful to express its Lie Algebra in a Cartan decomposition, $\mathcal{G} = \mathcal{K} \oplus \mathcal{P}$. With $\dim(\mathcal{K}) = d(d-1)/2 + 1$, it follows that $\dim(\mathcal{P}) = 2d$. It can be shown that the space \mathcal{G} can be spanned by \mathcal{K} , \mathcal{A} and \mathcal{N}_+ , with $\dim(\mathcal{N}_+) = 2d - 2$. This subset, \mathcal{N}_+ , can be chosen to be a set of “positive roots”, leading to a set of nilpotents. (It is worth noting that, for $SO(d+1, 1)$, one has $\dim(\mathcal{K}) = d(d+1)/2$, $\dim(\mathcal{A}) = 1$, and $\dim(\mathcal{N}_+) = d$.) This leads to a unique group decomposition

$$G = PK = N^+AK, \quad (\text{C.1})$$

known as **Iwasawa decomposition**, where A and N^+ are generated by \mathcal{A} and \mathcal{N}_+ respectively. (See Appendix C.3 for a simple illustration for $d = 1$.)

This decomposition can be considered as a generalization of the Gram-Schmidt procedure for organizing the Lie algebra. Schematically, in this picture, for each group element, one can choose A to be diagonal, with positive entries, N^+ is upper triangular, with 1 on the diagonal and 0 in the lower half, and K consists of orthogonal matrices. The details in arranging for N^+ , the set of positive roots, is the same as that done for compact groups which involves specifying its root-space structure. This will serve as our starting point for constructing induced representations for non-compact Lie groups.

C.2 Illustrative Features and Root Space

Will provide here explicit illustrations for $d = 2$. In anticipating generalizing to $d = 4$, we shall denote the embedding coordinates by $(X_{-2}, X_{-1}; X_0, X_3)$, with the understanding that X_3 is associated with the longitudinal coordinate, i.e., the z-axis. (Instead of subscripts 0 and 3, we will write these occasionally as t and z when the context is clear. When moving to $d = 4$, we will occasionally replace subscripts 1 and 2 by x and y .)

The dimension for the algebra is now 6, with $\dim(\mathcal{K}) = 2$ and $\dim(\mathcal{P}) = 4$. Each generator can be represented by a real 4×4 matrix. Let us designate compact rotational generators in the two-dimensional space-like $(X_{-1}-X_3)$ and time-like $(X_{-2}-X_0)$ and planes as $K_1 = \mathcal{L}_{-1,3} = -\mathcal{L}_{3,-1}$ and $K_2 = \mathcal{L}_{0,-2} = -\mathcal{L}_{-2,0}$ respectively. From (A.2), each is an anti-symmetric 4×4 matrix, with mostly vanishing elements except for two, e.g., $K_1 = \begin{pmatrix} 0 & 1 \\ -1 & 0 \end{pmatrix}$, acting on the space-like plane $X_{-1}-X_3$. Similarly, one also has $K_2 = \begin{pmatrix} 0 & 1 \\ -1 & 0 \end{pmatrix}$, acting on the $X_{-2}-X_0$ plane.

Of four noncompact generators, we have already indicated that we denote the generator for

scaling as $D = \mathcal{L}_{-1,-2} = -\mathcal{L}_{-2,-1}$ and the generator for Lorentz boost along “longitudinal” direction as $L = \mathcal{L}_{3,0} = -\mathcal{L}_{0,3}$. Other two “mixed” boosts are $B_1 = \mathcal{L}_{3,-2} = -\mathcal{L}_{-2,3}$ and $B_2 = \mathcal{L}_{0,-1} = -\mathcal{L}_{-1,0}$. All are symmetric 4×4 matrices, with mostly vanishing elements except two. They all take on the form $\begin{pmatrix} 0 & 1 \\ 1 & 0 \end{pmatrix}$ when acting on their respective two-dimensional Lorentzian plane.

From these, we note the following special features:

- **Commuting pairs and Cartan Subalgebras:** There are three commuting pairs,

$$[K_1, K_2] = [L_{-1,3}, L_{0,-2}] = 0, \quad [B_1, B_2] = [L_{3,-2}, L_{0,-1}] = 0, \quad [D, L] = [L_{-1,-2}, L_{3,0}] = 0, \quad (\text{C.2})$$

which can be identified with the three sets of allowed Cartan subalgebras, with (D, L) and (B_1, B_2) as the possible generators for the (non-compact) MASG. For CFT considerations, we shall adopt $\mathcal{A} = (D, L)$ as that for the MASG. (The option of adopting the pair (B_1, B_2) will re-emerge when we consider causal symmetric space below.)

- **Basis for \mathcal{G} :** With $\dim(\mathcal{G}) = 6$, the natural choice for its basis would be the three pairs (K_1, K_2) , (D, L) and (B_1, B_2) . However, there are several more meaningful options, e.g., by forming the following combinations,

$$T_z = -K_1 + B_1, \quad T_t = -K_2 + B_2, \quad C_z = K_1 + B_1, \quad C_t = K_2 + B_2. \quad (\text{C.3})$$

In the context of CFT, T_t and T_z serve as generators of translations and C_t and C_z as that for special conformal transformations. When represented as 4×4 matrices,

$$T_t = \begin{pmatrix} 0 & 0 & -1 & 0 \\ 0 & 0 & 1 & 0 \\ 1 & 1 & 0 & 0 \\ 0 & 0 & 0 & 0 \end{pmatrix}, \quad T_z = \begin{pmatrix} 0 & 0 & 0 & 1 \\ 0 & 0 & 0 & -1 \\ 0 & 0 & 0 & 0 \\ 1 & 1 & 0 & 0 \end{pmatrix}, \quad (\text{C.4})$$

with C_t and C_z given by the transpose of T_t and T_z . It is easy to check that these are nilpotent, i.e., $T_t^3 = T_z^3 = C_t^3 = C_z^3 = 0$.

Another useful set obtained by forming lightcone combinations, is $T_\pm = T_t \pm T_z$ and $C_\pm = C_t \pm C_z$. These lead to a simple set of commutation relations with D and L ,

$$[L, T_\pm] = \pm T_\pm, \quad [L, C_\pm] = \mp C_\pm, \quad [D, T_\pm] = -T_\pm, \quad [D, C_\pm] = C_\pm \quad (\text{C.5})$$

- **Root Space and Positive Roots:** As a linear vector space, the basis for \mathcal{G} can also be chosen to consist of independent eigenvectors of linear transformation on \mathcal{G} . Denote elements of \mathcal{A} by \mathcal{A}_i , e.g., with $\mathcal{A}_1 = L$ and $\mathcal{A}_2 = D$. The action of each \mathcal{A}_i with other

generators X via commutators now serves as a linear map for the algebra. Since L and D commute, \mathcal{G} can be spanned by a set of simultaneous eigenvectors, $\{\mathcal{L}_\alpha\}$, each associated with a root vector, $\vec{\alpha} = (\alpha_1, \alpha_2)$, via

$$[\mathcal{A}_i, \mathcal{L}_\alpha] = \alpha_i \mathcal{L}_\alpha. \quad (\text{C.6})$$

It is well known that the root vectors are one dimensional subspaces. That is, each root vector corresponds to a unique generator in the algebra. It can also be shown that, for $SO(d, 2)$, the root space spectrum of each element of \mathcal{A} takes on values $\{-1, 0, 1\}$.

It is useful to first focus on a decomposition according to eigenvalues relative to each \mathcal{A}_i . For instance, for L ,

$$\mathcal{G} = \mathcal{G}(-1, L) \oplus \mathcal{G}(0, L) \oplus \mathcal{G}(1, L), \quad (\text{C.7})$$

where $\mathcal{G}(\lambda, L)$ is the set with eigenvalue $\lambda = 0, \pm 1$. Clearly, $\mathcal{G}(0, L) = (L, D)$. From commutation relations given above, one has $\mathcal{G}(1, L) = (T_+, C_-)$ and $\mathcal{G}(-1, L) = (T_-, C_+)$. Similarly, $\mathcal{G} = \mathcal{G}(-1, D) \oplus \mathcal{G}(0, D) \oplus \mathcal{G}(1, D)$, with $\mathcal{G}(0, D) = (L, D)$, $\mathcal{G}(1, D) = (C_+, C_-)$ and $\mathcal{G}(-1, D) = (T_+, T_-)$.

This also leads to a natural decomposition of the group algebra dictated by its spectrum on each generator in the Cartan subalgebra, \mathcal{A} , i.e., associating generators as simultaneous eigenvectors of (L, D) , with eigenvalue, (root-vector), (α_1, α_2) . The allowed non-zero roots are $(1, 1)$, $(1, -1)$, $(-1, 1)$ and $(-1, -1)$, associated with generators, C_- and T_+ , C_+ and T_- respectively. Together with L and D , associated with the zero root, $(0, 0)$, they can serve as a basis for the group algebra.

Given a specific ordering, (α_1, α_2) , it selects out the set of positive roots, defined by:

$$\begin{aligned} \alpha_1 > 0, \quad \alpha_2 \in \{-1, 0, 1\}, \\ \text{or} \quad \alpha_1 = 0, \quad \alpha_2 > 0. \end{aligned} \quad (\text{C.8})$$

Associated with positive roots $(1, 1)$ and $(1, -1)$ are C_- and T_+ respectively. Other root vectors are C_+ and T_- , associated with roots $(-1, 1)$ and $(-1, -1)$.

- **Cayley Basis:** We can perform a change of basis such that the MASG A is diagonal. A familiar example of this is the map from $SO(2, 1)$ to $SL(2, R)$ which we shall discuss in the next subsection. (See Eq. (C.10).) For $SO(2, 2)$, however, there is a choice in the ordering of MASG. Let us adopt the order (L, D) , where, in this basis, the Lorentz boost generator L only has non-vanishing diagonal in the first and fourth entries, and scaling D has non-vanishing second and third entries. The nilpotents, corresponding to positive roots, $N_t^+(t_+) = e^{t_+(T_t+T_z)}$ and $N_c^+(c_-) = e^{c_-(C_t-C_z)}$, can be shown to take upper triangular forms. That is, with this choice for the Cayley basis, $a_L(y) = e^{\xi D}$, $a_D(\xi) = e^{\xi D}$, $N_t^+(t_+)$

and $N_c^+(c_-)$ are

$$\begin{pmatrix} e^y & 0 & 0 & 0 \\ 0 & 1 & 0 & 0 \\ 0 & 0 & 1 & 0 \\ 0 & 0 & 0 & e^{-y} \end{pmatrix}, \begin{pmatrix} 1 & 0 & 0 & 0 \\ 0 & e^\xi & 0 & 0 \\ 0 & 0 & e^{-\xi} & 0 \\ 0 & 0 & 0 & 1 \end{pmatrix}, \begin{pmatrix} 1 & -2t_+ & 0 & 0 \\ 0 & 1 & 0 & 0 \\ 0 & 0 & 1 & 2t_+ \\ 0 & 0 & 0 & 1 \end{pmatrix}, \begin{pmatrix} 1 & 0 & -2c_- & 0 \\ 0 & 1 & 0 & 2c_- \\ 0 & 0 & 1 & 0 \\ 0 & 0 & 0 & 1 \end{pmatrix}. \quad (\text{C.9})$$

Let us stress that the choice of Cayley basis corresponds to a particular ordering for positive roots, e.g., (L, D) , which affects which of the nilpotents are in this upper triangular form. This is equivalent to saying that the ordering of roots dictates the set N^+ . The Iwasawa decomposition is best understood in this Cayley basis where the Cartan subalgebra becomes diagonal.

C.3 Group Decompositions

We provide a simple illustration for the difference between Iwasawa and Cartan decompositions by considering $SO(2, 1)$. Instead of working with 3×3 matrices, we will instead consider the equivalent $SL(2, R)$ by working with real 2×2 matrices. There are three generators, one compact and two non-compact. Consider

$$X_0 = (1/2) \begin{pmatrix} 0 & 1 \\ -1 & 0 \end{pmatrix}, \quad X_1 = (1/2) \begin{pmatrix} 1 & 0 \\ 0 & -1 \end{pmatrix}, \quad X_2 = (1/2) \begin{pmatrix} 0 & 1 \\ 1 & 0 \end{pmatrix}. \quad (\text{C.10})$$

- **Iwasawa Decomposition:** Let us adopt $A = X_1$ as the generator for the MASG and X_0 as the generator for the compact subgroup K . Consider $\mathcal{N}^\pm = X_0 \pm X_2$, i.e., $\mathcal{N}^+ = \begin{pmatrix} 0 & 1 \\ 0 & 0 \end{pmatrix}$, which is upper triangular. One easily verifies that \mathcal{N}^\pm are root vectors, $[X_1, \mathcal{N}^\pm] = \pm \mathcal{N}^\pm$, with \mathcal{N}^+ being the positive root. For each element of the group, Iwasawa decomposition corresponds to $g(\theta, \eta, \xi) = k(\theta)a(\eta)n(\xi)$ where

$$k(\theta) = \begin{pmatrix} \cos \frac{\theta}{2} & \sin \frac{\theta}{2} \\ -\sin \frac{\theta}{2} & \cos \frac{\theta}{2} \end{pmatrix}, \quad a(\eta) = \begin{pmatrix} e^{\frac{\eta}{2}} & 0 \\ 0 & e^{-\frac{\eta}{2}} \end{pmatrix}, \quad n(\xi) = e^{\xi \mathcal{N}^+} = \begin{pmatrix} 1 & e^\xi \\ 0 & 1 \end{pmatrix}. \quad (\text{C.11})$$

- **Cartan Decomposition:** In addition to Iwasawa decomposition, another useful decomposition is of the Cartan type. Consider generalizations of Eulerian decomposition for $SO(3)$, $g(\varphi, \theta, \psi) = k_z(\varphi)k_y(\theta)k_z(\psi)$. For $SO(2, 1)$, there are two possibilities. Again fixing X_1 for the MASG, one involves K and the other involves H , generated by X_2 , i.e.,

$$g(\varphi, \eta, \psi) = k(\varphi)a(\eta)k(\psi), \quad \text{and} \quad g(\xi, \eta, \xi') = h(\xi)a(\eta)h(\xi'). \quad (\text{C.12})$$

where

$$h(\xi) = e^{\xi X_2} = \begin{pmatrix} \cosh \frac{\xi}{2} & \sinh \frac{\xi}{2} \\ \sinh \frac{\xi}{2} & \cosh \frac{\xi}{2} \end{pmatrix} \in H. \quad (\text{C.13})$$

These are Cartan type of decompositions. The first is of the type $G = KAK$, i.e., it involves a compact subgroup K . The second involves a non-compact subgroup, H , and will be referred to as the $G = HAH$ type.

D Causal Symmetric Spaces

In this appendix, we provide a background discussion to *non-Riemannian symmetric spaces*, or, more precisely, *causal symmetric spaces* [41]. This step is necessary in formulating **causality** for CFT group theoretically. In D.1, we discuss spacetime as a Symmetric Space. In D.2, we provide a first look at the Causal Semigroup. In D.3, we finally discuss causal semigroup for four-point CFT Amplitude.

The defining property of Riemannian spaces is that the separation between any two points on the manifold is positive definite. By way of two simple examples, i.e., $S_2 = SO(3)/SO(2)$ and $H_2 = SO(2,1)/SO(2)$ respectively, we briefly discussed coset construction of *Riemannian symmetric spaces* of the form G/H , with H compact. Although instructive, these spaces are not sufficient for discussing Lorentzian physics directly as the salient feature of Minkowski spacetime is that it admits a causal structure. That is, on the spacetime manifold, separation between two events can be positive, null or negative. Therefore, these spaces admit a lightcone description of causality. As stated earlier, these are *non-Riemannian causal symmetric spaces*. To understand spherical harmonics appropriate for studying Minkowski CFTs, we need to understand these causal symmetric spaces from a group theoretic perspective.

D.1 Spacetime as a Symmetric Space

The group $SO(d,2)$ can be realized via the exponentiation of $(d+2)(d+1)/2$ generators, (see Appendix-C). In Sec. 4, a *Cartan decomposition* for the Lie algebra, $\mathcal{G} = \mathcal{K} \oplus \mathcal{P}$ was introduced, where \mathcal{K} stands for generators for the maximal compact subgroup. We have also identified a particular set of non-compact generators, $\mathcal{A} = \{D, L\}$, $\mathcal{A} \subset \mathcal{P}$, as the preferred set of maximal Abelian subgroup in G .

The standard Cartan decomposition, $\mathcal{G} = \mathcal{K} \oplus \mathcal{P}$, corresponds to having an involution, s , with $s^2 = 1$, where $s(\mathcal{K}) = \mathcal{K}$ and $s(\mathcal{P}) = -\mathcal{P}$. In this section, we will introduce another decomposition, $\mathcal{G} = \mathcal{H}_0 \oplus \mathcal{Q}_0$, which is more useful in dealing with causality issues [38, 40]. This corresponds to introducing another involution, Θ , where $\Theta(\mathcal{H}_0) = \mathcal{H}_0$ and $\Theta(\mathcal{Q}_0) = -\mathcal{Q}_0$, with $\mathcal{G} = \mathcal{H}_0 \oplus \mathcal{Q}_0$. This new involution is compatible with that for the standard involution s in the sense that its MASG, \mathcal{A}_0 , can be chosen to also lie in \mathcal{P} , i.e., $\mathcal{A}_0 \subset \mathcal{P} \cap \mathcal{Q}_0$ [41].

It is important to consider the role of coordinate origin, $x_\mu = 0$, which lies on the null-cone at $\xi_0 = (1, 1; 0, 0, \dots)$. By construction, we have $Q^- \xi_0 = \xi_0$. Special attention should also be

paid to the subgroup H_0 associated with the algebra $\mathcal{H}_0 = \mathcal{L} \oplus D$, which serves as the isometry group of the point $\xi_0 = (1, 1; 0, 0, \dots)$, upto an overall scaling. That is, an element $h \in H_0$ acting on ξ_0 gives $h \cdot \xi_0 = (a, a; 0, 0, \dots) = a \xi_0$. For $d = 4$, the set $\mathcal{H}_0 = \mathcal{L} \oplus D$ consists of 7 elements,

$$\mathcal{H}_0 = \mathcal{L} \oplus D = \{B_{01}, B_{02}, B_{03} = L; R_{12}, R_{31}, R_{23}\} \oplus \{D\}. \quad (\text{D.1})$$

That is, \mathcal{L} consists of 6 generators, 3 for rotations and 3 for boosts. In particular, D is central in \mathcal{H}_0 , i.e., it commutes with all other generators. State it more simply, for $d = 4$, \mathcal{H}_0 consists of Lorentz generators and dilations. For $d = 2$, however, the set \mathcal{H}_0 is much smaller, consisting of only two elements $\mathcal{H}_0 = \{L, D\}$. We also note that the subalgebra \mathcal{Q}_0 , consists of $\mathcal{Q}_0 = \mathcal{Q}^- \oplus \mathcal{Q}^+$. Both associated subgroups Q^\pm are abelian.

The pair $(\mathcal{G}; \mathcal{H}_0)$ can be used to define a symmetric space ²². In particular, the quotient space

$$\mathcal{M} = G/H_0Q^- \quad (\text{D.2})$$

can be associated with our spacetime manifold. The construction here is the Lorentzian counterpart for the Euclidean spacetime identification $\mathcal{M}_E = G/MAN^-$ made in [39] where the subgroup MAN^- is maximal parabolic in $SO(d+1, 1)$. Similarly, H_0Q^- is a maximal parabolic in $SO(d, 2)$.

Generators of translations, traditionally denoted as \mathcal{T}_μ , are realized in the embedding space as discussed in App. C. To understand this identification intuitively, this means that the group parameters for Q^+ are the coordinates on the spacetime manifold, and they therefore act transitively on it. A generic element of Q^+, Q^- is given by:

$$Q^+(a^\mu) = \begin{pmatrix} 1 + a^2/2 & a^2/2 & a_\mu \\ -a^2/2 & 1 - a^2/2 & -a_\mu \\ a^\mu & a^\mu & \text{diag}(\mathbf{1}_d) \end{pmatrix}; \quad Q^-(b^\mu) = \begin{pmatrix} 1 + b^2/2 & -b^2/2 & (b^\mu)^t \\ b^2/2 & 1 - b^2/2 & (b^\mu)^t \\ (b_\mu)^t & -(b_\mu)^t & \text{diag}(\mathbf{1}_d) \end{pmatrix}. \quad (\text{D.3})$$

Transitive action of Q^+ on the spacetime manifold can be shown by projecting down onto ξ_0 , thus recovering our parabolic slice:

$$Q^+(x^\mu) \cdot \xi_0/2 = Q^+(x^\mu) \cdot \left(\frac{1}{2}, \frac{1}{2}; 0, \dots\right) = \left(\frac{1+x^2}{2}, \frac{1-x^2}{2}; x^\mu\right). \quad (\text{D.4})$$

D.2 A First Look at the Causal Semigroup

Our spacetime manifold \mathcal{M} thus obtained admits a causal structure in the sense that it carries a natural definition of lightcones. That is, for any given point $a \in \mathcal{M}$, we have a set of points b

²²The structure theory of symmetric spaces can be rather involved [41]. Here, we try to present the minimum required for our discussion. In particular, it needs to be shown that the following commutation relations hold: $[\mathcal{H}, \mathcal{H}] \subset \mathcal{H}; [\mathcal{H}, \mathcal{Q}] \subset \mathcal{Q}; [\mathcal{Q}, \mathcal{Q}] \subset \mathcal{H}$. This is true for all variations of $(\mathcal{G}, \mathcal{H})$ presented in this work.

in the future of a such that $(a - b)^2 \leq 0$ and $a_t \leq b_t$. The set of group transformations that take $a \rightarrow b$ form a semigroup in $SO(d, 2)$. A semigroup structure is characterized by the absence of an inverse. Intuitively, this can be understood by the fact that the future point b has a past lightcone which contains a , along with all other points c such that $(c - b)^2 \leq 0$ and $b_t \geq c_t$. (That is, the point b itself does not have any information about its past.)

For our choice of basepoint, this condition is trivially satisfied by time translations, Lorentz group and dilatations under the constraints that $x_t > 0$, where x_t is the time translation parameter. That is, the semigroup relative to the origin ξ_0 ,

$$S_0 = \{g \in G \mid \xi_0 \leq g \cdot \xi_0\}. \quad (\text{D.5})$$

can be expressed as

$$S_0 = H_0 \exp x_t \mathcal{T}_0. \quad (\text{D.6})$$

where the generators for H_0 are $\mathcal{H}_0 = \mathcal{L} \oplus D$, given earlier, (D.1). Any point x_a in the forward lightcone of the basepoint can be written as $\xi_a = S_0 \cdot \xi_0$.

Recall that the generator of time translations in the embedding formulation can be realized as $\mathcal{T}_0 = \mathcal{B}_{-1,0} + \mathcal{R}_{-2,0}$. These two generators, $\mathcal{B}_{-1,0}$ and $\mathcal{R}_{-2,0}$, have a special place in the structure theory of causal symmetric spaces. The non-compact generator $\mathcal{B}_{-1,0}$ is often called the *cone generating element* in \mathcal{Q}_0 . The compact rotation $\mathcal{R}_{-2,0}$ defines a gradation on \mathcal{G} such that $\mathcal{G}(0, R_{-2,0}) = \mathcal{K}$ are generators for the maximal compact subgroup. (That is, we have a decomposition analogous to Eq. (C.7) such that $\mathcal{G} = \mathcal{G}(-1, R_{-2,0}) \oplus \mathcal{G}(0, R_{-2,0}) \oplus \mathcal{G}(1, R_{-2,0})$.) Together with D , they form an $SO(2, 1)$ subalgebra. In general, given the symmetry group $SO(d, 2)$, $R_{-2,0}$ is the central element of \mathcal{K} in \mathcal{K} . With a choice of \mathcal{H} , there is a central element Y of \mathcal{H} in \mathcal{H} . Taking the commutator $[R_{-2,0}, Y]$ and completing the $SO(2, 1)$ algebra gives the cone generating element.

The cone generating element, $\mathcal{B}_{-1,0}$, also belongs to the set \mathcal{A}_0 , which allows an analogous Iwasawa-like decomposition

$$S_0 \subset N_0^+ A_0 H_0. \quad (\text{D.7})$$

The set of positive roots N_0^+ is ordered such that the cone generating element is the leading root [41]. That is, fixing \mathcal{H} not only determines \mathcal{A} completely, it also tells us the ordering with respect to which positive roots are defined in the induced representation picture. Therefore, fixing the cone-generating element determines the Weyl vector $\vec{\rho}$ and hence plays a central role in determining the leading behaviour of representation functions defined over the semigroup (see Sec. 3). We also note that this is where the ambiguity pointed out earlier (in section 3.2) is resolved. The subalgebra \mathcal{A} used for induced representations is maximal abelian in $\mathcal{Q} \cap \mathcal{P}$.

For the purposes of harmonic analysis, a particularly important decomposition of the causal

semigroup is a Cartan-like decomposition of the form:

$$S_0 = H_0 A_{0+} H_0 \quad (\text{D.8})$$

where A_{0+} is a subset of $\mathcal{A}_0 = \{\mathcal{B}_{-1,0}, \mathcal{B}_{-2,3}\}$, the maximal abelian subalgebra in $\mathcal{Q}_0 \cap \mathcal{P}_0$ introduced earlier. As was outlined in Sec. 3, for CFTs, we will be interested in studying the H -bi-invariant zonal spherical functions. A Cartan-like decomposition makes the identification of these functions more natural. The restriction to A_{0+} is such that boost parameters satisfy the inequality

$$\text{param}(\mathcal{B}_{\beta_0}) - \text{param}(\mathcal{B}_{\alpha_3}) > 0 \quad (\text{D.9})$$

to ensure the final point lies in the forward lightcone. This can be shown by considering points $\xi = A_0 \cdot \xi_0$ and imposing the constraint that $(x - x_0)^2 < 0$. It is worth stressing that the choice of maximal abelian subalgebra is associated with the choice of basepoint ξ_0 .

Let the subgroup A_0 be parametrized by (y_0, η_0) . The basepoint of interest is $\xi_0 = \{1, 1; 0, 0\}$, which maps to the origin of the spacetime manifold. Under action of A_0 , this point moves and is given by:

$$\xi = \begin{pmatrix} \cosh \eta_0 & 0 & 0 & \sinh \eta_0 \\ 0 & \cosh y_0 & \sinh y_0 & 0 \\ 0 & \sinh y_0 & \cosh y_0 & 0 \\ \sinh \eta_0 & 0 & 0 & \cosh \eta_0 \end{pmatrix} \begin{pmatrix} 1 \\ 1 \\ 0 \\ 0 \end{pmatrix} = \begin{pmatrix} \cosh \eta_0 \\ \cosh y_0 \\ \sinh y_0 \\ \sinh \eta_0 \end{pmatrix} \quad (\text{D.10})$$

On the spacetime manifold, this point maps to:

$$x = (t, z) = \left(\frac{\sinh y_0}{\cosh \eta_0 + \cosh y_0}, \frac{\sinh \eta_0}{\cosh \eta_0 + \cosh y_0} \right). \quad (\text{D.11})$$

Requiring this point to lie in the forward lightcone of $x_0 = (0, 0)$ leads to:

$$x^2 - x_0^2 < 0 \quad (\text{D.12})$$

$$- \sinh^2 y_0 + \sinh^2 \eta_0 < 0 \quad (\text{D.13})$$

which leads to our causal condition:

$$y_0 - \eta_0 > 0; \quad y_0 > 0. \quad (\text{D.14})$$

This analysis applies for general d in the antipodal frame where $\vec{b}_\perp = 0$. For non-zero impact parameter, we discussed similar constraints in Sec. 5.5.

D.3 Causal Semigroup for Four-point CFT Amplitude

As we have shown in Sec. 3 that, for causal consideration CFT amplitude, it is necessary to consider semigroup relative to a basepoint other than ξ_0 . A generic point x_a on the manifold

can be arrived at from the basepoint by some transformation $\tilde{g} \in G$. Therefore, we find that the semigroup S_a with respect to the basepoint $\xi_a = \tilde{g} \cdot \xi_0$ given by

$$S_a = \tilde{g} \cdot S_0 \cdot \tilde{g}^{-1} \quad (\text{D.15})$$

That is, the semigroup at any point ξ_a on the manifold can be obtained via a shift by \tilde{g} where $\tilde{g} \cdot \xi_0 = \xi_a$. With similarly shifted generators, one has a different set of maximal abelian subgroup, $\mathcal{A}_a = \tilde{g} \mathcal{A}_0 \tilde{g}^{-1}$, cone generating element, etc.

As was discussed in Sec. 3.2, the relevant basepoint can be chosen to be the point $\xi_a = \{1, 0; 0, 0, 0, 1\}$, which can be translated from ξ_0 by

$$\tilde{g} = \exp\left(\frac{\pi}{2} \mathcal{R}_{-1,3}\right). \quad (\text{D.16})$$

This translates from S_0 to S_a by conjugation, i.e., $S_a = \tilde{g} \tilde{S}_0 \tilde{g}^{-1}$. Therefore, in terms of algebra we have that, after conjugating $\mathcal{H} = \tilde{g} \mathcal{H}_0 \tilde{g}^{-1}$, for $d = 2$,

$$\mathcal{H} = \{B_{-2,z}, B_{-1,t}\}. \quad (\text{D.17})$$

For $d = 4$,

$$\mathcal{H} = \{B_{-2,z}, B_{-1,t}, R_{-1,x}, R_{-1,y}, B_{tx}, B_{ty}, R_{xy}\} \quad (\text{D.18})$$

where $B_{-2,z}$ is central. More explicitly, the causal condition for the semigroup relative to ξ_a becomes

$$S_a = \{g \in G \mid \xi_a \leq g \cdot \xi_a\}. \quad (\text{D.19})$$

and it can be expressed as

$$S_a = H \exp x_t T_a, \quad (\text{D.20})$$

where $T_a = \tilde{g}(R_{-2,t} + B_{-1,t})\tilde{g}^{-1} = R_{-2,t} + L$, with L as the cone generating element. The generators for the MASG, A , are $\mathcal{A} = \tilde{g} \mathcal{A}_0 \tilde{g}^{-1} = \{L, D\}$. More interestingly, the semigroup can now be expressed as

$$S_a = H A_+ H \quad (\text{D.21})$$

The restriction on A_+ , changing from (D.9), is $y - \eta > 0$. Note that this is precisely the condition defining the physical causal scattering discussed in Sec. 2.2.

E Spherical Functions for $SO(3)$

We review the concept of spherical functions by looking at the simple example of $SO(3)$. Here, we shall adopt a procedure more appropriate for an induced representation, with emphasis on the coset construction.

Spherical Functions and Coset: In terms of Euler angles, each group element can be parametrized as a product, e.g., $g(\varphi, \theta, \psi) = R_z(\varphi)R_y(\theta)R_z(\psi)$. For the familiar case of $SO(3)$, a UIR corresponds to eigenfunction of the Casimir operator with the eigenvalue $\lambda = \ell(\ell + 1)$, where ℓ is a non-negative integer. A function over the group can be expanded in terms of a set of Wigner D -functions, $F(g) = \sum_{\ell} \sum_{m,n} f_{mn}^{\ell} D_{mn}^{\ell}(\varphi, \theta, \psi)$, $-\ell \leq m, n \leq \ell$.

Consider next functions over a coset G/K . By choosing $K = R_z(\psi)$, the coset $SO(3)/SO(2)$ can be identified with $R_z(\varphi)R_y(\theta)$. As a manifold, it corresponds to S^2 , which can be parametrized by two variables, (φ, θ) . The subgroup K can be understood as isometries of a **basepoint** ξ_0 in the embedding space, e.g., a point on the z-axis, $k \cdot \xi_0 = \xi_0$. Functions over this coset can be expanded in terms of a restricted set of Wigner functions independent of ψ , i.e., the subset $D_{m,0}^{\ell}(\varphi, \theta, \psi) = Y_{\ell,m}(\theta, \varphi)$, which is $(2\ell + 1)$ -dimensional. These are **spherical functions** for $SO(3)$ relative to the subgroup $SO(2)$.

Zonal Spherical functions and Two-sided Coset: These spherical functions, $Y_{\ell,m}$, can also be characterized by the condition of “right- K -invariance”, $F(gk) = F(g)$, with $k \in SO(2)$, consistent with Eq. (4.4). However, they are not “left- K -invariant”, $F(kg) \neq F(g)$, i.e., a left-rotation mixes $Y_{\ell,m}(\theta, \varphi)$ with $Y_{\ell,m'}(\theta, \varphi')$. The exception is the special vector $m = 0$, i.e., $Y_{\ell,0}(\theta, \varphi) = P_{\ell}(\cos \theta) = \langle \ell 0 | D_{00}^{\ell}(\varphi, \theta, \psi) | \ell 0 \rangle$, which can be considered as a function over the two-sided coset, $K \backslash G/K$. (We adopt the convention where the two-sided coset is denoted by $G//K$.)

This further reduction leads to an invariant subspace, the **zonal spherical functions** for $SO(3)$, consisting of Legendre functions of the first kind, $P_{\ell}(\cos \theta)$. They can also be characterized by the K bi-invariant condition,

$$f(kgk') = f(g). \quad (\text{E.1})$$

This is analogous to Eq. (3.12), except for the fact that $k, k' \in SO(2)$, which is compact.

Integral Representation and Inductive Character: Spherical harmonics for $SO(3)$ can be given by an integral representation ²³

$$Y_{\ell,m}(\theta, \varphi) = \langle \ell, m | g(\varphi, \theta, \psi) | \ell, 0 \rangle = c_{\ell,m} e^{im\varphi} \int_0^{2\pi} (\cos \theta + i \sin \theta \cos \varphi')^{\ell} e^{-im\varphi'} d\varphi'. \quad (\text{E.2})$$

Let us denote the first factor under the integral by

$$W(\theta, \varphi; \ell) = (\cos \theta + i \sin \theta \cos \varphi)^{\ell} \equiv e^{i\ell\theta'(\theta, \varphi)} \quad (\text{E.3})$$

²³For integral representations of special functions and their further generalizations, see [45, 46, 89].

For reason explained in the text, it will be referred to as the *inductive character* for $SO(3)$. Here, it simply serves as the generating function for spherical functions $Y_{\ell,m}$. (More generally, it can also serve as the generating function for the Wigner D-functions.)

For $m = 0$, it leads to ordinary Legendre polynomials,

$$P_{\ell}(\cos \theta) = \langle \ell, 0 | g(\varphi, \theta, \psi) | \ell, 0 \rangle = 4\pi \int_0^{2\pi} W(\theta, \varphi; \ell) d\varphi. \quad (\text{E.4})$$

It is a function of a single variable, and the integral can be interpreted as “averaging” over the subgroup $K = SO(2)$, a typically procedure in arriving at the “S-wave” projection. This provides a useful perspective in deriving zonal spherical functions for non-compact groups, (5.10).

Generalization: In this example of $SO(3)$, the group $R_y(\theta)$ plays the role of the Cartan subgroup and its representation is one-dimensional, i.e., $e^{i\ell\theta}$, with ℓ integer. As indicated earlier, we shall refer to $W(\theta, \varphi; \ell) = e^{i\ell\theta'(\theta, \varphi)}$, (5.2), the character for $R_y(\theta')$, as the inductive character for $SO(3)$. Above construct can be generalized for more general cosets, e.g., G non-compact, with a subgroup H , which can also be non-compact, leading to generalized spherical functions. By enforcing the H bi-invariant condition, (3.12), it leads to a subset of **zonal spherical functions** for non-compact groups where $f(hah') = f(a)$, with $a \in A$.

Our ultimate goal is to obtain these functions for the split rank-2 case of $SO(d, 2)$ relative to a non-compact subgroup H by generalizing the formula $P_{\ell}(\cos \theta) = \langle \ell, 0 | R_z(\varphi) R_y(\theta) R_z(\psi) | \ell, 0 \rangle = \langle \ell, 0 | R_y(\theta) | \ell, 0 \rangle$. Note that taking the matrix element between $|\ell, 0\rangle$ can be replaced by the trace of an operator \mathcal{O}_{λ} with a projection operator $\hat{P}_0 = |\ell, 0\rangle\langle \ell, 0|$. For $SO(3)$, this is fixed by $|\ell, 0\rangle$ being invariant under $R_z(\psi)$. This procedure also applies to non-compact group, $SO(2, 1)$. For each case, the relevant operator \mathcal{O}_{λ} can be reduced to its inductive character, W , and taking trace can in turn be replaced by an averaging over appropriate subgroup.

F Inductive Characters & Zonal Spherical Functions

In this appendix, we begin by considering zonal spherical functions for $SO(2, 1)$ relative to its subgroups, following the procedure as done for $SO(3)$ via Euler-type group expansions. We next introduce a “doubling procedure” in App. F.3, which facilitates our treatment for the rank 2 case in App. F.4.

There are two possible zone spherical functions, one for compact subgroup $K = SO(2)$ and the second for non-compact subgroup $H = SO(1, 1)$. We are only interested in the latter; however,

the treatment for both are instructive. The associated zonal spherical functions are

$$\varphi_K(\eta, \lambda) = P_\lambda(\cosh \eta) = \int_0^{2\pi} d\varphi (\cosh \eta + \cos \varphi \sinh \eta)^\lambda, \quad (\text{F.1})$$

$$\varphi_H(\eta, \lambda) = Q_{-\lambda-1}(\cosh \eta) = \int_0^\infty ds (\cosh \eta + \cosh s \sinh \eta)^\lambda. \quad (\text{F.2})$$

The integrands are the inductive characters, $W_K(\cosh \eta, \varphi; \lambda)$ and $W_H(\cosh \eta, s; \lambda)$, for $SO(2, 1)$ over $SO(2)$ and $SO(1, 1)$ respectively, with $\lambda = -1/2 + \tilde{\ell}$. We also record here, for $SO(d+1, 1)/SO(d+1)$, and $SO(d+1, 1)/SO(d, 1)$, the corresponding zonal spherical functions can also be expressed as [45, 46]

$$\varphi_K(\eta, \lambda) = \int d\varphi (\cosh \eta + \cos \varphi \sinh \eta)^\lambda \sin^{d-1} \varphi, \quad (\text{F.3})$$

$$\varphi_H(\eta, \lambda) = \int ds (\cosh \eta + \cosh s \sinh \eta)^\lambda \sinh^{d-1} s. \quad (\text{F.4})$$

with $\lambda = -d/2 + \tilde{\ell}$. Let us begin by listing various basic facts, with $d = 1$.

Homogenous Functions and Null-Cone: Consider $SO(2, 1)$ acting transitively on the null-cone, $x_1^2 - x_2^2 - x_3^2 = 0$. In anticipation of a CFT reduction, we introduce a space of homogeneous functions on the null cone, $\mathcal{F}_\lambda = \{F(x) \mid F(\sigma x) = \sigma^\lambda F(x)\}$. This homogeneity condition can be realized with different ‘‘slices’’ of the null-cone, dictated by certain subgroup of $SO(2, 1)$, acting transitive on the slice.

For instance, with $\sigma = x_1^{-1}$, the slice γ_1 is $\Gamma_1 = \{x \mid x(\varphi) = (1, \cos \varphi, \sin \varphi), \varphi \in [0, 2\pi]\}$ and the compact subgroup $K = R_{23} = SO(2)$, i.e., rotations in 2-3 plane, acts transitively on Γ_1 . Another choice, $\sigma = x_2^{-1}$, leads to a difference slice, $\Gamma_2 = \Gamma_{2,+} \cup \Gamma_{2,-}$, $\Gamma_{2,\pm} = \{x \mid x_\pm(s) = (\cosh s, \pm 1, \sinh s), s \in R\}$, with a non-compact subgroup $H = B_{13} = SO(1, 1)$, e.g., boosts in 1-3 plane, acting transitively on Γ_2 . The space of homogeneous functions for each slice can be characterized by a reduced function, f_i , defined on Γ_i , $i = 1, 2$, respectively,

$$\mathcal{F}_{\lambda,1} = \left\{ F(x) \mid F(x) = x_1^\lambda f_1(x_2/x_1, x_3/x_1) \right\}, \quad \mathcal{F}_{\lambda,2} = \left\{ F(x) \mid F(x) = |x_2|^\lambda f_2(x_1/x_2, x_3/x_2) \right\}. \quad (\text{F.5})$$

Choice of Basis for $\mathcal{F}_{(\lambda,i)}$: Each $\mathcal{F}_{(\lambda,i)}$ is still infinite-dimensional; a natural choice for each consists of eigenfunctions of the relevant subgroup, i.e., K for Γ_1 and H for Γ_2 . For $\mathcal{F}_{(\lambda,1)}$, we choose the discrete Fourier basis, labelled by $|\lambda, m\rangle$, m integers, $-\infty \leq m \leq \infty$, corresponding to $K = R_{23}$ diagonal. For \mathcal{F}_{γ_2} , the basis for $\mathcal{F}_{(\lambda,2)}$ can be labelled by a continuous Fourier basis, $|\lambda, p\rangle$, $-\infty \leq p \leq \infty$, with $H = B_{13}$ non-compact and diagonal.

Consider $\mathcal{F}_{(\lambda,1)}$ first. Let us adopt an Eulerian parametrization where $g = R_{23}(\varphi)B_{12}(\eta)R_{23}(\psi)$, with B_{12} serving as boosts and R_{23} and R_{23} serving as rotations. That is, we consider a Cartan decomposition for $SO(2, 1)$ where $g \in KAK$, with $B_{12}(\eta)$ serving as the MASG. With

$K = R_{23}$ diagonal, the action of a group element can be represented as $\langle \lambda, m | T_\lambda(g) | \lambda, n \rangle = e^{-im\varphi} e^{in\psi} t_{\lambda; m, n}(\eta)$, where

$$t_{m, n}^\lambda(\eta) = \langle \lambda, m | A(\eta) | \lambda, n \rangle = \langle \lambda, m | B_{12}(\eta) | \lambda, n \rangle. \quad (\text{F.6})$$

We need to find matrix elements $t_{m, n}^\lambda(\eta)$, leading to a group representation.

Consider $\mathcal{F}_{(\lambda, 2)}$ next. With H non-compact, we consider an alternative group decomposition. Staying with $A = B_{12}(\eta)$, consider $g = B_{23}(\zeta) B_{12}(\eta) B_{23}(\zeta')$, i.e., it is of the type HAH . With $B_{23}(\zeta)$ and $B_{23}(\zeta')$ diagonal on the continuous basis, $|\lambda, p\rangle$, $-\infty \leq p \leq \infty$, we have explicit representation $\langle \lambda, p | T_\lambda(g) | \lambda, q \rangle = e^{-ip\zeta} e^{iq\zeta'} t^\lambda(p, q; \eta)$ again with

$$t^\lambda(p, q; \eta) = \langle \lambda, p | A(\eta) | \lambda, q \rangle = \langle \lambda, p | B_{12}(\eta) | \lambda, q \rangle. \quad (\text{F.7})$$

The challenge is again in evaluating $t^\lambda(p, q; \eta)$.

Unitary Irreducible Representation: By specifying a group action on each functional space via “shifting”, e.g.,

$$T_\lambda(g) F_{(\lambda, i)}(x) = F_{g; (\lambda, i)}(x) = F_{(\lambda, i)}(gx), \quad (\text{F.8})$$

where $F_{(\lambda, \gamma_i)}(x) \in \mathcal{F}_{\gamma_i}$, it can be shown that this leads to a representation, T_λ , for $SO(2, 1)$. One can also show that, with λ complex, each leads to a distinct representation in general, with λ and $-1 - \lambda$ being equivalent. By restricting the scaling label $\lambda = -1/2 + \tilde{\lambda}$ where $\tilde{\lambda}$ is purely imaginary, an inner product can be introduced, leading to a unitary irreducible principal series representation. Representations for different slices can be shown to be equivalent.

F.1 Spherical Functions for $SO(2, 1)/SO(2)$

A function in $\mathcal{F}_{(\lambda, 1)}$ can be treated as a vector $|F\rangle$. As a function over the null-cone, it can be expanded in a Fourier series, $F(x) = \langle x | F \rangle = x_1^\lambda \sum_n a_n e^{in\varphi}$, where $e^{i\varphi} = (x_2 + ix_3)/x_1$, i.e., a_n are Fourier coefficients for the function $\tilde{F}(x) = x_1^{-\lambda} F(x)$. Consider next the action of a group element g on $F(x)$ specified by (F.8). It is sufficient for us to consider $g = B_{12}(\eta)$, i.e., a boost in the 1-2 plane. It leads to a new function $F_g(x)$, which can again be expressed as $F_g(x) = x_1^\lambda \sum_n a'_n e^{in\varphi}$, with a'_n a new set of Fourier coefficients. On the other hand, by (F.8), one has $F_g(x) = x_1'^\lambda \sum_n a_n e^{in\varphi'}$, with $x' = gx = (x'_1, x'_2, x'_3) = x'_1(1, \sin \varphi', \cos \varphi')$, where $x'_1 = (\cosh \eta + \cos \varphi_1 \sinh \eta) x_1$ and $\varphi' = \tan^{-1}[(\sin \varphi) / \sinh \eta + \cos \varphi \cosh \eta]$. It follows that the new set of Fourier coefficients a'_n are related to the initial set, a_n , linearly, $a'_m = \sum_n t_{\lambda, (m, n)} a_n$, with $t_{\lambda, (m, n)}$ given by the matrix elements (F.6).

A direct calculation leads to

$$t_{m, n}^\lambda(\eta) = \int d\varphi (\cosh \eta + \cos \varphi \sinh \eta)^\lambda e^{-im\varphi + in\varphi'}, \quad (\text{F.9})$$

with φ' a function of η and φ given above and $\lambda = -1/2 + \tilde{\lambda}$. Let us make the following observations:

- **Spherical functions:** Representation via shifts allows the identification of a subspace of $\mathcal{F}_{\lambda,1}$ which is right-K-invariant, i.e., $F(gk) = F(g)$. It follows that all a_n vanish except for a_0 . This subspace can be identified with the coset, $SO(2,1)/SO(2)$. It follows that the integrand of (F.6), with $n = 0$ serves as the generating function for spherical functions for $SO(2,1)$ over a compact subgroup $SO(2)$.
- **K-bi-invariance and Zonal spherical functions:** One can further identify the K-bi-invariant subspace, i.e., $F(kgk') = F(g)$. It follows that only $t_{0,0}^\lambda$ survives, leading to zonal spherical function, Eq. (F.1). From the integrand, the inductive character, $W_K(\eta, \varphi)$ for $SO(2,1)/SO(2)$, can be expressed as in (5.10).

F.2 Spherical Functions for $SO(2,1)/SO(1,1)$

The analysis follows analogously as for the compact case, except. The main difference is the fact that a function in $\mathcal{F}_{(\lambda,2)}$, treated as a vector $|F\rangle$, can be expanded in a Fourier integral, $F(x) = \langle x|F\rangle = |x_2|^\lambda \int dp a(p) e^{ip\zeta}$, where $x = (x_1, x_2, x_3) = |x_2|(\cosh \zeta, \pm, \sinh \zeta)$, $e^\eta = (x_1 + x_3)/|x_2|$ and \pm stands for sign x_2 . It is again sufficient to consider action of $B_{12}(\eta)$ on $F(x)$, leading to a new function $F_g(x)$, where $F_g(x) = F(x') = |x_2|^\lambda \int dp a'(p) e^{ip\zeta} = |x'_2|^\lambda \int dp' a(p') e^{ip'\zeta'}$, with $x' = gx = (x'_1, x'_2, x'_3) = |x'_2|(\cosh \zeta', \pm 1, \sinh \zeta')$, $x'_2 = (\pm \cosh \eta + \cosh \zeta \sinh \eta) |x_2|$ and $\zeta' = \tanh^{-1}(\sinh \zeta)/(\pm \sinh \eta + \cosh \zeta \cosh \eta)$. It follows that the Fourier coefficients $a'(p)$ are related to $a(p)$ by $a'(p) = \int dt t^\lambda(p, p'; \eta) a(p')$, with $t^\lambda(p, p'; \eta)$ given by the matrix elements (F.7) and

$$t^\lambda(p, p'; \eta) = \int d\zeta |\cosh \eta \mp \cosh \zeta \sinh \eta|^\lambda e^{-ip\zeta + ip'\zeta'} \quad (\text{F.10})$$

with ζ' a function of η and ζ and $\lambda = -1/2 + \tilde{\lambda}$. It is now possible to make the following observations:

- **Spherical functions:** Representation via shifts leads to a subspace of $\mathcal{F}_{\lambda,2}$ which is right-H-invariant, i.e., $F(gh) = F(g)$. It follows that $a(q) = 0$ except for $a(0)$, i.e., it is given by a delta-function. It follows that (F.7), with $q = 0$ and $\lambda = \ell = -1/2 + \tilde{\ell}$, serves as the generating function for spherical functions over the coset, $SO(2,1)/SO(1,1)$.
- **H-bi-invariance and zonal spherical functions:** For the H-bi-invariant subspace, i.e., $F(hgh') = F(g)$, only $t^\lambda(0, 0; \eta)$ survives, leading to Eq. (5.8), i.e., Legendre function of the second kind, $Q_{-1/2+\tilde{\ell}}(\cosh \eta)$. From the integrand, one obtains the inductive character $W_H(\eta, \zeta)$ for $SO(2,1)/SO(1,1)$, given by (5.9).

We also note, due to the appearance of \pm sign, care must be exercised in interpreting (F.10), leading to restriction on region where it is defined. A similar question will emerge in dealing

with split-rank 2 case of interest to us.

F.3 Generalized Doubling Procedure for Inductive Character

As explained in Sec. 3, our ultimate goal is to calculate group harmonics for H -bi-invariant functions with split-rank 2 which can be obtained by the appropriate inductive character via Eq. (5.10) for $d = 2$. In what follows, we introduce an alternative procedure of arriving at the inductive character, which can be generalized more easily to the case of split-rank 2.

As shown earlier, zonal spherical functions for $SO(2,1)/SO(1,1)$ are given by matrix element $t^\lambda(p, p')$ with $p = p' = 0$, which can be thought as the generalization for the case of $SO(3)/SO(2)$ where $P_\ell(\cos \theta) = \langle \ell, 0 | R_z(\varphi) R_y(\theta) R_z(\psi) | \ell, 0 \rangle$. In moving to $SO(2,1)/SO(1,1)$, we replace $R_z(\varphi) R_y(\theta) R_z(\psi)$ by $B_{12}(\zeta) B_{13}(\eta) B_{12}(\zeta')$. The absence of ψ for dependence $SO(3)/SO(2)$ can be understood as due to action of $R_z(\psi)$ on a basepoint on the z-axis. As such, the inductive character, $W_K(\theta, \varphi)$ serves as the generator for spherical function, $Y_{\ell, m}$. The zonal spherical function can be obtained by averaging the inductive character $W_K(\theta, \varphi)$ over the subgroup, $R_z(\varphi)$.

Similarly, the absence of ζ' dependence should be understood as having B_{12} the isotropy of the basepoint $\xi_0 = (1, 1, 0)$. Notice that we have moved to the null cone and this isotropy is only upto a scale and the dependence on ζ' does not drop out explicitly. Let us define a space of matrices $X = g \cdot P \cdot g^T$ where P is diagonal, with $\text{diag}(P) = (-1, 1, 0)$. The important feature of P is that $h \cdot P \cdot h^T = P$. That is, the dependence on ζ' drops out explicitly. Further, because of this property, the space of matrices X carries an image of each element of the coset $g \in G/H$.

Since we are now working with non-Riemannian manifolds, in the framework of induced representations, we decompose a semigroup element $g = na_+h$. The induced representation of this group element is given by

$$\mathcal{F}(g) = e^{\lambda \eta_I} F(h) = e^{\lambda \eta_I} e^{ip\zeta} \quad (\text{F.11})$$

where we write η_I to remind ourselves that this is the parametrization of a in the Iwasawa-like decomposition. Further, $\lambda = \tilde{\lambda} - \rho = \tilde{\lambda} - 1/2$. Setting $p = 0$ takes us to the coset G/H .

The same semigroup element g also carries the Cartan-like decomposition $g = h_1 a_+ h_2$. The function $\mathcal{F}(g) = e^{\lambda \eta_I}$ is on the one-sided coset G/H . For H -bi-invariant functions, we can expand this function in a basis such that h_1 is diagonal. We can then project out the invariant vector by

$$\varphi_\lambda(a) = c'_{\lambda, 0} \int_{h_1} e^{\lambda \eta_I} dh_1, \quad (\text{F.12})$$

much in analogy with the $SO(3)$ discussion. The challenge then is to find the dependence of η_I on $h_1(s)$.

Recall that under $SO(2) \cong U(1)$, the inductive character $e^{i\ell\theta}$ is simply the trace of the one dimensional representation. This identification can be made in general by performing a Cayley transform so that A is diagonal. For the compact case, this is often referred to as the maximal torus. We can generalize this appropriately for the non-compact case and write more explicitly. After the Cayley transformation, A can be written as:

$$A = \begin{pmatrix} e^\eta & 0 & 0 \\ 0 & 1 & 0 \\ 0 & 0 & e^{-\eta} \end{pmatrix}. \quad (\text{F.13})$$

This is in the form of a 3×3 matrix since we are working with the adjoint representation of $SO(2, 1)$.

In the space of matrices X for the two decompositions of g discussed, we have that

$$na_+^I \cdot P \cdot a_+^{I T} n^T = h_1 a_+ \cdot P \cdot a_+^T h_1^T. \quad (\text{F.14})$$

We can solve this equation for e^{η_I} . Notice that in the left hand side, the first entry in the matrix is $e^{2\eta_I}$. We can therefore find the square of the inductive character by finding the first matrix element on the right hand side. We therefore have:

$$\varphi_H(\eta, \lambda) = Q_\lambda(\cosh \eta) = \int ds (\cosh \eta + \cosh s \sinh \eta)^\lambda. \quad (\text{F.15})$$

in agreement with that obtained earlier.

F.4 Rank 2 Case: $SO(2, 2)$

For the rank-2 case, the same construction applies. The adjoint representation now is in terms of 4×4 matrices. We need to solve Eq. (F.14) for two characters e^{y_I}, e^{η_I} . In the Cayley basis of Eq. (C.9), we have

$$a \cdot P \cdot a^T = \begin{pmatrix} e^{2y} & 0 & 0 & -1 \\ 0 & -e^{2\eta} & -1 & 0 \\ 0 & -1 & -e^{-2\eta} & 0 \\ -1 & 0 & 0 & e^{-2y} \end{pmatrix}. \quad (\text{F.16})$$

It is sufficient to consider the 2×2 minor of $na \cdot P \cdot a^T n^T$ which is given by

$$\text{Minor}_1 = (e^{2y_I}); \quad \text{Minor}_2 = \begin{pmatrix} e^{2y_I} & -2e^{2y_I} t_+ \\ -2e^{2y_I} t_+ & 4e^{2y_I} t_+^2 - e^{2\eta_I} \end{pmatrix}. \quad (\text{F.17})$$

The determinant is given by $|\text{Minor}_2| = -e^{2y_I} e^{2\eta_I}$. We can therefore solve for both e^{y_I} and e^{η_I} in terms of $h_1(\alpha, \beta)$. This leads to Eq. (5.17).

References

- [1] Simon Caron-Huot. Analyticity in spin in conformal theories. *Journal of High Energy Physics*, 2017(9):1–44, 2017.
- [2] David Simmons-Duffin, Douglas Stanford, and Edward Witten. A spacetime derivation of the lorentzian ope inversion formula. *Journal of High Energy Physics*, 2018(7):1–40, 2018.
- [3] Richard C. Brower, Joseph Polchinski, Matthew J. Strassler, and Chung-I Tan. The Pomeron and Gauge/String Duality. *Journal of High Energy Physics*, 12:005, 2007.
- [4] Lorenzo Cornalba, Miguel S. Costa, Joao Penedones, and Ricardo Schiappa. Eikonal Approximation in AdS/CFT: Conformal Partial Waves and Finite N Four-Point Functions. *Nuclear Physics*, B767:327–351, 2007.
- [5] Lorenzo Cornalba, Miguel S. Costa, Joao Penedones, and Ricardo Schiappa. Eikonal Approximation in AdS/CFT: From Shock Waves to Four-Point Functions. *Journal of High Energy Physics*, 08:019, 2007.
- [6] Richard C. Brower, Matthew J. Strassler, and Chung-I Tan. On the Eikonal Approximation in AdS Space. *Journal of High Energy Physics*, 2009(03):050, 2009.
- [7] Richard C. Brower, Matthew J. Strassler, and Chung-I Tan. On The Pomeron at Large t Hooft Coupling. *Journal of High Energy Physics*, 03:092, 2009.
- [8] Lorenzo Cornalba, Miguel S. Costa, and Joao Penedones. Eikonal approximation in AdS/CFT: Resumming the gravitational loop expansion. *Journal of High Energy Physics*, 09:037, 2007.
- [9] Lorenzo Cornalba. Eikonal methods in AdS/CFT: Regge theory and multi-reggeon exchange. *arXiv:hep-th/0710.5480*, 2007.
- [10] Diego M. Hofman and Juan Maldacena. Conformal collider physics: Energy and charge correlations. *Journal of High Energy Physics*, 05:012, 2008.
- [11] Matthew J. Strassler. Why Unparticle Models with Mass Gaps are Examples of Hidden Valleys. *arXiv preprint arXiv:0801.0629*, 2008.
- [12] Lorenzo Cornalba, Miguel S. Costa, and Joao Penedones. Eikonal Methods in AdS/CFT: BFKL Pomeron at Weak Coupling. *Journal of High Energy Physics*, 06:048, 2008.
- [13] Lorenzo Cornalba, Miguel S. Costa, and Joao Penedones. Deep Inelastic Scattering in Conformal QCD. *Journal of High Energy Physics*, 03:133, 2010.
- [14] Miguel S. Costa, Vasco Goncalves, and Joao Penedones. Conformal Regge theory. *Journal*

- of High Energy Physics*, 12:091, 2012.
- [15] Richard C. Brower, Miguel S. Costa, Marko Djuric, Timothy Raben, and Chung-I Tan. Strong Coupling Expansion for the Conformal Pomeron/Odderon Trajectories. *Journal of High Energy Physics*, 02:104, 2015.
 - [16] A. V. Belitsky, S. Hohenegger, G. P. Korchemsky, E. Sokatchev, and A. Zhiboedov. From correlation functions to event shapes. *Nuclear Physics*, B884:305–343, 2014.
 - [17] A. V. Belitsky, S. Hohenegger, G. P. Korchemsky, E. Sokatchev, and A. Zhiboedov. Energy-Energy Correlations in N=4 Supersymmetric Yang-Mills Theory. *Phys. Rev. Lett.*, 112(7):071601, 2014.
 - [18] Tom Banks and Guido Festuccia. The Regge Limit for Green Functions in Conformal Field Theory. *Journal of High Energy Physics*, 06:105, 2010.
 - [19] Richard Nally, Timothy Raben, and Chung-I Tan. Inclusive production through ads/cft. *Journal of High Energy Physics*, 2017(11):1–56, 2017.
 - [20] Timothy G. Raben and Chung-I Tan. Minkowski conformal blocks and the Regge limit for Sachdev-Ye-Kitaev-like models. *Physical Review*, D98(8):086009, 2018.
 - [21] Dean Carmi and Simon Caron-Huot. A conformal dispersion relation: correlations from absorption. *Journal of High Energy Physics*, 2020(9):1–39, 2020.
 - [22] Juan Maldacena, Stephen H. Shenker, and Douglas Stanford. A bound on chaos. *Journal of High Energy Physics*, 08:106, 2016.
 - [23] Yingfei Gu and Alexei Kitaev. On the relation between the magnitude and exponent of OTOCs. *Journal of High Energy Physics*, 02:075, 2019.
 - [24] Yingfei Gu, Alexei Kitaev, and Pengfei Zhang. A two-way approach to out-of-time-order correlators. *Journal of High Energy Physics*, 03:133, 2022.
 - [25] Stephen H. Shenker and Douglas Stanford. Stringy effects in scrambling. *Journal of High Energy Physics*, 05:132, 2015.
 - [26] Alexei Kitaev. A simple model of quantum holography (part 1). Talk given at KITP Program: Entanglement in Strongly-Correlated Quantum Matter, April 2015.
 - [27] A. Kitaev. A simple model of quantum holography (part 2). Talk given at KITP Program: Entanglement in Strongly-Correlated Quantum Matter, May 2015.
 - [28] Juan Maldacena and Douglas Stanford. Comments on the Sachdev-Ye-Kitaev model. *Physical Review*, D94(10):106002, 2016.

- [29] Joseph Polchinski and Vladimir Rosenhaus. The Spectrum in the Sachdev-Ye-Kitaev Model. *Journal of High Energy Physics*, 04:001, 2016.
- [30] Ana-Maria Raclariu. Lectures on celestial holography. *arXiv preprint arXiv:2107.02075*, 2021.
- [31] Andrew Strominger. *Lectures on the infrared structure of gravity and gauge theory*. Princeton University Press, 2018.
- [32] Adam Ball, Monica Pate, Ana-Maria Raclariu, Andrew Strominger, and Raju Venugopalan. Measuring color memory in a color glass condensate at electron-ion colliders. *Annals Phys.*, 407:15–28, 2019.
- [33] Petr Kravchuk, Jiaxin Qiao, and Slava Rychkov. Distributions in CFT. Part I. Cross-ratio space. *JHEP*, 05:137, 2020.
- [34] Petr Kravchuk, Jiaxin Qiao, and Slava Rychkov. Distributions in CFT. Part II. Minkowski space. *JHEP*, 08:094, 2021.
- [35] Joshua D Qualls. Lectures on conformal field theory. *arXiv preprint arXiv:1511.04074*, 2015.
- [36] Slava Rychkov. *EPFL lectures on conformal field theory in $D \geq 3$ dimensions*. Springer, 2017.
- [37] Petr Kravchuk and David Simmons-Duffin. Light-ray operators in conformal field theory. *Journal of High Energy Physics*, 2018(11):1–111, 2018.
- [38] Gerhard Mack. Conformal field theory in $d > 2$ dimensions, representations and harmonic analysis. *arXiv preprint arXiv:1902.03812*, 2019.
- [39] V. K. Dobrev, G. Mack, V. B. Petkova, S. G. Petrova, and I. T. Todorov. *On the n -Dimensional Lorentz Group and Its Application to Conformal Quantum Field Theory*. Springer Berlin, Heidelberg, 1977.
- [40] Gerhard Mack and Mathias de Riese. Simple space-time symmetries: generalizing conformal field theory. *Journal of mathematical physics*, 48(5):052304, 2007.
- [41] Gestur Ólafsson and Joachim Hilgert. *Causal Symmetric Spaces*. Elsevier Science & Techn., 1996.
- [42] A. Bassetto and M. Toller. Harmonic analysis on the one-sheet hyperboloid and multiperipheral inclusive distributions. *Annales de l’institut Henri Poincaré. Section A, Physique Théorique*, 18(1):1–38, 1973.
- [43] G. A. Viano. On the harmonic analysis of the elastic scattering amplitude of two spinless

- particles at fixed momentum transfer. *Annales de l'I.H.P. Physique théorique*, 32(2):109–123, 1980.
- [44] J. Faraut and G. A. Viano. Volterra algebra and the bethe–salpeter equation. *Journal of Mathematical Physics*, 27(3):840–848, mar 1986.
- [45] N. Ja. Vilenkin and A. U. Klimyk. *Representation of Lie Groups and Special Functions*, volume 1. Springer Netherlands, 1991.
- [46] N. Ja. Vilenkin and A. U. Klimyk. *Representation of Lie Groups and Special Functions*, volume 2. Springer Netherlands, 1993.
- [47] N. Ja. Vilenkin and A. U. Klimyk. *Representation of Lie Groups and Special Functions*, volume 3. Springer Netherlands, 1992.
- [48] M. Toller. Three-dimensional lorentz group and harmonic analysis of the scattering amplitude. *Il Nuovo Cimento*, 37:631, 1965.
- [49] A.W. Knap. *Representation Theory of Semisimple Groups: An overview based on examples*. Princeton mathematical series. Princeton University Press, Princeton, New jersey, 1986.
- [50] A.W. Knap. *Lie Groups Beyond an Introduction*. Progress in Mathematics. Birkhäuser Boston, 2002.
- [51] S. Helgason. *Groups and Geometric Analysis: Integral Geometry, Invariant Differential Operators, and Spherical Functions*. Mathematical Surveys and Monographs. American Mathematical Society, 2022.
- [52] Pulkit Agarwal, Richard C. Brower, Timothy G. Raben, and Chung-I Tan. Conformal Blocks and Harish Chandra c-Functions. *To appear*, 2023.
- [53] Pulkit Agarwal, Richard Brower, Timothy G Raben, and Chung-I Tan. Application of lorentzian cft principal series representation to near forward scattering. *SciPost Physics Proceedings*, (10):026, 2022.
- [54] F. A. Dolan and H. Osborn. Conformal Partial Waves: Further Mathematical Results. *arXiv:hep-th1108.6194*, 2011.
- [55] Volker Schomerus, Evgeny Sobko, and Mikhail Isachenkov. Harmony of spinning conformal blocks. *Journal of High Energy Physics*, 2017(3), 2017.
- [56] Volker Schomerus and Evgeny Sobko. From spinning conformal blocks to matrix calogero-sutherland models. *Journal of High Energy Physics*, 2018(4), 2018.
- [57] Mikhail Isachenkov and Volker Schomerus. Integrability of conformal blocks. part i.

- calogero-sutherland scattering theory. *Journal of High Energy Physics*, 2018(7), 2018.
- [58] Ilija Burić, Volker Schomerus, and Mikhail Isachenkov. Conformal group theory of tensor structures. *Journal of High Energy Physics*, 2020(10), 2020.
- [59] Ilija Buric and Volker Schomerus. Universal Spinning Casimir Equations and Their Solutions. *arXiv:hep-th/2211.14340*, 11 2022.
- [60] Dalimil Mazáč. A Crossing-Symmetric OPE Inversion Formula. *JHEP*, 06:082, 2019.
- [61] Matthijs Hogervorst and Slava Rychkov. Radial Coordinates for Conformal Blocks. *Physical Review*, D87:106004, 2013.
- [62] Richard C Brower, George T Fleming, Andrew D Gasbarro, Dean Howarth, Timothy G Raben, Chung-I Tan, and Evan S Weinberg. Radial lattice quantization of 3d φ^4 field theory. *Physical Review D*, 104(9):094502, 2021.
- [63] R. Hermann. *Lie Groups for Physicists*. Mathematical physics monograph series. W. A. Benjamin, 1966.
- [64] Wu-Ki Tung. *Group Theory in Physics*. WORLD SCIENTIFIC, 1985.
- [65] V. Bargmann. Irreducible unitary representations of the lorentz group. *Annals of Mathematics*, 48(3):568–640, 1947.
- [66] Simon Caron-Huot, Dalimil Mazáč, Leonardo Rastelli, and David Simmons-Duffin. Dispersive cft sum rules. *Journal of High Energy Physics*, 2021(5):1–112, 2021.
- [67] Jiaxin Qiao. Classification of convergent ope channels for lorentzian cft four-point functions. *SciPost Physics*, 13(4):093, 2022.
- [68] Richard C. Brower, Marko Djuric, and Chung-I Tan. Odderon in Gauge/String Duality. *Journal of High Energy Physics*, 07:063, 2009.
- [69] Jean-Philippe Anker and Bent Orsted, editors. *Lie Theory*. Birkhäuser Boston, 2005.
- [70] Juan Maldacena, Stephen H. Shenker, and Douglas Stanford. A bound on chaos. *JHEP*, 08:106, 2016.
- [71] Joao Penedones, Joao A. Silva, and Alexander Zhiboedov. Nonperturbative Mellin Amplitudes: Existence, Properties, Applications. *JHEP*, 08:031, 2020.
- [72] A. V. Kotikov, L. N. Lipatov, A. I. Onishchenko, and V. N. Velizhanin. Three loop universal anomalous dimension of the Wilson operators in N=4 SUSY Yang-Mills model. *Phys. Lett.*, B595:521–529, 2004. [Erratum: *Phys. Lett.*B632,754(2006)].
- [73] Chung-I Tan. The Pomeron - A Bootstrap Story. *arXiv:hep-ph/2201-00216*, 2022.

- [74] Lars Brink, Richard C. Brower, Carleton DeTar, Chung-I Tan, and K. K. Phua. *Geoffrey Chew: Architect of the Bootstrap*. World Scientific, 2022, 2022.
- [75] Simon Caron-Huot and Joshua Sandor. Conformal Regge Theory at Finite Boost. *Journal of High Energy Physics*, 05:059, 2021.
- [76] B. Basso. An exact slope for AdS/CFT. *arXiv preprint arXiv:1109.3154*, 2011.
- [77] Nikolay Gromov, Fedor Levkovich-Maslyuk, Grigory Sizov, and Saulius Valatka. Quantum spectral curve at work: from small spin to strong coupling in $n=4$ sym. *Journal of High Energy Physics*, 2014(7):1–53, 2014.
- [78] Nikolay Gromov, Fedor Levkovich-Maslyuk, and Grigory Sizov. Quantum Spectral Curve and the Numerical Solution of the Spectral Problem in AdS₅/CFT₄. *Journal of High Energy Physics*, 06:036, 2016.
- [79] C Cronström and WH Klink. Generalized $O(2, 1)$ expansions of multiparticle amplitudes. *Annals of Physics*, 69(1):218–278, 1972.
- [80] Robert Hermann. *Fourier Analysis on Groups and Partial Wave Analysis*. Mathematical Lecture Notes Series (W. A. Benjamin, Inc.), 1969.
- [81] A. V. Kotikov and L. N. Lipatov. Pomeron in the $N=4$ supersymmetric gauge model at strong couplings. *Nuclear Physics*, B874:889–904, 2013.
- [82] Yuri V. Kovchegov and Eugene Levin. *Quantum chromodynamics at high energy*. Cambridge Monographs on Particle Physics, Nuclear Physics and Cosmology, Vol. 33. Cambridge University Press, 2012, 2013.
- [83] V. M. Braun, G. P. Korchemsky, and Dieter Mueller. The Uses of conformal symmetry in QCD. *Progress in Particle and Nuclear Physics*, 51:311–398, 2003.
- [84] António Antunes, Miguel S. Costa, Tobias Hansen, Aaditya Salgarkar, and Sourav Sarkar. The perturbative CFT optical theorem and high-energy string scattering in AdS at one loop. *Journal of High Energy Physics*, 2021(4):088, 2021.
- [85] A. H. Mueller. Unitarity and the BFKL Pomeron. *Nuclear Physics*, 107(B 437), 2023.
- [86] Miao Li and Chung-I Tan. High energy scattering in $(2+ 1)$ -dimensional qcd: A dipole picture. *Physical Review D*, 51(7):3287, 1995.
- [87] Yizhuang Liu, Maciej A Nowak, and Ismail Zahed. Rapidity evolution of the entanglement entropy in quarkonium: Parton and string duality. *Physical Review D*, 105(11):114028, 2022.
- [88] Dalimil Mazáč, Leonardo Rastelli, and Xinan Zhou. A basis of analytic functionals for cfts

in general dimension. *Journal of High Energy Physics*, 2021(8):1–52, 2021.

- [89] Loyal Durand. Product formulas and nicholson-type integrals for jacobi functions. i: Summary of results. *SIAM Journal on Mathematical Analysis*, 9(1):76–86, 1978.